LEABHARLANN CHOLÁISTE NA TRÍONÓIDE, BAILE ÁTHA CLIATH | TRINITY COLLEGE LIBRARY DUBLIN
Ollscoil Átha Cliath | The University of Dublin

Terms and Conditions of Use of Digitised Theses from Trinity College Library Dublin

Copyright statement

All material supplied by Trinity College Library is protected by copyright (under the Copyright and Related Rights Act, 2000 as amended) and other relevant Intellectual Property Rights. By accessing and using a Digitised Thesis from Trinity College Library you acknowledge that all Intellectual Property Rights in any Works supplied are the sole and exclusive property of the copyright and/or other IPR holder. Specific copyright holders may not be explicitly identified. Use of materials from other sources within a thesis should not be construed as a claim over them.

A non-exclusive, non-transferable licence is hereby granted to those using or reproducing, in whole or in part, the material for valid purposes, providing the copyright owners are acknowledged using the normal conventions. Where specific permission to use material is required, this is identified and such permission must be sought from the copyright holder or agency cited.

Liability statement

By using a Digitised Thesis, I accept that Trinity College Dublin bears no legal responsibility for the accuracy, legality or comprehensiveness of materials contained within the thesis, and that Trinity College Dublin accepts no liability for indirect, consequential, or incidental, damages or losses arising from use of the thesis for whatever reason. Information located in a thesis may be subject to specific use constraints, details of which may not be explicitly described. It is the responsibility of potential and actual users to be aware of such constraints and to abide by them. By making use of material from a digitised thesis, you accept these copyright and disclaimer provisions. Where it is brought to the attention of Trinity College Library that there may be a breach of copyright or other restraint, it is the policy to withdraw or take down access to a thesis while the issue is being resolved.

Access Agreement

By using a Digitised Thesis from Trinity College Library you are bound by the following Terms & Conditions. Please read them carefully.

I have read and I understand the following statement: All material supplied via a Digitised Thesis from Trinity College Library is protected by copyright and other intellectual property rights, and duplication or sale of all or part of any of a thesis is not permitted, except that material may be duplicated by you for your research use or for educational purposes in electronic or print form providing the copyright owners are acknowledged using the normal conventions. You must obtain permission for any other use. Electronic or print copies may not be offered, whether for sale or otherwise to anyone. This copy has been supplied on the understanding that it is copyright material and that no quotation from the thesis may be published without proper acknowledgement.

MicroRNA regulation of the bovine alveolar macrophage response to *Mycobacterium bovis*

A thesis submitted to the University of Dublin for the degree of
Doctor of Philosophy

2015

PETER VEGH

School of Genetics and Microbiology,
Trinity College, University of Dublin

Supervisors: Associate Professor David J. Lynn and Professor Daniel G. Bradley

TRINITY COLLEGE
0 6 OCT 2015
LIBRARY DUBLIN

Thesis 10878

Declaration

I declare that this thesis has not been submitted as an exercise for a degree at this or any other university and it is entirely my own work.

I agree to deposit this thesis in the University's open access institutional repository or allow the library to do so on my behalf, subject to Irish Copyright Legislation and Trinity College Library conditions of use and acknowledgement.

Peter Vegh

Peter Vegh

Summary

Bovine tuberculosis is one of the most economically significant infectious diseases of cattle in Ireland and globally, resulting in economic losses of approximately €2 billion annually. The causative agent is *Mycobacterium bovis*, a rod-shaped, Gram positive, acid-fast bacterium that is a member of the *Mycobacterium tuberculosis* complex (MTBC), a group of highly related pathogens that are spread via an airborne route. Alveolar macrophages (AMs) are the natural host cell for inhaled mycobacteria and constitute the front line of host defence. In this thesis, I sought to investigate the role that microRNAs play in regulating immune responses in AMs. MicroRNAs (miRNAs) are short non-coding RNAs that post-transcriptionally regulate gene expression and are known to play important roles in regulating both adaptive and innate immunity. I first established the profile of miRNA expression in uninfected bovine alveolar macrophages isolated from lung lavages of eight different healthy Holstein–Friesian male calves. Employing a next-generation sequencing (RNA-seq) approach to profile the expression levels of known and novel miRNAs, 80 different miRNAs were identified as being expressed in bovine AMs at a threshold of at least 100 reads per million. The expression levels of miRNAs varied over a large dynamic range, with a few miRNAs expressed at very high and the majority lowly expressed. Notably, many of the most highly expressed miRNAs in bovine AMs have known roles in regulating immunity in other species.

Next we implemented a similar RNA-seq approach to temporally profile miRNA expression in primary bovine AMs post-infection with *M. bovis*. In total, 2.5 billion sequencing reads were generated from the 88 miRNA RNA-seq libraries prepared from AMs isolated from ten different animals. One, six, and forty miRNAs were identified as significantly differentially expressed at 2, 24 and 48 hours post-infection, respectively. The differential expression of three miRNAs (miR-142-5p, miR-146a, and miR-423-3p) was confirmed by reverse transcription quantitative real-time PCR (RT-qPCR). Pathway analysis of the predicted mRNA targets of differentially expressed miRNAs suggests that these miRNAs preferentially target several pathways that are functionally relevant for mycobacterial pathogenesis, including endocytosis and lysosome trafficking, IL-1 signalling and the TGF-β pathway. Transfection of a synthetic mimic of miR-146 into a bovine macrophage cell-line (Bomac) confirmed the

predicted targeting of two key genes in the innate immune response to *M. bovis* by this miRNA, IL-1 receptor-associated kinase 1 *(IRAK1)* and TGF-β receptor 2 *(TGFBR2).* We next sought to identify the genes regulated by miR-146a on a genome-wide scale. RNA-seq was again used to profile global gene expression changes in Bomacs transfected with the synthetic mimic of miR-146 in comparison to a scrambled negative control synthetic RNA. 125 differentially expressed genes were identified following miR-146a transfection and confirmed the targeting of *IRAK1* and *TGFBR2* by this miRNA. Pathway analysis revealed that differentially expressed genes were enriched for roles in macrophage activation and immune responses.

One of the potential applications of this work is the identification of novel miRNA biomarkers of *M. bovis* infection. To investigate this, we profiled miRNA expression in peripheral blood mononuclear cells isolated from five animals naturally infected with *M. bovis* and four healthy animals. Nine miRNAs were found to be differentially expressed between healthy and infected animals and multi-dimensional scaling analysis revealed the clear separation of infected and control animals based on their miRNA expression profiles. The differentially expressed miRNAs were found to preferentially target cell cycle regulation and TGF-β receptor signalling. This pilot study is supportive of the potential of using miRNAs as biomarkers of *M. bovis* infection and now needs further investigation in a larger number of animals.

In conclusion, the work presented in this thesis has for the first time identified the differential expression of more than 40 miRNAs in AMs at several time-points following infection with *M. bovis* and revealed that these miRNAs play important roles in targeting genes that are functionally relevant for mycobacterial pathogenesis, suggesting that miRNAs play a key role in tuning the complex interplay between *M. bovis* survival strategies and the host immune response.

Publications

P. Vegh, A. B. K. Foroushani, D. A. Magee, M. S. McCabe, J. A. Browne, N. C. Nalpas, K. M. Conlon, S. V. Gordon, D. G. Bradley, D. E. MacHugh, D. J. Lynn, *Profiling microRNA expression in bovine alveolar macrophages using RNA-seq.* Veterinary Immunology and Immunopathology (2013) 155, 238-244

N. Lawless*, P. Vegh*, C. O'Farrelly, D. J. Lynn, *The role of microRNAs in bovine infection and immunity.* Frontiers in Immunology (2014) 5:611

P. Vegh, D. A. Magee, N. C. Nalpas, K. Bryan, M. S. McCabe, J. A. Browne, K. M. Conlon, S. V. Gordon, D. G. Bradley, D. E. MacHugh, D. J. Lynn, *MicroRNA profiling of the bovine alveolar macrophage response to Mycobacterium bovis infection suggests pathogen survival is enhanced by microRNA regulation of endocytosis and lysosome trafficking.* Tuberculosis (2015) 95(1):60-67

* These authors contributed equally

Table of Contents

Declaration i

Summary ii

Publications iv

Table of Contents v

Index of Figures x

Index of Tables xii

Index of Appendices xiii

Acknowledgements xiv

Abbreviations xv

1 Chapter 1 Introduction 1

1.1 Tuberculosis 2

1.1.1 Bovine tuberculosis 2

1.1.2 Lung alveoli: the site of infection 3

1.1.3 Macrophages 3

1.1.4 Innate immune stage 5

1.1.5 Immunological equilibrium 7

1.1.6 Reactivation 10

1.1.7 Transmission of disease 11

1.1.8 Genetics and gene regulation of mycobacterial infections 11

1.2 MicroRNAs 13

1.2.1 Biogenesis and function in gene expression regulation 13

1.2.2 MicroRNAs in the immune system 16

1.2.3 MicroRNAs in mycobacterial infections 17

1.2.4 MicroRNAs in cattle 18

1.2.5 Application of miRNAs in diagnosis and therapy 19

1.3 Transcriptomics 20

1.3.1 Next-generation sequencing 20

1.3.2 Bioinformatics 22
1.4 Thesis hypothesis, aim, and specific objectives 25
2 Chapter 2 Profiling microRNA expression in bovine alveolar macrophages using RNA-seq 27
2.1 Introduction 28
2.2 Materials and methods 29
2.2.1 Ethics statement 29
2.2.2 Animals 29
2.2.3 Lung lavages, alveolar cell preparation and storage 29
2.2.4 Alveolar cell culture 30
2.2.5 Small RNA 31
2.2.6 RNA-seq libraries 31
2.2.7 Analysis of RNA-seq data 31
2.2.8 RT-qPCR validation 33
2.3 Results and discussion 35
2.3.1 AM-expressed miRNAs 35
2.3.2 Relative expression of miR-21, miR-148a and miR-708 39
2.3.3 Analysis of predicted miRNA target genes 40
2.3.4 IsomiR expression in AMs 40
2.3.5 Prediction of novel bovine miRNAs expressed in AMs 43
2.3.6 Conclusion 43
3 Chapter 3 MicroRNA profiling of the bovine alveolar macrophage response to Mycobacterium bovis infection suggests pathogen survival is enhanced by microRNA regulation of endocytosis and lysosome trafficking 45
3.1 Introduction 46
3.2 Materials and methods 47
3.2.1 Ethical approval 47
3.2.2 Animals 47

3.2.3 Alveolar macrophage in vitro infection 47
3.2.4 Small RNA preparation 48
3.2.5 RNA-seq library preparation 48
3.2.6 Analysis of RNA-seq data 48
3.2.7 Co-expression and target analysis of miRNA and mRNA data 50
3.2.8 Pathway analysis of predicted miRNA target genes 50
3.2.9 RT-qPCR validation of differentially expressed miRNA genes 50
3.2.10 Transfection of Bomac cells with miRNA mimics 51
3.2.11 RT-qPCR analysis of target gene downregulation 52
3.3 Results 53
3.3.1 Multiple differentially expressed miRNAs were detected at 2, 24, and 48 hours post infection with M. bovis 56
3.3.2 Validation of three differentially expressed miRNAs using RT-qPCR 59
3.3.3 Two potentially novel bovine miRNAs are predicted from the sequencing data 63
3.3.4 The predicted targets of upregulated miRNAs are enriched for roles in endocytosis and lysosome function 64
3.3.5 Overexpression of miR-146 results in the transcriptional suppression of IRAK1 and TGFBR2 66
3.4 Discussion 68
4 Chapter 4 Transcriptomic (RNA-seq) analysis of Bomac cells overexpressing miR-146a 71
4.1 Introduction 72
4.2 Materials and methods 73
4.2.1 Transfection of Bomac cells with bta-miR-146a mimics 73
4.2.2 RNA-seq library preparation 74
4.2.3 RNA-seq data analysis 74
4.3 Results and discussion 75

4.3.1 Sequencing data 75
4.3.2 Upregulated genes in the negative control miRNA treated cells 78
4.3.3 Downregulated genes in the negative control miRNA treated cells 81
4.3.4 Differentially expressed genes in miR-146a mimic transfected cells, in comparison to the negative control mimic 84
4.3.5 Differentially expressed genes with seed match to miR-146a 88
4.3.6 Pathway analysis of differentially expressed genes 88
4.3.7 Conclusion 91
5 Chapter 5 MicroRNA-seq profiling of PBMCs of *Mycobacterium bovis* infected cattle shows regulation of cell cycle and TGF-β receptor signalling by differentially expressed miRNAs 93
5.1 Introduction 94
5.2 Materials and methods 95
5.2.1 Animals 95
5.2.2 Haematological analysis and PBMC isolation 95
5.2.3 Small RNA preparation 96
5.2.4 RNA-seq library preparation and sequencing data analysis 96
5.2.5 Target prediction and pathway analysis 97
5.2.6 RT-qPCR validation of differentially expressed miRNA genes 98
5.3 Results and discussion 98
5.3.1 IFN-γ testing 98
5.3.2 Haematological analysis 100
5.3.3 Small RNA 100
5.3.4 The miRNA-seq profile of healthy animals 100
5.3.5 Nine miRNAs are differentially expressed miRNAs between PBMCs of healthy and infected cattle 104
5.3.6 Differentially expressed miRNAs target cell cycle regulation and TGF-β receptor signalling 107

5.3.7 Validation of three miRNAs using RT-qPCR 109
5.3.8 Conclusion 111
6 Chapter 6 General discussion 113
6.1 General discussion 114
6.1.1 MicroRNA expression studies in cattle 115
6.1.2 Role of microRNAs in regulating host responses to infection in cattle.. 116
6.1.3 Validating miRNA targets 118
6.1.4 MicroRNAs as novel biomarkers 120
6.1.5 Future directions 121
6.1.6 Conclusion 123
References 125
Appendix 151
Electronic Appendix 169

Index of Figures

Figure 1-1 | Functions of autophagy in the immune system. 9
Figure 1-2 | The standard pathway of miRNA processing. 14
Figure 1-3 | The role of miRNAs in mycobacterial infection. 18
Figure 1-4 | The FASTQ format. 23
Figure 2-1 | Bioinformatics analysis pipeline overview. 32
Figure 2-2 | The proportion of reads aligning uniquely to annotated bovine genes (averaged across eight samples) 35
Figure 2-3 | Distribution of miRNAs in the bovine genome. 36
Figure 2-4 | Box plot of miRNAs expressed in AMs 37
Figure 2-5 | Scatter plots of miRNAs expressed at a threshold above 100 RPM in AMs. 39
Figure 3-1 | Scatter plot of miRNAs expressed above 100 RPM in the ten 0 h control samples 54
Figure 3-2 | MicroRNA expression in unchallenged bovine alveolar macrophages. 55
Figure 3-3 | Upregulated (A) and downregulated (B) miRNAs in bovine alveolar macrophages isolated from nine animals at 48 hours post infection with *M. bovis*. 57
Figure 3-4 | Fold changes of four miRNAs across four time points. 60
Figure 3-5 | The differential expression of three (bta-miR-142-5p, bta-miR-146a, and bta-miR-423-3p) out of four miRNAs for the nine animals at 48 hpi was confirmed with RT-qPCR (white). 60
Figure 3-6 | Fold changes of differentially expressed miRNAs across four time points. 63
Figure 3-7 | Two-dimensional cluster analysis and heatmap visualization of significant correlations (shown as coloured lines) between miRNA and mRNA expression at 48 hpi. 65
Figure 3-8 | A network of the predicted mRNA targets of differentially expressed miRNAs at 48 hpi with *M. bovis*. 66
Figure 3-9 | Transfection of miRNA mimics for miR-146a or miR-146b into a bovine macrophage cell line (Bomac) led to a 3 fold decrease in *IRAK1* transcript levels, and a 1.5 fold downregulation of *TGFBR2* in comparison to a scrambled control miRNA, as measured by RT-qPCR. 67

Figure 4-1 | Scatter plot of genes expressed above 10 RPM in all samples. 77
Figure 4-2 | Multi-dimensional scaling (MDS) plots comparing transcriptomic profiles of untreated and miRNA-mimic treated cells. 78
Figure 4-3 | Volcano plot of differentially expressed genes. 85
Figure 4-4 | Signalling by HMGB1. 91
Figure 5-1 | Whole blood cell counts for infected and control samples. 99
Figure 5-2 | The proportion of reads aligning uniquely to annotated bovine genes. 103
Figure 5-3 | Scatter plot of miRNAs expressed above 100 reads per million in healthy (C) and the infected (I) samples. 103
Figure 5-4 | The miRNA expression profile of PBMCs of healthy animals. 104
Figure 5-5 | Multidimensional scaling (MDS) plot comparing samples in the healthy (C) and infected (I) groups. 105
Figure 5-6 | Volcano plot showing edgeR results. 106
Figure 5-7 | Dotplot of ΔC_t results for infected and control samples. 110
Figure 5-8 | RNA-seq count numbers for miR-222 and miR-423-3p. 111

Index of Tables

Table 2-1 | RNA quality and read numbers. 34
Table 2-2 | The RT-qPCR results for miR-21, miR-148a and miR-708 in four samples. 40
Table 2-3 | Summary of isomiR expression across samples. 42
Table 3-1 | Summary of number of reads at each data processing step. 49
Table 3-2 | Sequences of primers used in the RT-qPCR 53
Table 3-3 | Differentially expressed microRNAs in alveolar macrophages challenged with *M. bovis* 58
Table 4-1 | Summary of read counts. 76
Table 4-2 | Upregulated genes in Bomac cells treated with scrambled negative control miRNA mimic, in comparison with untreated cells 80
Table 4-3 | Overrepresented KEGG pathways among upregulated genes. 81
Table 4-4 | Downregulated genes in Bomac cells treated with scrambled negative control miRNA mimic, in comparison with untreated cells. 83
Table 4-5 | Overrepresented KEGG pathways among downregulated genes. 84
Table 4-6 | Downregulated genes in miR-146a overexpressed Bomac cells, in comparison with scrambled negative control miRNA mimic treated cells. 86
Table 4-7 | Upregulated genes in miR-146a overexpressed Bomac cells, in comparison with scrambled negative control miRNA mimic treated cells. 87
Table 4-8 | Downregulated genes with seed match to miR-146a. 88
Table 4-9 | IPA analysis of downregulated and upregulated genes. 90
Table 5-1 | IFN-γ release assay results for all animals. 99
Table 5-2 | Sample RNA concentrations 100
Table 5-3 | Read numbers at each data processing step. 101
Table 5-4 | Differentially expressed miRNAs in PBMCs of TB reactor animals. 106
Table 5-5 | Pathway overrepresentation analysis of targets of upregulated miRNAs. 107
Table 5-6 | Pathway overrepresentation analysis of targets of downregulated miRNAs. 108

Index of Appendices

Appendix 1 151
Appendix 2 152
Appendix 3 154
Appendix 4 156
Appendix 5 156
Appendix 6 157
Appendix 7 161
Appendix 8 164
Appendix 9 165

Acknowledgements

First and foremost I would like to thank my supervisor, Professor David Lynn for his patience, mentoring, and guidance over the years.

I also wish to thank my university supervisor at Trinity College Dublin, Professor Daniel Bradley, for overseeing my PhD work, and providing invaluable advice.

I would like to thank my co-supervisor at University College Dublin, Professor David MacHugh, and the members of the UCD group, Professor Stephen Gordon, Dr. David Magee, Dr. John Browne, and Nicolas Nalpas for their work on our project. I wish to thank the staff at UCD College of Agriculture, Food Science and Veterinary Medicine, and the UCD Lyons Research Farm for their assistance and help.

I would like to thank the members of our group, firstly Nathan, who taught me several laboratory techniques and introduced me to work in the labs at Teagasc Grange. Also thanks to Heather, Ken, Manuel, Amir, Brian, and Theodosia for the several discussions and conversations in the office and the canteen.

I thank everyone in Grange. I would especially like to thank Dr. Kieran Meade, Dr. Matt McCabe, Dr. Paul Cormican, Margaret Murray, Joe Larkin, Joe Gill, and Peter Grimes for their help in my research, and Jenna, Rachael, Anthony, Bojan, and Francesco for ideas, suggestions, discussions, and the good times we spent together during the PhD.

I am very grateful for Teagasc and the Walsh Fellowship scheme for providing me an opportunity for professional and personal growth and development.

Finally, I thank my parents and my family for their support throughout the years.

Abbreviations

AGO	Argonaute
AIDS	acquired immune deficiency syndrome
AM	alveolar macrophage
BCG	bacille Calmette-Guérin
bp	basepair
CCL	chemokine (C-C motif) ligand
CD	cluster of differentiation
CDKN	cyclin dependent kinase inhibitor
cDNA	complementary DNA
CFU	colony-forming unit
CPM	count per million
C_q or C_t	quantification cycle
CR	complement receptor
CXCL	chemokine (C-X-C motif) ligand
DC	dendritic cell
DE	differentially expressed
DNA	deoxyribonucleic acid
EEA1	early endosome antigen 1
Eis	enhanced intracellular survival protein
FBS	fetal bovine serum
FC	fold change
FDR	false discovery rate
GEO	Gene Expression Omnibus
GWAS	genome-wide association study
HBSS	Hank's Balanced Salt Solution
HIV/AIDS	human immunodeficiency virus infection and AIDS
hpi	hours post infection
HSC	hematopoietic stem cell
IFN-γ	interferon-gamma
IL	interleukin
IPA	Ingenuity Pathway Analysis

IRAK1	interleukin-1 receptor-associated kinase 1
lncRNA	long non-coding RNA
MAPK	mitogen-activated protein kinase
MDS	multi-dimensional scaling
MHC	Major Histocompatibility Complex
miRNA	microRNA
mRNA	messenger RNA
MTBC	*Mycobacterium tuberculosis* complex
mTOR	mammalian target of rapamycin
mtRNA	mitochondrial RNA
ncRNA	non-coding RNA
NGS	next-generation sequencing
NK	natural killer
NKT	natural killer T
nt	nucleotide
PAMP	pathogen associated molecular pattern
PBMC	peripheral blood mononuclear cell
PBS	phosphate-buffered saline
PCR	polymerase chain reaction
PI3	phosphatidylinositol-3
PPD	purified protein derivative
PRR	pattern recognition receptor
QTL	quantitative trait loci
RILP	Rab-interacting lysosomal protein
RIN	RNA integrity number
RISC	RNA-induced silencing complex
RLE	relative log expression
RNA	ribonucleic acid
RNA-seq	next-generation sequencing applied to RNA sequencing
RPM	read per million
rRNA	ribosomal RNA
RT-qPCR	reverse transcription quantitative polymerase chain reaction
snoRNA	small nucleolar RNA
snRNA	small nuclear RNA

TB	tuberculosis
TGF-β	transforming growth factor beta
T_H1	T helper cell type 1
TLR	Toll-like receptor
TMM	trimmed mean of M-values
TNF-α	tumour necrosis factor alpha
tRNA	transfer RNA
UCD	University College Dublin
UTR	untranslated region

CHAPTER 1

INTRODUCTION

1.1 Tuberculosis

1.1.1 Bovine tuberculosis

Bovine tuberculosis (TB) is an infectious disease of cattle *(Bos taurus),* caused by *Mycobacterium bovis,* a rod-shaped, Gram positive, acid-fast bacterium in the *Mycobacterium tuberculosis* complex of the family *Mycobacteriaceae.* Its primary host are cattle, and is found throughout the world. It is a significant problem for Irish and global agriculture, resulting in economic losses of approximately US$3 billion annually (Garnier *et al.*, 2003). The bacterium can cause disease in many other species, for example, in sheep *(Ovis aries),* badgers *(Meles meles),* deer *(Cervidae),* and in humans *(Homo sapiens)* (Ayele *et al.*, 2004). The main route of infection is airborne, from other livestock. It was recently reported that movement of infected animals between herds in the United Kingdom was responsible for 84% of newly infected animals (Brooks-Pollock *et al.*, 2014). Calves and humans can also become infected by consumption of raw milk from infected animals. Another route of infection is transmission from the local environment; through contact with contaminated water or farm machinery and facilities. Wildlife, especially badgers, may also serve as vectors of infection (Menzies and Neill, 2000).

Prevention is achieved mainly via separation of infected animals from the herd, and the separation of the herd, food and water both from other domestic animals with unknown status, and wildlife (Menzies and Neill, 2000). Maintenance of good farming practice, including regular cleaning and disinfecting of equipment, performing TB tests before moving animals is also important. Vaccination is not used, as its efficiency is poor, and interferes with diagnosis of the disease (Sopp *et al.*, 2008).

The standard diagnosis method is the tuberculin skin test, where a small amount of mycobacterial antigen (purified protein derivative) is injected into the skin and the immune reaction is measured. The test is not reliable, and this contributes to the spread of the disease (McDonald, 2014). A better diagnosis can be made by IFN-γ release assays, or by growing the bacteria in the laboratory, which takes at least eight weeks. Infected animals can be treated by administration of isoniazid and rifampicin for six months, however, due to the cost and length of the treatment, culling is the main method employed (Fitzgerald *et al.*, 2010). Slaughtering the whole herd upon detection of bovine TB is effective in control the disease spread, however, it is very costly to the cattle industry (Brooks-Pollock *et al.*, 2014).

The infection starts with inhalation of mycobacteria-containing aerosols into lung alveoli where the bacteria is taken up by alveolar macrophages. However, the bacteria usually survive within the phagocyte, and modulate its behaviour to avoid lysis. The resulting immune response is not sterilising, but leads to tubercle formation which protects by confining the infection. Certain causes (such as weakened immune system) may reactivate the infection, which develops into a contagious form. Finally, the bacteria are transmitted via sputum particles, which are expelled from the lung into the air by coughing. Our knowledge of tuberculosis immunobiology originates mostly from human and from mouse models, not cattle. Reflecting this, the following sections outline what is currently known about the host immune response to *Mycobacteria* in general and not specifically to *M. bovis*.

1.1.2 Lung alveoli: the site of infection

The main site of tuberculous infection is the lung, specifically, the lung *alveoli,* in which the airways terminate. The alveoli are the site of gas exchange. Two major types of epithelial cells constitute the alveolus; the thin type I alveolar epithelial cells provide structure, and the cuboidal type II alveolar epithelial cells produce components of the surfactant layer (Huether and McCance, 2004). Pulmonary surfactant is a fluid coating the walls of the alveoli of the lungs, with the primary role of lowering the surface tension. It consists of phospholipids, plasma proteins, cholesterol, surfactant proteins, among other substances. In addition to its role of easing the inflation of alveoli during inhalation, it enhances pathogen clearance and regulates innate and adaptive immune-cell functions. Surfactant protein A and D bind to the lipoarabinomannan of *M. tuberculosis,* enhancing uptake by immune cells (Wright, 2005). Other humoral and cellular elements of immunity are also found in the alveoli. Elements of the humoral arm are lactoferrins, lysozyme, mannose binding lectin, and defensins (Huether and McCance, 2004).

1.1.3 Macrophages

Cells of the immune system are grouped by their origin as lymphoid or myeloid cells. Members of the lymphoid lineage are B cells, T cells and innate lymphoid cells. Cells of the myeloid lineage are granulocytes, dendritic cells (DCs), monocytes, and macrophages (Murphy *et al.*, 2008). Macrophages originate from bone marrow hematopoietic stem cells (HSCs) which undergo several differentiation stages, namely,

common myeloid progenitor, granulocyte-monocyte colony-forming unit (CFU), monocyte-CFU, monoblast and finally the monocyte, which enters the bloodstream. These circulating peripheral blood mononuclear cells (PBMCs) migrate into almost all tissues and differentiate into macrophages (Mosser and Edwards, 2008).

The main role of macrophages is to maintain homeostasis by regulating immunity, controlling infection, assisting wound healing and removing cell debris by *phagocytosis* (from Greek *phagein,* "to eat"), a process by which unwanted or foreign material is endocytosed into the *phagosome,* a membrane-bounded organelle in the cytoplasm (Lambrecht, 2006). Other types of endocytosis are clathrin-mediated, caveolar-type, flotillin-dependent endocytosis, and pinocytosis (from Greek *pino,* "to drink"). These differ in the type of material internalised, the membrane morphology and proteins involved (Doherty and McMahon, 2009).

Phagocytosis is receptor-mediated and depends on remodelling of the actin cytoskeleton, which forms pseudopods, membrane invaginations, and closes the phagosome. The receptors that mediate phagocytosis are scavenger receptors, phosphatidyl serine receptors, the thrombospondin receptor, integrins, and complement receptors (Groves *et al.*, 2008). The phagosome matures through a series of fusions and fissions. The early phagosomes fuse with multivesicular bodies, and have a pH of 6.3. It carries the early endosome antigen 1 (EEA1), which bridges membranes during interactions, and the GTPase Rab5, which is involved in endosomal trafficking and membrane fusion (Flannagan *et al.*, 2009). The resulting intermediate phagosome contains Rab5, but not EEA1. The fusion with the late endosome gives rise to the late phagosome, which has a pH of 5.5, several lysosome-associated membrane proteins, and Rab7 (Flannagan *et al.*, 2009). The fusion event with the lysosome, resulting in the phagolysosome is dependent on Rab7A and the Rab-interacting lysosomal protein (RILP) for bridging the phagosomal membrane to microtubules, necessary for movement within the cell and for membrane extensions (Flannagan *et al.*, 2009). At the final stage, the phagolysosome environment is microbicidal with its acidic pH of 4.5–5, hydrolases (cathepsin D), reactive oxygen and nitrogen species, and antimicrobial peptides (Flannagan *et al.*, 2009); and completely disintegrates the ingested microorganism.

Upon stimulation, macrophages change their morphology and expression of surface molecules, in a process termed *activation* (Mosser and Edwards, 2008). Activated macrophages were originally referred to as classically activated macrophages

(M1) – which exhibit enhanced killing of intracellular microorganisms, secretion of cytokines and expression of co-stimulatory molecules – and alternatively activated macrophages (M2), which participate in tissue repair and produce anti-inflammatory cytokines. More recently a new grouping is suggested, in which macrophages are characterized by the relative exertion of their separate functions of microbicidal activity, tissue repair, anti-inflammatory activity, at the same time emphasizing the plasticity of these categories (Mosser and Edwards, 2008).

Alveolar macrophages, a subset of macrophages, reside in the alveoli of the lung. Alveolar macrophages closely adhere to alveolar epithelial cells, and this contact induces suppression of phagocytosis and cytokine production by integrin-activated transforming growth factor beta (TGF-β) (Lambrecht, 2006). Upon encountering pathogens, integrin expression, and thus TGF-β inhibition, is lost, and macrophages exert innate immune functions. At the same time, inflammatory monocytes are recruited to the alveolar space to help fight infection. Alveolar macrophages also suppress induction of adaptive immunity by alveolar DCs, to which they are in close proximity (Lambrecht, 2006, Marriott and Dockrell, 2007). This regulatory function makes the alveolar macrophage a critically important cell in several diseases, such as asthma, pneumonia, tularemia and particularly tuberculosis (Peters-Golden, 2004).

Four stages of the tuberculosis infection life cycle are distinguished: (1) the early innate immune stage is followed by (2) a dormant stage in granulomas. Certain events facilitate (3) reactivation of TB, leading to the last stage of (4) transmission (Ernst, 2012).

1.1.4 Innate immune stage

The infection starts with inhalation of mycobacteria-containing sputum released by an infected individual. The bacterium is recognised by host pattern recognition receptors (PRRs), namely, Toll-like receptors (TLR), NOD-like receptors, C-type lectin receptors, scavenger receptors, CD14, and also by complement receptors (CR1, CR3, CR4). These receptors bind pathogen associated molecular patterns (PAMPs), such as lipoarabinomannan and its precursor lipomannan, or opsonizing agents on the bacterial surface (Bhatt and Salgame, 2007, Natarajan *et al.*, 2011). TLR2 has the largest number (99) of mycobacterial agonists, and TLR9 senses mycobacterial DNA.

The bacterium is then phagocytosed by alveolar macrophages and lives intracellularly in the phagosome (Ernst, 2012). Opsonisation of bacteria by complement

component C3 and surfactant proteins enhances uptake (Kaufmann and Rubin, 2008). The *Mycobacterium* has a complex cell wall, which is instrumental in manipulation of host immunity such that the bacterium is able to avoid innate antimicrobial defense mechanisms of the macrophage and find a safe niche in the phagosome for intracellular growth (Kaufmann and Rubin, 2008).

The bacterium thus survives, reproduces, and modulates trafficking and maturation of phagosomes in which it resides (Ernst, 2012). It also enhances phagosome fusion with early endosomes, possibly providing access to host nutrients and secreted glycoproteins (Vergne *et al.*, 2004). On the other hand, mycobacteria prevent fusion of the phagosome with the lysosome (Ernst, 2012), by suppressing actin assembly and the recruitment of sorting proteins, thus avoiding the acidic pH (4.8) and host effector molecules of this organelle. Products of the phosphatidylinositol-3 (PI3) kinases have been shown to be involved in endosomal trafficking. Recruit of PI3 kinases is dependent on Rab5, to generate PI3 phosphate on endosomal membranes. These in turn bind to proteins, including EEA1, which are required for the membrane fusion. Retention of EEA1 among others is inhibited by mycobacteria, thus blocking lysosomal fusion of mycobacterial phagosomes (Houben *et al.*, 2006). This blocking is achieved possibly through inhibition of Ca^{2+} signalling, and secretion of SapM, an acid phosphatase and protein kinase G, and the mycobacterial cell wall lipids, such as mannose-capped lipoarabinomannan, which may be competing with PI3 phosphates (Houben *et al.*, 2006). The bacterial cell wall provides further defense, and the production of enzymes counteract host effector molecules (Apt and Kondratieva, 2008). The bacterium can also be found in the cytosol, however, it remains to be determined whether this is a strategy used by it to avoid the hostile environment, and enable faster replication and access to nutrients in the cytosol, or whether it is only a consequence of membrane lysis during cell death induced by it (Welin and Lerm, 2012).

Proinflammatory signalling through the inflammasome, a multiprotein complex, results in production and cleavage of pro-interleukin-1β (pro-IL-1β) and release of the mature cytokine. IL-1β receptor signalling, together with IFN-γ and tumour necrosis factor alpha (TNF-α), improve phagosomal maturation (Flannagan *et al.*, 2009). On the other hand, IL-10 attenuates phagosomal maturation.

Ligand binding by PRRs triggers a signalling cascade, which leads to the nuclear translocation of NF-kB and the induction of proinflammatory cytokines (IL-1-α, IL-1β, and IL-18) and chemokines (chemokine (C-C motif) ligand 2 (CCL2),

chemokine (C-X-C motif) ligand 10 (CXCL10)). It has been shown that IL-1β is important for upregulating mediators for the control of TB infection (Sasindran and Torrelles, 2011), and IL-1 receptor signalling is required for the innate response to *M. tuberculosis* (Fremond *et al.*, 2007). Moreover, these steps are crucial in initiating the adaptive immune response (Natarajan *et al.*, 2011). IL-1β augments TNF signalling by upregulating TNF receptor 1 expression (Jayaraman *et al.*, 2013). TNF-α facilitates the subsequent cell migration and activation of macrophages, and also induces apoptosis, which is found to be essential for host resistance to infection (Rodrigues *et al.*, 2013, Apt and Kondratieva, 2008). The process of efferocytosis, re-uptake of apoptotic vesicles containing mycobacteria, is also an efficient clearance mechanism (Jayaraman *et al.*, 2013). IL-12, IL-23, IL-27 are also important for inducing naive T cells toward T_H1 (T helper cell type 1) differentiation, which in turn activate infected macrophages.

1.1.5 Immunological equilibrium

In response to chemokine secretion, neutrophils, followed by mononuclear phagocytes, migrate to the site of infection. Mycobacteria inhibit host apoptosis as it is toxic to them, and this inhibition also provides time for proliferation before release. Instead, the mycobacterial type VII secretion system promotes necrosis of infected cells, and the recruitment of macrophages (Ernst, 2012). This allows the bacteria to infect recruited cells, and expand its population. Recruited phagocytes differentiate into macrophages and take up bacteria released by the initially infected macrophages. These cells form the core of the developing *granuloma* (Ramakrishnan, 2012). Granulomas are a collection of cells formed by Type 4 (delayed type) hypersensitivity responses (Kaufmann and Rubin, 2008). This cell-mediated response, initiated by $CD4^+$ T cells, restricts infection dissemination and inhibits bacterial growth by subjecting mycobacteria to stress, starvation, reactive oxygen and nitrogen intermediates, hypoxia, and by forming the battlefield for protective immunity (Huynh *et al.*, 2011). However, granuloma formation also compromises the respiratory capacity of the lung (Apt and Kondratieva, 2008). The core of the granuloma is surrounded by foamy macrophages that contain fatty vacuoles which may serve as lipid source for mycobacteria. Core cells express chemokine ligands of the CXCR3 receptor (CXCL9, CXCL10, and CXCL11). These mobilize lymphocytes, first natural killer T (NKT) cells, then $CD4^+$, $CD8^+$, γδ T cells, and B cells, which surround the macrophage core. The central zone is gradually necrotized (Apt and Kondratieva, 2008).

Evidence suggests that the most important component of protective immunity is the recognition of mycobacterial proteins (peptides) presented on macrophages by MHC (major histocompatibility complex) class II molecules to $CD4^+$ T cells. Upon antigen recognition, T cells produce IFN-γ, which induces macrophage mycobactericidal functions (such as the production of bacteriostatic and bactericidal molecules: oxygen and nitrogen radicals), and makes them produce TNF-α, and IL-12, the main inducer of IFN-γ itself (Apt and Kondratieva, 2008). Mycobactericidal function of macrophages is dependent on IFN-γ, initially produced by innate immune cells such as natural killer (NK) cells and later on provided by effector T cells. IFN-γ also promotes phagolysosomal fusion and bacterium killing. IFN-γ induces production of the bactericidal peptide cathelicidin, oxygen and nitrogen radicals, promotes phagolysosomal fusion and *autophagy,* a cytoplasmic, homeostatic process, by which cells break down their components by delivery to lysosomes (Bhatt and Salgame, 2007, Deretic *et al.*, 2009). In this, a portion of cytoplasm is engulfed by the phagophore, a membrane from the endoplasmic reticulum, resulting in the double-membrane structured autophagosome. These fuse with lysosomes, and the resulting autolysosome breaks down the enclosed material (Levine *et al.*, 2011). Autophagy is induced by nutrient starvation through the inhibition of mammalian target of rapamycin (mTOR). Autophagy also has functions in innate and adaptive immunity, and acts as effector during infection (Figure 1-1).

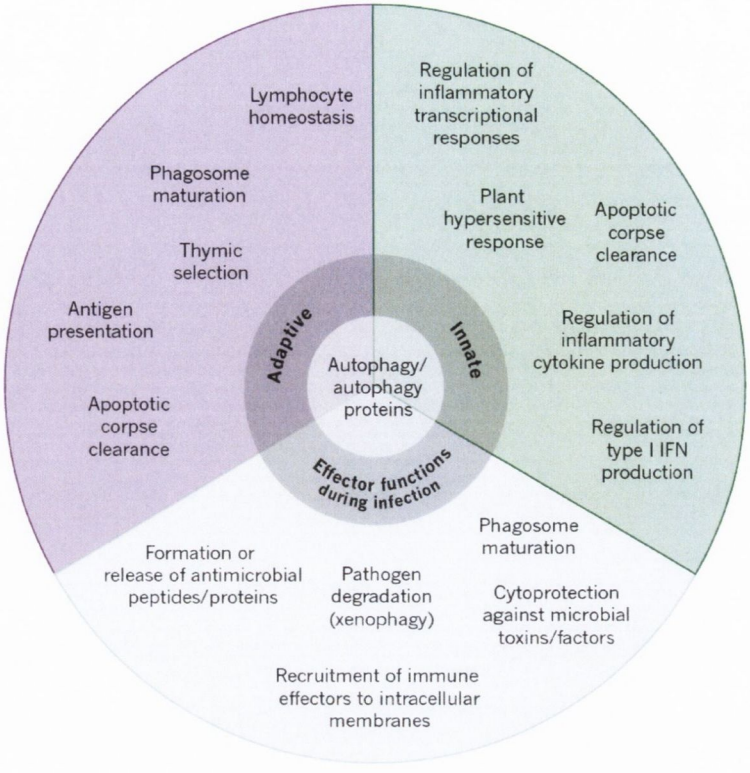

Figure 1-1 | Functions of autophagy in the immune system. Autophagy can be induced by PRRs, IFN-γ, TNF-α, and immunity-related GTPases. Autophagy proteins function in the development and homeostasis of the immune system, in the regulation of innate immune signalling, in antigen presentation, and in inflammation. Source: Levine et al., 2011, *Nature, 469(7330), pp. 323-35.*

Autophagy is stimulated by T_H1 cytokines (TNF-α, IFN-γ), and is inhibited by the T_H2 cytokines (IL-4, IL-13, IL-10). Additionally, vitamin D (via cathelicidin), and TLR-mediated signals can also induce autophagy (Ni Cheallaigh *et al.*, 2011). Autophagy is important in the immune response against *Mycobacterium*; it kills intracellular mycobacteria, enhances antigen presentation and modulates the secretion of important cytokines thus and suppressing damaging inflammation (Castillo *et al.*, 2012). In accordance with this, *Mycobacteria* defend itself with several anti-autophagy factors, such as lipoarabinomannan and Eis (enhanced intracellular survival protein) and ESAT-6, which inhibit autophagy (Bradfute *et al.*, 2013). $CD8^+$ T cells produce the antimicrobial granulysin, which together with perforin forms pores in the macrophage membrane (Apt and Kondratieva, 2008). Recruited DCs also capture the bacteria, undergo maturation, and migrate to the draining lymph nodes. The adaptive immune

response is initiated in the draining lymph nodes wherein naive antigen-specific T cells are primed by DCs to become T_H1 and T_C cell types. However, the transport of bacteria by DCs from lung to lymph nodes, and DC maturation, and thus the initiation of adaptive immune response are delayed by the bacteria (Bhatt and Salgame, 2007). IL-1β release from mycobacteria-infected antigen-presenting cells inhibits DC maturation. Several other mechanisms limit the ability of the adaptive response, such as impaired MHC class II-mediated antigen presentation; induction of the anti-inflammatory lipoxin; restriction by regulatory T cells; downregulation of bacterial antigen gene expression; and resistance to the macrophage-activating effects of IFN-γ (Ernst, 2012).

After TLR2 ligand binding, IL-10 is released during the induction of innate immune response and subsequent T_H1 induction. The anti-inflammatory IL-10 – together with the other discussed cytokines here – appears to play a central role in the outcome of the disease (Redford *et al.*, 2011). The role of IL-10 is to control the magnitude of the T_H1 response by down-regulating antigen-presentation function or inducing T regulatory cells. The strategy on the part of the bacterium may be to induce T_H1 immunity sufficient to controls its replication, but does not to cause its complete eradication. During the early phases of *M. tuberculosis* infection *in vivo,* IL-10 hinders optimum protective immunity (Cyktor *et al.*, 2013), and it blocks phagosome maturation in human macrophages (O'Leary *et al.*, 2011).

1.1.6 Reactivation

Known causes of TB reactivation are $CD4^+$ T cell defects (particularly HIV/AIDS), therapeutic neutralization of TNF (administration of anti-TNF antibodies), and diabetes mellitus. Additional risk factors are treatment with glucocorticoids, thin body habitus, silicosis, haematological malignancies, cancer chemotherapy, uraemia, gastrectomy, and advanced age. However, these account only for a minority of reactivation cases, therefore the 'weakened immune system' model of reactivation needs reconsideration. There are four possible alternative explanations (Ernst, 2012): In the *T cell exhaustion model*, the T cells exhibit inhibitory receptors that prevent their proliferation and ability to mediate effector functions. Another explanation is that *altered bacterial antigen expression profiles* at distinct stages of infection allow bacteria to evade T cell recognition. The *altered cell trafficking model* is based on the idea that the kinetics of cell turnover in granulomas changes over the decades that the

infection can persist. Finally, *bacteria-initiated reactivation* is also a possible explanation.

The activated disease is characterized by shedding of bacteria in respiratory secretions, especially during coughing. A highly contagious form, *cavitary TB,* is characterised by lung tissue destruction and macroscopic open spaces that contain bacilli. This leads to discharge of infectious debris from necrotizing granulomas into the bronchial airways and subsequent airborne transmission between individuals (Ernst, 2012).

1.1.7 Transmission of disease

In experiments with rabbits, only particles containing 1–3 bacteria were infectious, because these remain suspended in the air and reach the alveoli. Heavier particles settle on the mucosal surface, then moved out from the respiratory tract by cilia and swallowed: the mucosal surfaces and the gastrointestinal tract are resistant to tuberculosis (Dannenberg, 2006). Moisture in air helps transmission of bacilli by preventing drying out of infectious particles, meanwhile UV light kills bacteria; thus dark and damp places facilitate spread of disease (Dannenberg, 2006). A small percentage of infected individuals clear infection, likely because of their strong innate immune response. It has been suggested, that the early innate immune response largely determines the outcome of the infection (Subbian *et al.*, 2013). The majority of individuals will induce adaptive immunity, but often this does not clear infection; the individuals remain latently infected, and the disease may reactivate later (Bhatt and Salgame, 2007). It has been confirmed that TB can reactivate after more than 30 years of latent infection in humans (Lillebaek *et al.*, 2002). TB patients with a weak adaptive immune response will develop *miliary TB,* a disseminated form of the disease, meanwhile an excessively strong adaptive response will cause *caseous pneumonia*, both fatal conditions (Apt and Kondratieva, 2008). Individuals with low innate immune activity will develop primary tuberculosis upon the first infection (Bhatt and Salgame, 2007).

1.1.8 Genetics and gene regulation of mycobacterial infections

Host genetics partly explains differences in susceptibility for TB. Studying the genetic background responsible for this complex polygenic quantitative trait is a promising area for research. *Quantitative trait loci* (QTLs) of TB susceptibility are

regions of the genome which are responsible for the variation in susceptibility. Genome-wide approaches to identify these QTLs include *genome-wide association studies* (GWAS), which identified associations with genes primarily in innate immunity pathways (e.g. *TNF, IL10,* IL1R agonist, *TLR8). Genome-wide siRNA screens* have also identified roles for specific kinases, autophagy, IFN-γ and TGF-β in regulating *M. tuberculosis* survival in human macrophages (Ottenhoff, 2012). There are several other known genes responsible for susceptibility including genes encoding macrophage receptors, soluble C-type lectins, and other molecules of innate immunity, such as inducible nitric oxide synthase (iNOS) (Azad *et al.*, 2012). Host *epigenomic profiling* uncovers epigenetic regulation of genes. There is a limited number of studies on TB-specific epigenetic changes. In a recent work with bacille Calmette-Guérin (BCG) vaccination, increased histone methylation was shown in monocytes, and this is thought to be responsible for the long-term modulation of cytokine production (Kleinnijenhuis *et al.*, 2012).

Transcriptional profiling studies have uncovered the change in expression of several thousand mRNA transcripts in monocyte-derived macrophages challenged *in vitro* with live *M. bovis* (Magee *et al.*, 2012) and its purified protein derivative (PPD) (Taraktsoglou *et al.*, 2011). In the most recent analysis, using RNA sequencing, 2,584 genes were found differentially expressed, which were found to be involved in immunity, apoptosis, cell signalling (Nalpas *et al.*, 2013). In primary bovine alveolar macrophages, significant changes were found four hours after infection with *M. bovis.* Members of the TNF/NFκB signalling pathway were found to be involved, together with the upregulation of a number of genes transcribed by NFκB, ten chemokines and genes involved in apoptosis and the MHC I antigen processing pathway (Widdison *et al.*, 2011). More recently, however, it has emerged that a new layer of regulation, microRNAs, may play a critical role in regulating the host responses to TB.

1.2 MicroRNAs

1.2.1 Biogenesis and function in gene expression regulation

MicroRNAs (miRNAs) are a ≈22 nucleotide (nt) long subset of non-coding RNAs, which post-transcriptionally regulate gene expression by pairing with target mRNAs and preventing translation or causing mRNA degradation. The miRNAs are transcribed by RNA Polymerase II or III as pri-miRNAs in the nucleus (Figure 1-2), and then processed into pre-miRNAs by the Microprocessor multiprotein complex, which is made up by Drosha (an RNase III enzyme family member), and the cofactor DiGeorge Syndrome Critical Region 8 (DGCR8/Pasha), which contains a double-stranded RNA-binding domain. After export to the cytoplasm by exportin 5, the last step is the formation of a mature 22 nt duplex by Dicer. The duplex, together with trans-activation responsive RNA-binding protein 2 (TARBP2) and Argonaute (AGO), form a complex which triggers the assembly of the RNA-induced silencing complex (RISC). One miRNA strand is then incorporated into the RISC, and guides it to its target mRNA via base-pairing (Winter *et al.*, 2009, Holley and Topkara, 2011). Perfect pairing facilitates endonucleolytic cleavage of target mRNA. In the case of imperfect pairing, the *seed region* (nucleotides 2–7 at the 5' end) usually perfectly pairs, but other types of pairing have also been observed. This results in translation inhibition, mRNA destabilization, and eventual degradation (Krol *et al.*, 2010).

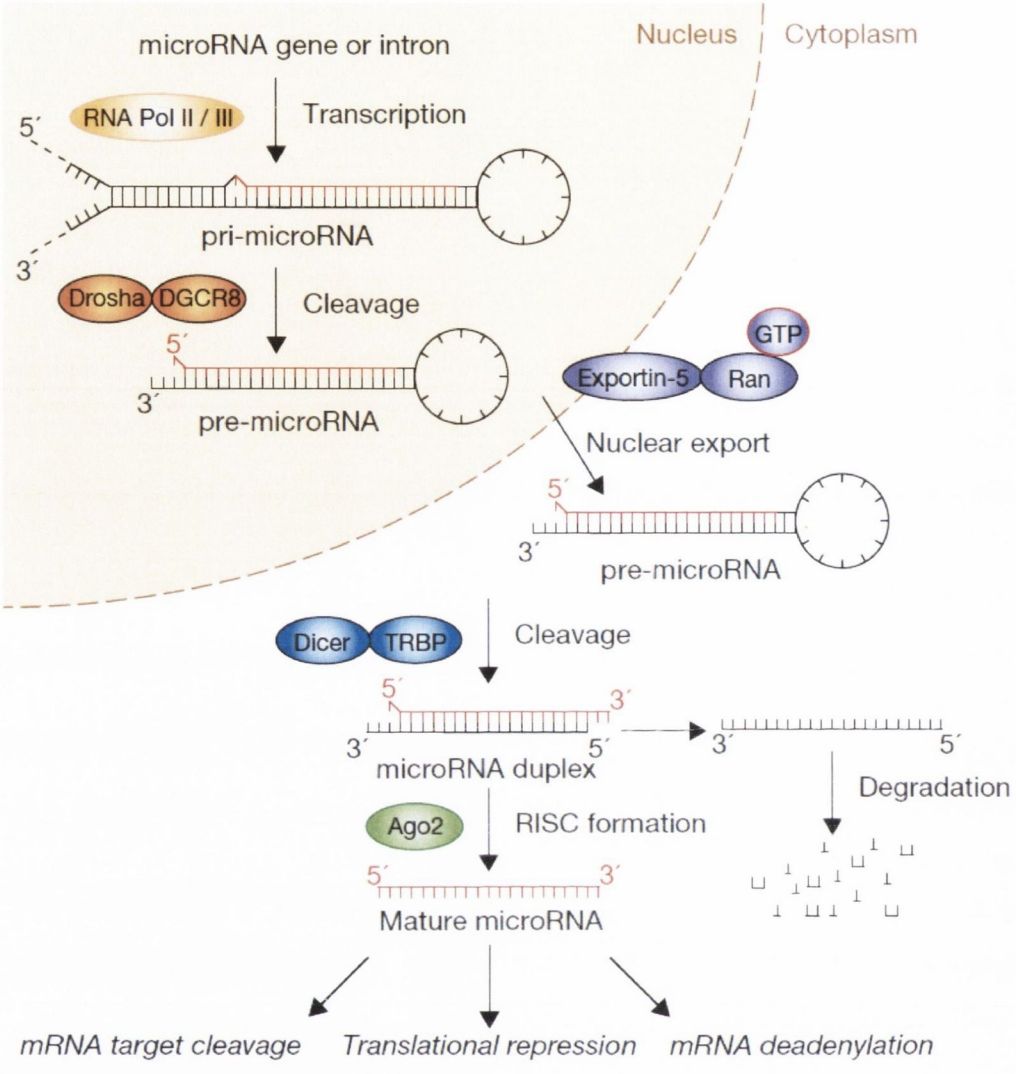

Figure 1-2 | The standard pathway of miRNA processing. The production of the primary miRNA transcript (pri-microRNA) is followed by cleavage of by the microprocessor complex Drosha–DGCR8 (Pasha) in the nucleus. The resulting precursor (pre-microRNA) is exported from the nucleus and then further cleaved in the cytoplasm. The functional strand of the mature miRNA is then loaded into the RNA-induced silencing complex (RISC), where it guides RISC to silence target mRNAs. Source: Winter et al., 2009, *Nature Cell Biology, 11(3), pp. 228-34.*

Mature miRNA originating from the 5' end of the pre-miRNA is marked with the -5p suffix, and likewise, the strand from the 3' end is noted with the -3p suffix (e.g. miR-21-3p). This notation replaced the old nomenclature, where the degraded strand

was marked with an asterisk (e.g. miR-21*). MicroRNAs are grouped by their location in the genome, or by similarity to each other: miRNAs on a single polycistronic transcript are in the same *cluster,* and miRNAs with sequence similarity across the whole hairpin precursor are in the same *family* (Tanzer and Stadler, 2004). Mature miRNAs which are encoded by the same gene but which differ by a few nucleotides are called *isomiRs*. These variants arise from imprecise cleavage, exonuclease activity, or addition of bases; and their functional significance is unresolved (Neilsen *et al.*, 2012). Multiple nonstandard methods for miRNA production are known – one of these is the *mirtron* pathway, where short introns are excised by splicing to generate intermediates of the RNA interference pathway, with no cleavage by the microprocessor. These mirtrons function as miRNAs (Curtis *et al.*, 2012).

Gene expression is regulated at each of the many steps of RNA (and protein) production: at the *transcriptional* level, or at the *posttranscriptional* level of mRNA processing, transport and localization, translation, and degradation. miRNAs serve as an additional layer of gene regulation, regulating mRNA translation and/or degradation (Pasquinelli, 2012). Originally, miRNAs were thought to regulate expression primarily via translation inhibition, however, more recently the degradation of target mRNAs has been shown to be primarily responsible for repression in mammals (Huntzinger and Izaurralde, 2011). Additionally, activation of gene expression by miRNAs has also been observed (Huntzinger and Izaurralde, 2011).

Biogenesis of miRNAs is well-controlled. Transcription of miRNAs is regulated through their promoters, and transcription factors (e.g. p53, MYC) and epigenetic controls – miRNAs which reside in introns of other genes usually share the promoter of the gene (Ha and Kim, 2014). Processing in the nucleus by Microprocessor and subsequently by Dicer is regulated by their cofactors and posttranslational modifications (Ha and Kim, 2014). Several factors affect the function of miRNAs, including the location and number of target sites within mRNA 3' UTRs, RNA-binding proteins which interfere with RISC binding, RISC cofactors, and the modification of Argonaute proteins (Pasquinelli, 2012). Presence of target sites can also protect miRNAs from degradation, in a feedback process called *target mediated miRNA protection.* Additionally, during the process of target mimicry, transcripts with target sites for a common miRNA compete for recognition. These *competing endogenous RNAs,* such as mRNAs, long non-coding RNAs (lncRNA), pseudogene transcripts and

independently transcribed UTR regions, can inhibit the activity of specific miRNAs *in vivo* (Pasquinelli, 2012).

1.2.2 MicroRNAs in the immune system

The observation that a given miRNA can have many targets, and similarly, a given mRNA can have several regulator miRNAs, explains how a relatively small number of miRNAs have a huge impact on gene regulation. Indeed, several diseases and conditions are linked to abnormal expression of miRNAs (Bushati and Cohen, 2007, Alvarez-Garcia and Miska, 2005), as they govern most biological processes, such as differentiation, apoptosis, development (Ivey and Srivastava, 2010). There is a growing body of evidence in several species and cell types that miRNAs widely regulate immunity as well (Xiao and Rajewsky, 2009). Haematopoietic stem cell differentiation into common lymphoid progenitor or common myeloid progenitor has been shown to be under the influence of miR-196b, miR-126, miR-221 and miR-222 (O'Connell *et al.*, 2010). Similarly, several miRNAs are involved in the differentiation and function of myeloid and lymphoid cells (O'Connell *et al.*, 2010, Rossi *et al.*, 2011). It has also been shown that miRNAs are expressed in macrophages, for example, miR-155, miR-146, miR-21 (Alam and O'Neill, 2011, Quinn and O'Neill, 2011), and miR-147 (Liu *et al.*, 2009), and govern macrophage functions during inflammation through TLR signalling. Substantial evidence has been accumulated that miRNAs also regulate the autophagy pathway in all five steps of induction, vesicle nucleation and elongation, retrieval, and fusion (Frankel and Lund, 2012).

The involvement of several miRNAs in intracellular bacterial infections is also established (Eulalio *et al.*, 2012). For example, hsa-miR-21 in monocytes is able to alter the outcome of infection with mycobacteria, through regulation of the vitamin D-dependent antimicrobial pathway (Liu *et al.*, 2012). Another example is miR-29, which has been shown to suppress IFN-γ production, and is down-regulated in response to intracellular infection by *Listeria monocytogenes* or *Mycobacterium bovis* (Ma *et al.*, 2011). The role of miRNAs in macrophages is also confirmed in multiple studies, where infection of human macrophages with virulent *M. tuberculosis* resulted in high hsa-miR-125b and low hsa-miR-155 expression when compared to infection with the non-virulent *M. smegmatis,* causing lowered TNF-α production (Tili *et al.*, 2007) (Rajaram *et al.*, 2011). Transfection of mouse macrophages with miR-155 resulted in decreased *M. tuberculosis* survival (Kumar *et al.*, 2012). The antimicrobial activity of

miR-155 possibly acts through the regulation of macrophage apoptosis and autophagy (Mehta and Liu, 2014). Intriguingly, a recent study has also suggested that miRNAs may play a regulatory role in immunity by binding to TLRs *as ligands*, thus triggering inflammatory response (Fabbri *et al.*, 2012).

1.2.3 MicroRNAs in mycobacterial infections

The involvement of miRNA genes in TB is well-established, and there have been multiple studies which have demonstrated that miRNA expression is altered in response to mycobacterial infections (Harapan *et al.*, 2013). These miRNAs target several genes that are important in tuberculosis immunity (Figure 1-3). The examples include miR-29, which is thought to suppress the immune response by down-regulating IFN-γ. Another miRNA, miR-147, which was found to be upregulated in the sputum of tuberculosis patients, is upregulated upon TLR signalling, and suppresses expression of proinflammatory cytokines (e.g. TNF-α, IL-6). The anti-inflammatory miR-21 also appears to be an important player in mycobacterial infections. For example, in *M. leprae* infected monocytes, miR-21 inhibits the expression of two vitamin D dependent antimicrobial peptides (CAMP and DEFB4A), by downregulating IL-1β expression, and indirect upregulation of IL-10 (Singh *et al.*, 2013a).

Similarly to other pathogenic bacteria, miR-155 expression is upregulated upon mycobacterial infection, leading to increased apoptosis of infected cells, and stimulation of TNF-α synthesis. This effect is dependent on the balance between miR-125b and miR-155 levels (Maudet *et al.*, 2014). Another miRNA, miR-142-3p, is downregulated upon *M. bovis* infection, and the de-repression of the target IRAK1 (IL-1 receptor-associated kinase 1) results in the activation of the NF-κB pathway (Xu *et al.*, 2013). In macrophages and DCs, *M. tuberculosis* infection upregulates miR-99b, dampening the inflammatory response. Direct targets of miR-99b are TNF-α and its receptor TNFRSF-4 (TNF receptor superfamily, member 4), and inhibition of this miRNA activates the production of TNF-α, and the inflammatory cytokines IL-6, IL-12 and IL-1β (Maudet *et al.*, 2014). In alveolar macrophages, miR-124 is upregulated in response to *M. bovis* infection, and targets TLR signalling (Ma *et al.*, 2014).

Interestingly, the *Mycobacterium* genome also codes for non-coding RNA, including intergenic small RNA molecules, which are analogous to eukaryotic microRNAs. This network of RNAs provides a level of control of bacterial gene regulation (Arnvig *et al.*, 2011).

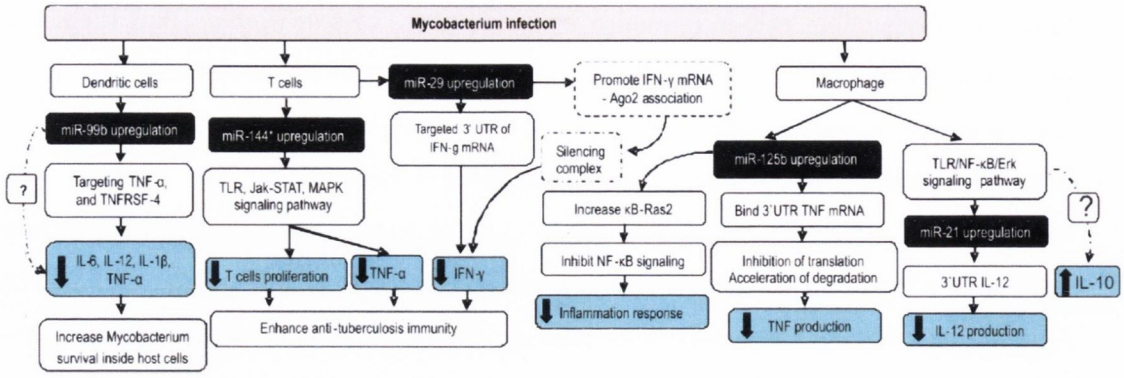

Figure 1-3 | The role of miRNAs in mycobacterial infection. The effect of five miRNAs (miR-99b, miR-144, miR-29, miR-125b, and miR-21) in *Mycobacterium* infections are shown. These upregulated miRNAs help mycobacteria to survive inside host cells, inhibit production of proinflammatory cytokines and induce the anti-inflammatory IL-10. Abbreviations: Ago2: Argonaute 2, Jak-STAT: Janus kinase/signal transducers and activators of transcription, MAPK: mitogen-activated protein kinase, TNFRSF-4: TNF receptor superfamily, member 4. Source: Harapan et al., 2013, *Tuberculosis, 93(6), pp. 596-605.*

1.2.4 MicroRNAs in cattle

Currently, 793 mature miRNAs are annotated in the bovine genome (Kozomara and Griffiths-Jones, 2011). Due to their evolutionarily conserved nature, many miRNAs found in other species, for example, miR-146, or miR-155, can also be found in cattle, however there are also differences. These may be due to better miRNA annotation of better studied species, but genuine differences are present: the human miR-198, for example, which targets the Cyclin T1 gene, a co-factor for HIV-1, has no homolog in the bovine genome (Sung and Rice, 2009).

Research on miRNAs in cattle has focused on tissues relevant to economically important traits: muscle, milk production, immunity. Expression of miRNAs have been confirmed in several bovine tissues: bovine embryo, thymus, small intestine, mesenteric lymph node, abomasum lymph node, monocytes isolated from blood and milk, mammary epithelial cells, mammary tissue, and the MDBK cell line (Jin *et al.*, 2014,

Coutinho *et al.*, 2007, Dilda *et al.*, 2011, Lawless *et al.*, 2013, Lawless *et al.*, 2014, Naeem *et al.*, 2012, Glazov *et al.*, 2009). Multiple studies have examined changes in miRNA expression during bacterial infections causing bovine mastitis, a disease of the mammary gland which causes great losses to the dairy industry. Using RT-qPCR (reverse transcription quantitative PCR), Naeem et al. have found four differentially expressed miRNAs (miR-223, -16a, -31, and -181a) in mammary tissue (Naeem *et al.*, 2012). More recent studies have used high-throughput sequencing to measure transcriptome-wide changes in miRNA expression. For example, Lawless et al. identified twenty-one miRNAs in mammary epithelial cells, in response to *in vitro* challenge with live *Streptococcus uberis* (Lawless *et al.*, 2013). In another study, transcriptome-wide mRNA and miRNA expression at multiple time-points were simultaneously measured in both milk- and blood-isolated $CD14^+$ monocytes infected with *S. uberis* (Lawless *et al.*, 2014). Twenty-six miRNAs and more than 3500 genes were found differentially expressed over the 48 hour time-course.

1.2.5 Application of miRNAs in diagnosis and therapy

MicroRNAs are also being intensively investigated as potential diagnostic or prognostic biomarkers of disease, as they have many properties that make them suitable as non-invasive biomarkers: miRNAs are abundantly expressed, in a stable form and in a range of extracellular fluids, are easily measured, and in many cases exhibit temporal and spatial specificity (Chen *et al.*, 2010, Hata *et al.*, 2010, Kosaka *et al.*, 2010, Kusuda *et al.*, 2011). Moreover, a small numbers of miRNAs can serve as accurate biomarkers. There has been interest in finding biomarkers of tuberculosis in humans. Multiple experiments have been performed on samples, derived from TB patients. One recent study of human tuberculosis patients, for example, has shown that 95 miRNAs are differentially expressed in sputum of infected patients (Yi *et al.*, 2012). To date, three miRNAs have been evaluated for use as biomarkers: miR-155-3p and miR-155-5p in stimulated PBMCs (Wu *et al.*, 2012a), and miR-29a in pooled serum (Fu *et al.*, 2011). In a recent publication, hsa-miR-196b and hsa-miR-376c were identified as potential markers of active TB disease in the serum of patients (Zhang *et al.*, 2014).

In addition to their utility as biomarkers, miRNAs also have significant potential as therapeutic targets or agents. MicroRNA function can be augmented either by over-expression approaches, using miRNA mimics or vector based overexpression, or by inhibition, using miRNA sponges or antimiR oligonucleotides (van Rooij and

Kauppinen, 2014). Several miRNAs are currently in preclinical and clinical trials as novel therapeutics in human cancer, viral infections and cardiovascular disease (van Rooij and Kauppinen, 2014). For example, human miR-122 is being investigated for its therapeutic potential to modulate cholesterol metabolism (Rottiers and Naar, 2012). Moreover, targeting miR-122 with an anti-miR induces antiviral activity against hepatitis C virus, and the clinical utility of this is currently being investigated in Phase II clinical trials (Li *et al.*, 2011b). Similarly, miR-208 has been shown to have an important role in modulating cardiac function and remodelling in humans (van Rooij *et al.*, 2007), and is currently in preclinical trials. Interestingly from an agricultural perspective, this miRNA also has a big impact on metabolism: treatment with anti-miR-208 prevented weight gain in aging mice, by reducing fat weight (Grueter *et al.*, 2012).

The miRNAs with therapeutic potential mentioned above have orthologs in cattle, and these examples suggest that miRNA-based therapeutic strategies may be used to combat disease and regulate metabolism in cattle in order to influence important economic traits, such as growth, feed efficiency, or milk production. Although the cost of miRNA therapy and the large size of animals may prevent agricultural use, bovine research models still could be valuable, as the evolutionarily conserved nature of miRNAs facilitates translation of research to human application (van Rooij and Kauppinen, 2014).

1.3 Transcriptomics

Transcriptomics is the study of the *transciptome*, the complete set of transcripts (i.e. all RNA molecules) in a population of cells (Wang *et al.*, 2009). The main aims of transcriptomics are finding and classifying all RNA types, determining the structure of RNAs, including post-transcriptional modifications, and quantifying the expression levels of each transcript in different cells and conditions. Methods for studying the transcriptome are Sanger sequencing, RT-qPCR, DNA microarrays; and in the following we discuss in detail the more recent high-throughput sequencing technology, which is used in this research project.

1.3.1 Next-generation sequencing

A recent sequencing technology, called *next-generation sequencing* (NGS), makes it possible to sequence whole genomes or transcriptomes of multiple samples in

a short time. Currently, several synonyms are used in the literature; NGS is also called *second-generation sequencing* or *high-throughput sequencing* technology. The term *digital gene expression* refers to that the unique sequences (tags) are counted: each is assigned a number expressing how many identical copies were sequenced. *Deep sequencing* refers to the increased sequencing depth (i.e. the average number a nucleotide in the sample is sequenced), an important additional advantage, which allows relative expression profiling. When applied to RNA sequencing, the term *RNA-seq* or *whole transcriptome shotgun sequencing* is used.

The first papers using RNA-seq appeared in 2008, which established several advantages of this technology, including a better picture of transcription than was possible before (Blair, 2013). Marioni et al. performed differential expression analysis with RNA-seq, and the high technical reproducibility of this technology was established (Marioni *et al.*, 2008). New applications of RNA-seq are being continuously developed and techniques to identify splice variants, strand specific analysis, small RNA-seq are now all available. In 2009, RNA-seq analyses on single embryonic cells were published (Tang *et al.*, 2009). Developments in bioinformatics analysis of data paralleled these advancements. TopHat, an important program which aligns reads to a reference genome, was published in 2009 (Trapnell *et al.*, 2009). Reference-free transcriptome assembly software, Trans-ABySS, Oases, and Trinity, were published in 2010 (Blair, 2013). The same year, widely-used differential expression analysis tools, DEseq (Anders and Huber, 2010), and edgeR (Robinson *et al.*, 2010) were published.

There are several advantages of using NGS over microarrays, the other technology that is often applied to miRNA profiling. Advantages of an RNA-seq based approach include the ability to accurately measure the expression of all miRNAs simultaneously, with single-nucleotide resolution and across the broad dynamic range of expression. Moreover, as prior knowledge of the sequences is not needed, RNA-seq has the ability to identify the expression of new miRNAs as well as known ones, and to discriminate between miRNA isoforms known as isomiRs (Wang *et al.*, 2009, Illumina, 2011). Furthermore, RNA-seq is also highly reproducible with little technical variation (Marioni *et al.*, 2008). RNA-seq results have also been found to be highly correlated to RT-qPCR results (Pradervand *et al.*, 2010). An additional advantage is that the sequencing data can be reanalysed as novel miRNAs are discovered and published (Marioni *et al.*, 2008, Illumina, 2011). Disadvantages of RNA-seq are the high cost, the requirement of bioinformatics knowledge, and of infrastructure for analysing data.

RNA-seq being a new technology, it also suffers from lack of standards and knowledge for analysing and publishing data. Additionally, not all biases introduced by this technique are known. The use of different adapters and barcodes during ligation, and the complex RNA structures and modifications drastically influence cDNA synthesis efficacies and are sources of bias. In addition, polymerase chain reaction amplification efficiency depends on G/C-content of RNA (Raabe *et al.*, 2014).

Currently several NGS platforms exist, developed by Illumina, 454 Life Sciences, Life Technologies, Pacific Biosciences and Oxford Nanopore Technologies. Of these, the Illumina NGS technology is used in the project as it is the most established and most widely used technology. Firstly, NGS libraries are prepared from the RNA samples: adapter sequences are attached to both ends of miRNAs (and small RNAs). This is followed by PCR amplification and acrylamide gel purification. Before sequencing, the prepared libraries are immobilized on a flow cell. In a process called cluster generation, many copies (up to 1000) are created of each sample molecule. A final density of ten million clusters per square centimetre is reached. The *sequencing by synthesis* technology uses four fluorescently labelled nucleotides to sequence the clusters on the flow cell surface. Samples are sequenced simultaneously: each sequencing cycle adds a labelled deoxynucleoside triphosphate (dNTP), which prevents further polymerization. Base calls are made directly from the fluorescent signal intensity measurements during each cycle, and enzymatic cleavage of the dye allows incorporation of the next nucleotide (Illumina, 2010). Finally, we get a sequence read for each cluster, supplied in a text file.

1.3.2 Bioinformatics

The sequencing output text file is in FASTQ format (Figure 1-4). In this format, each sequence tag (read) is described in four lines. The title line, marked with '@', contains information on the sequence. The second line is the actual sequence, followed by a separator line. The last line gives quality scores for each base, coded as characters (Cock *et al.*, 2010), as illustrated in Figure 1-4.

1) @DJDP4KN1:68:D0GGHACXX:3:1101:7177:2235 1:N:0:CGATGT

2) TTCACAGTGGCTAAGTTCCGAGATCGGAAGAGCACACGTCTGAACTCCAG

3) +

4) 1?:=ABDBFHHGGIJIJIJGHIIDGIIEGHEHIJJ)?@FDHIEHIIII=C

Figure 1-4 | The FASTQ format. The FASTQ format describes each sequence tag (read) in four lines. The title line (1), marked with '@', contains the following information on the sequence, with the categories separated by a colon: the unique instrument identifier, run and flowcell ids, flowcell lane number, tile number within the flowcell lane, 'x' and 'y' coordinates of the cluster within the tile, the member of a pair (value is '1' for single reads), whether read fails filter (Y = yes, N = no), control bits (0 = off), index sequence. The second line (2) is the actual sequence, followed by a separator line (3). The last line (4) gives quality scores for each base, coded as characters. The example miRNA *(bta-mir-27a)* sequence is underlined (red), and the remaining part is adapter sequence (blue).

The adapter sequence contains a six-nucleotide-long index *(barcode)* sequence, which allows sequencing multiple samples on the same flowcell lane *(multiplexing)*: the reads can be grouped by their different barcodes corresponding to each sample. The reads are supplied by the sequencing provider with their 5' adapters already trimmed. As the sequencing length is 50 basepair (bp), and miRNAs are usually 21 nt long, that means part of all reads contain adapter sequences. In the case of miRNA analysis, the reads are therefore subjected to adapter trimming and quality control steps, using Cutadapt (Martin, 2011) and the FASTX Toolkit. The reads are then aligned to the reference bovine genome (UMD3.1) (Zimin *et al.*, 2009), or another reference database (e.g. miRBase), using Novoalign (Novocraft Technologies). HTSeq (Anders *et al.*, 2015) is used to count aligned reads overlapping known miRNA genes. The analysis parameters are given in the 'Materials and Methods' sections in each Chapter. A similar analysis pipeline is followed for analysing mRNA reads, as described in CHAPTER 4.

One possible problem is the alignment of these short miRNA sequences to the genome. As an alternative, alignment to a miRNA-only database (such as miRBase) avoids this issue. An additional problem is that miRNAs from the 3' and 5' arms cannot be distinguished if the strand-information is not preserved during library preparation

and sequencing. In some cases, miRNAs can be transcribed from either strand of DNA, therefore miRNA annotations may overlap, and this results in ambiguous alignments, which are discarded.

The outcome of this analysis is a table of count numbers for each feature (gene) of each sample. The numbers of sequencing reads for each feature are then compared across groups. The data is normalised in two ways during analysis. Firstly, all libraries (samples) will have different count numbers, therefore a correction for this sequencing depth is needed. Secondly, RNA-seq provides a measure of relative abundance of each gene in each sample, but does not provide measure on total RNA output (Robinson and Oshlack, 2010). If one or more genes are very highly expressed in a particular sample, but not in the other samples, then the other genes will be under-sampled in that sample. This *RNA composition effect* must be adjusted for, or else the other genes may falsely appear downregulated in that sample. Multiple normalization methods exist, of which the TMM (trimmed mean of M-values) is the default in edgeR for mRNA analysis, and the quantile normalization is recommended for miRNA analysis (Garmire and Subramaniam, 2012). Gene length and GC content for each gene do not change from sample to sample, therefore it can be expected to have little effect on differential expression analyses. Data can also be analysed to compare relative abundance of isomiRs. In addition to analysis of known miRNAs, another line of investigation may be discovery of new genes from the sequencing data.

There are multiple software packages facilitating statistical tests to identify significantly differentially expressed miRNAs, such as DEseq or edgeR. These model the count data using the negative binomial distribution, and test differential expression between two experimental conditions. One test is performed for each gene, therefore correction for multiple testing is necessary, for example with the Benjamini-Hochberg method (Benjamini and Hochberg, 1995). For the discovery of new miRNAs, miRDeep is used. Details and parameters used are described in the Materials and Methods sections in each Chapter.

1.4 Thesis hypothesis, aim, and specific objectives

Research in other species has proved the involvement of miRNA regulation of gene expression in multiple host cell types, in response to TB. However, the understanding of this in alveolar macrophages, the primary host for *Mycobacterium,* is limited, and transcriptome-wide NGS experiments have not been carried out to date.

The primary goal of the thesis project is to investigate the role that microRNAs play in the regulation of the alveolar macrophage response to bovine tuberculosis. The underlying **hypothesis** of our work was that miRNAs are important regulators in bovine alveolar macrophages during their encounter with *Mycobacterium bovis*.

Our **aim** was to uncover both new insights into the regulatory role miRNAs play in *M. bovis* infection as well as to identify potential biomarkers of bovine TB.

Our specific **objectives** were to:

1. Set up and verify a protocol for isolating and sequencing miRNAs from alveolar macrophages, and establish the miRNA profile of unchallenged alveolar macrophages. This is described in CHAPTER 2.
2. Sequence miRNAs at four time-points in *M. bovis* infected and control alveolar macrophage cells to identify the miRNAs that are differentially expressed in response to infection, using a next-generation sequencing based approach, their differentially expressed target genes and the pathways and cellular processes that are involved in the response (CHAPTER 3).
3. Functionally characterise at least one of the miRNAs that are identified as being important regulators of the host response to *M. bovis* (CHAPTERS 3 and 4).
4. Investigate miRNA expression in peripheral blood mononuclear cells (PBMCs) in healthy and TB infected cattle, using a transcriptome-wide approach (CHAPTER 5).

CHAPTER 2

PROFILING MICRORNA EXPRESSION IN BOVINE ALVEOLAR MACROPHAGES USING RNA-SEQ

2.1 Introduction

MicroRNAs are an approximately 22 nucleotide long subset of non-coding RNAs, which post-transcriptionally regulate gene expression by base-pairing with target messenger RNAs (mRNAs). miRNAs are transcribed as pri-miRNAs in the nucleus and are then processed into pre-miRNAs. After export to the cytoplasm, a mature 22 nt duplex is formed. One miRNA strand is then incorporated into the RNA-induced silencing complex, and interacts with its target mRNA via base-pairing at binding sites usually located within 3' UTRs, meanwhile the other strand is usually degraded (Holley and Topkara, 2011). Depending on the level of miRNA-mRNA complementarity, the target mRNA can be degraded or its translation repressed (Bartel, 2009). Several diseases and conditions, such as cancer, cardiovascular disease, or autoimmune disease, have been linked to abnormal expression of miRNAs (Bushati and Cohen, 2007, Alvarez-Garcia and Miska, 2005), as they have a regulatory role in most biological processes, such as differentiation, apoptosis, and development (Xiao and Rajewsky, 2009, Ivey and Srivastava, 2010, O'Connell *et al.*, 2010).

It is also becoming increasingly clear that both adaptive and innate immunity are finely regulated by miRNAs. In the adaptive immune system, the differentiation of B cells, antibody generation, and T cell development and function, are all influenced by miRNAs (Belver *et al.*, 2011). Innate immune cell activation is also regulated by miRNAs, including miR-155, miR-146a, miR-21, and miR-9 (Gantier, 2010). For example, miR-155 is a positive regulator of TLR signalling, and is induced upon stimulation of murine macrophages with IFN-β or TLR ligands (Liston *et al.*, 2010, O'Connell *et al.*, 2007).

Furthermore, TNF biosynthesis has been shown to be inhibited by *Mycobacterium tuberculosis,* an intracellular mycobacterial pathogen that infects alveolar macrophages, by regulating levels of a human macrophage miRNA, miR-125b (Rajaram *et al.*, 2011). Alveolar macrophages have important roles in lung homeostasis and in many respiratory diseases, such as asthma in humans (Peters-Golden, 2004), and are the first cells to encounter several respiratory pathogens during the early stages of infection (Lambrecht, 2006, Marriott and Dockrell, 2007). In cattle, bovine alveolar macrophages (AMs) are the major target cell type infected by *M. bovis*, the causative agent of bovine tuberculosis (Pollock *et al.*, 2006), which results in losses of approximately US$3 billion to global agriculture annually (Garnier *et al.*, 2003).

Currently, 755 bovine miRNAs are annotated in miRBase (version 19, http://www.mirbase.org) (Kozomara and Griffiths-Jones, 2011), of which only 22 have been shown to be expressed in bovine AMs (Xu *et al.*, 2009). In this study, we present the first next-generation sequencing approach to profile miRNA expression in unchallenged bovine AMs, providing an important reference atlas for further elucidating the role miRNAs play in regulating immune networks in this important immune cell type.

2.2 Materials and methods

2.2.1 Ethics statement

All animal procedures were performed according to the provisions of the Irish Cruelty to Animals Act, and ethical approval for the study was obtained from the University College Dublin (UCD) Animal Ethics Committee (protocol number AREC-13-14-Gordon).

2.2.2 Animals

Eight unrelated Holstein-Friesian male calves (aged between 7-12 weeks old) were used in this study. All animals were maintained under uniform housing conditions and nutritional regimens at the UCD Lyons Research Farm (Newcastle, County Kildare, Ireland). The animals were selected from a herd without a recent history of bovine tuberculosis infection.

2.2.3 Lung lavages, alveolar cell preparation and storage

AMs were harvested by pulmonary lavage of lungs obtained post-mortem from eight animals. Lungs were washed using a total of 3 l of calcium- and magnesium-free sterile Hank's Balanced Salt Solution (HBSS, Invitrogen, Life Technologies Ltd., Paisley, UK); HBSS was infused into the lungs (500 ml per infusion) via the trachea. After each 500 ml infusion of HBSS, the lungs were gently massaged and resulting HBSS-cell suspension was collected into sterile beakers. All lung washes were performed in a laminar flow hood.

50 ml of HBSS-cell suspension collected from the first 500 ml wash was centrifuged (200 × g for 10 min at room temperature) and the resulting cell pellet was resuspended in 10 ml HBSS and screened for microbial contamination by incubation on

agar plates using the following conditions: Columbia blood agar with 5% defibrinated sheep blood (aerobic and CO_2-enriched atmosphere, 37°C, 36 h); Chocolate agar (CO_2-enriched atmosphere, 37°C, 36 h); Columbia-colistin-nalidixic acid agar (aerobic, 37°C, 36 h); MacConkey agar number 2 (aerobic, 37°C 36 h); Sabouraud dextrose agar (aerobic, 37°C, 5 days); and Mycoplasma agar (CO_2-enriched atmosphere, 14 days). All media was obtained from Oxoid Ltd. (Basingstoke, Hampshire, UK). All animals were negative for microbial contamination.

The remaining HBSS-cell suspension (~2 l) was transferred to 50 ml sterile tubes and centrifuged (200 × g for 10 min at room temperature). After centrifugation, the supernatants were discarded and the resulting cell pellets were pooled and resuspended in 50 ml cold R10 media (RPMI 1640 medium [Invitrogen], supplemented with 10% fetal bovine serum [FBS; Sigma-Aldrich, Dublin, Ireland], 2.5 μg/ml amphotericin B [Sigma-Aldrich], 2 mM L-glutamine [Sigma-Aldrich]). The cell suspension was repelleted (200 × g for 10 min at room temperature) and resuspended in 10 ml $R10^+$ media (RPMI 1640 medium supplemented with 10% FBS, 2.5 μg/ml amphotericin B, 2 mM L-glutamine, 100 ug/ml ampicillin [Sigma-Aldrich] and 25 ug/ml gentamycin [Sigma-Aldrich]). Cells were then counted using a haemocytometer, recentrifuged at 200 × g for 10 min and re-suspended in freezing solution (10% DMSO [Sigma-Aldrich], 90% FBS) at a density of 2.5×10^7 cell/ml. 1 ml cell aliquots were made in 2 ml sterile cryovials (Sarstedt Ltd., Wexford, Ireland) and placed into Mr. Frosty Cryo 1°C Freezing Containers (Nalgene, Thermo Fisher Scientific, Waltham, MA, USA) containing 100% isopropanol. Cryovials were stored at −80°C for a period of 18 h after which they were removed from the freezing containers and transferred to −140°C storage conditions until required for further use.

2.2.4 Alveolar cell culture

Cells were thawed and incubated in a 175 cm^2 flask (Cellstar, Greiner Bio-One Ltd., Stonehouse, UK) in $R10^+$ media for 24 h at 37°C, 5% CO_2. After incubation, media was removed together with non adherent cells, and replaced with HBSS. After removing HBSS, adherent cells were dissociated with 15 ml 1× non-enzymatic cell dissociation solution (Sigma-Aldrich). Collected cells were pelleted at 400 × g for 5 min, then resuspended in 10 ml sterile PBS (Invitrogen). Cells were counted with a haemocytometer (BRAND, Wertheim, Germany), and then 4×10^6 cells were pelleted

and lysed for each RNA extraction, except for sample BAM-8 which had a cell count of 0.8×10^6.

2.2.5 Small RNA

In total, eight RNA-seq libraries were prepared for sequencing. Eight small and total RNA fractions were prepared from the pelleted cells, using the RNeasy Plus Mini kit and RNeasy MinElute Cleanup Kit (Qiagen Ltd., Manchester, UK), according to the appendix E part of the manufacturer's protocol. The quality and quantity of the prepared total and small RNA were assessed using an Agilent 2100 Bioanalyzer (Agilent Technologies Ireland Ltd., Cork, Ireland) with the 6000 Nano and small RNA LabChip kits (Agilent Technologies). For the Bioanalyzer data, please see Appendix 1. Total RNA had RNA Integrity Number (RIN) values of 9.4–9.8 and 28S/18S rRNA ratios of 1.5–1.9. Small RNA concentrations were 10,000–25,000 pg/µl, and miRNA concentrations were ≈ 660–1900 pg/µl (Table 2-1). Samples were stored at −80°C until further use.

2.2.6 RNA-seq libraries

Illumina RNA-seq libraries were prepared with the Epicentre Scriptminer multiplex kit (Epicentre Biotechnologies, Illumina Inc., Madison, WI, USA), according to the manufacturer's protocol, using 8 µl of the prepared small RNA. The Epicentre FailSafe Enzyme mix was used in the PCR amplification step, and Epicentre RNA-Seq barcode primers (Epicentre Biotechnologies) were used for indexing. Libraries were sequenced (50 bp single-end) on one lane with an Illumina HiSeq 2000 machine (Norwegian Sequencing Centre, Oslo, Norway).

2.2.7 Analysis of RNA-seq data

The quality and number of the reads for each sample were assessed using FASTQC v0.10.0 (http://www.bioinformatics.bbsrc.ac.uk/projects/fastqc/). For the FASTQC results, please see Electronic Appendix 1. Cutadapt v1.0 (http://code.google.com/p/cutadapt/) was used to trim 3' Illumina adapter sequences from reads. Reads which were less than 18 nt after trimming and all untrimmed reads were discarded. The remaining reads were then further filtered using FASTQ Quality Filter (FASTX Toolkit v0.0.13; http://hannonlab.cshl.edu/fastx_toolkit/). Reads where at least 50% of the bases had a Phred score < 20 were removed. Finally, reads passing

all the above filters were also trimmed at their ends using FASTQ Quality Trimmer (FASTX Toolkit v0.0.13) to remove low quality bases (Phred score < 20), and reads less than 18 nt after the trimming were discarded.

Reads which passed all quality control steps were aligned to the bovine genome (UMD3.1 assembly (Zimin *et al.*, 2009)) using Novoalign (Novocraft Technologies, version 2.07.11) in 'miRNA' mode. HTSeq-count (part of the HTSeq framework, version 0.5.3p3) in 'union' mode was then used to count aligned reads that overlapped with known miRNA gene annotation from Ensembl version 66 (www.ensembl.org). To investigate the proportion of reads sequenced from non-miRNA genes, HTSeq-count was also separately used to count aligned reads that overlapped with all bovine gene annotations from Ensembl. A graphical depiction of the analysis pipeline is shown in Figure 2-1.

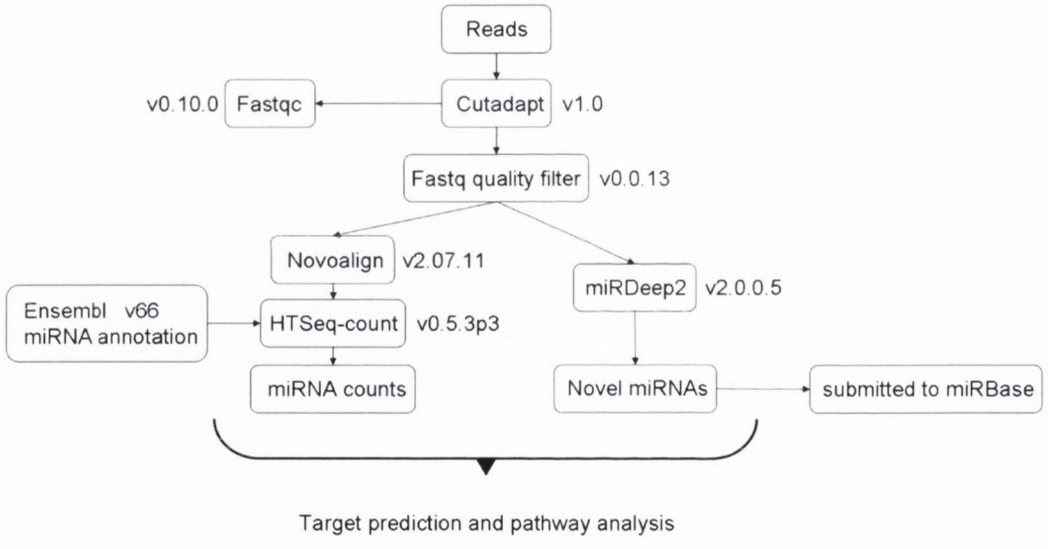

Figure 2-1 | Bioinformatics analysis pipeline overview.

miRDeep2 (version 2.0.0.5) (Friedlander *et al.*, 2008) was used to identify potentially novel miRNAs from the data. The predicted novel miRNAs that were independently predicted in at least three samples and fulfilled all of the following criteria were submitted to miRBase: both the mature and star strand had a minimum five reads each; the predicted miRNA had a high (> 90%) probability of being a true miRNA by miRDeep2; the hairpin structure had a RandFold p-value < 0.05. Customised Perl scripts were also written in house to examine the miRDeep2 output for

the presence of miRNA isomiRs as described recently by us (Lawless *et al.*, 2013). The Perl code is available upon request from the authors.

Target genes that are potentially regulated by expressed miRNAs were predicted using the consensus of two computational approaches, miRanda v3.3a (Betel *et al.*, 2008) and TargetScan v6.2 (Lewis *et al.*, 2005, Grimson *et al.*, 2007, Friedman *et al.*, 2009). Given the high false positive rates for miRNA target prediction, we identified only those potential target genes that were predicted by both methods as described in detail previously (Lawless *et al.*, 2013). The InnateDB (www.innatedb.com) (Lynn *et al.*, 2008) pathway analysis tool was used to identify potential pathways that were statistically overrepresented among predicted targets. Predicted target genes with a role in innate immunity were also identified using InnateDB and a hypergeometric test was used to investigate whether innate immune genes were statistically overrepresented. R (v2.14.0, http://r-project.org) was used to create the boxplot showing the miRNA expression levels, and the scatter plots showing the correlation between samples. The RNA-seq fastq files have been uploaded to the NCBI Gene Expression Omnibus (GEO) database (Barrett *et al.*, 2011) with experiment series accession number GSE41138.

2.2.8 RT-qPCR validation

The relative expression of three miRNAs (bta-miR-21, bta-miR-148a, and bta-miR-708) in BAM-5 and BAM-7 was also determined by RT-qPCR, using the Taqman MicroRNA Reverse Transcription Kit (Applied Biosystems, Life Technologies Ltd.), according to the manufacturer's protocol, and using 5 µl of 1:30 dilution of the prepared small RNA fraction, in 15 µl reverse transcription reaction (30 min 16°C, 30 min 42°C, 5 min at 85°C, and then maintained at 4°C). Taqman MicroRNA Assays (Applied Biosystems) with TaqMan Universal Master Mix II (no UNG) (Applied Biosystems), were used according to the manufacturer's protocol. A four-point 1:10 serial dilution of miR-21 and a 1:10 dilution of miR-148a was also measured. Additionally, the expression of miR-21 and miR-148a were also measured in BAM-3 and BAM-4.

RT-qPCR was performed on a 7500 Fast Real-Time PCR System (Applied Biosystems) with 7500 Software (version 2.0.6), using MicroAmp Fast optical 96-well plate and Optical Adhesive Film (Applied Biosystems). 20 µl reaction volumes were used for each well and amplification was performed using the following thermal cycle: 95°C 10 min, and 40 cycles: 95°C for 15 s, 60°C for 1 min. Technical replication was performed in triplicate. Non-template controls had no amplification.

Table 2-1 | RNA quality and read numbers. RNA Integrity Number (RIN) values were above 9 for all samples.

Sample ID	BAM-1	BAM-2	BAM-3	BAM-4	BAM-5	BAM-6	BAM-7	BAM-8
RNA conc. [ng/ul]	383	530	483	446	372	470	656	80
rRNA ratio (28s/18s)	1.6	1.6	1.7	1.6	1.7	1.7	1.5	1.9
RIN	9.4	9.4	9.4	9.6	9.7	9.6	9.4	9.8
Small RNA conc. [pg/µl]	15674	19602	18441	13306	17380	11565	9854	9869
miRNA conc. [pg/µl]	746	1144	1404	1005	1875	1830	1820	660
Index (barcode) sequence	CGATGT	TTAGGC	TGACCA	ACAGTG	GCCAAT	CAGATC	ACTTGA	ATCACG
Total # of reads	11268106	10359205	8379883	11322893	9957402	13108422	10561796	11380422
# of reads after quality control steps	7767806	6486994	5628363	8759869	8195175	9174465	8550114	8018972
# of uniquely aligned reads	5370197	4657271	3867637	5928652	5641224	6270685	5941310	4916793
Uniquely aligned as % of total	0.47658382	0.449578032	0.461538305	0.523598695	0.566536	0.478371	0.562528	0.43204

2.3 Results and discussion

2.3.1 AM-expressed miRNAs

The aim of this study was to identify, catalogue and quantify the expression of all known and novel miRNAs in non-activated AMs using RNA-seq. In total, 86 million reads were generated by sequencing the eight libraries. After the sequence processing steps of quality control and adapter removal, 62.5 million reads remained for further analysis; 86% of these reads were 19–24 nt long, thus validating the miRNA extraction and library preparation procedure (Table 2-1).

42.5 million reads aligned uniquely to the reference genome. 96.6% of reads aligning to known gene annotations from Ensembl (v66) aligned to miRNAs (Figure 2-2), 2.1% to small nucleolar RNAs (snoRNAs), 0.5% to small nuclear RNAs (snRNAs), and the rest to other RNA species including mRNAs, transfer RNAs (tRNAs), ribosomal RNAs (rRNAs) and mitochondrial RNAs (mtRNAs). Approximately one million reads aligned to unannotated regions of the genome; these possibly include novel miRNAs, other novel non-coding RNAs (ncRNAs), or mRNA degradation products. Highly expressed miRNAs were distributed relatively evenly across the genome (Figure 2-3).

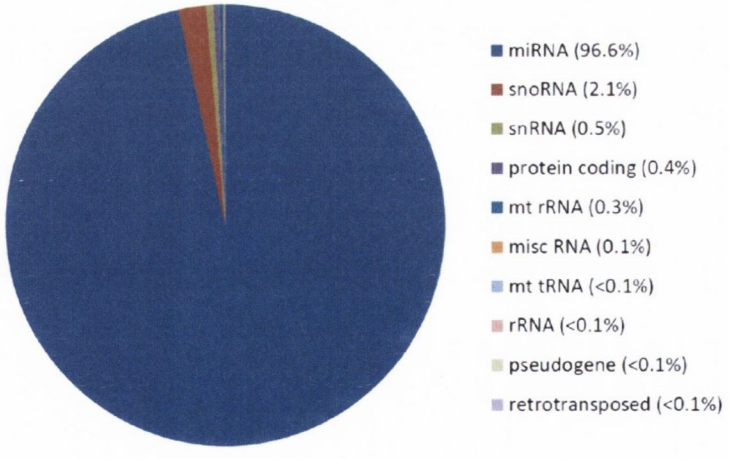

Figure 2-2 | The proportion of reads aligning uniquely to annotated bovine genes (averaged across eight samples). 96.6% of annotated reads aligned to known miRNAs. snoRNA: small nucleolar RNA; snRNA: small nuclear RNA; mt: mitochondrial; rRNA: ribosomal RNA; tRNA: transfer RNA.

Recently, it has been reported that miRNAs expressed below 100 reads per million (RPM) are unlikely to be functional (Mullokandov *et al.*, 2012). Using 100 RPM as a threshold for functional expression, we found that more than 10% (80/755) of known bovine miRNAs were expressed in AMs. As has been previously reported in the RAW 264.7 mouse macrophage cell line (Garmire *et al.*, 2010), there is a large dynamic range in the expression of known miRNAs – a few miRNAs (bta-mir-21, miR-27a and bta-let-7i) are expressed at very high levels (up to 800,000 RPM), with the majority being expressed at low levels (around 1,000 RPM). Figure 2-4 shows all miRNAs expressed in AMs above 100 RPM (the read counts for all known bovine miRNAs expressed in AMs can be found in Electronic Appendix 2). Read counts were highly correlated between biological replicates (Figure 2-5).

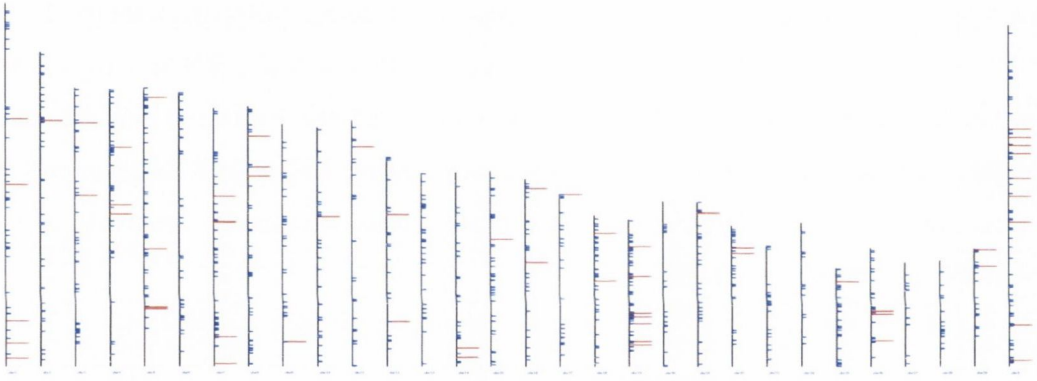

Figure 2-3 | Distribution of miRNAs in the bovine genome. Highly expressed miRNAs were relatively evenly distributed across the genome. Vertical bars represent chromosomes, blue horizontal bars known miRNA locations. Red horizontal bars show highly expressed (> 100 RPM) miRNA locations.

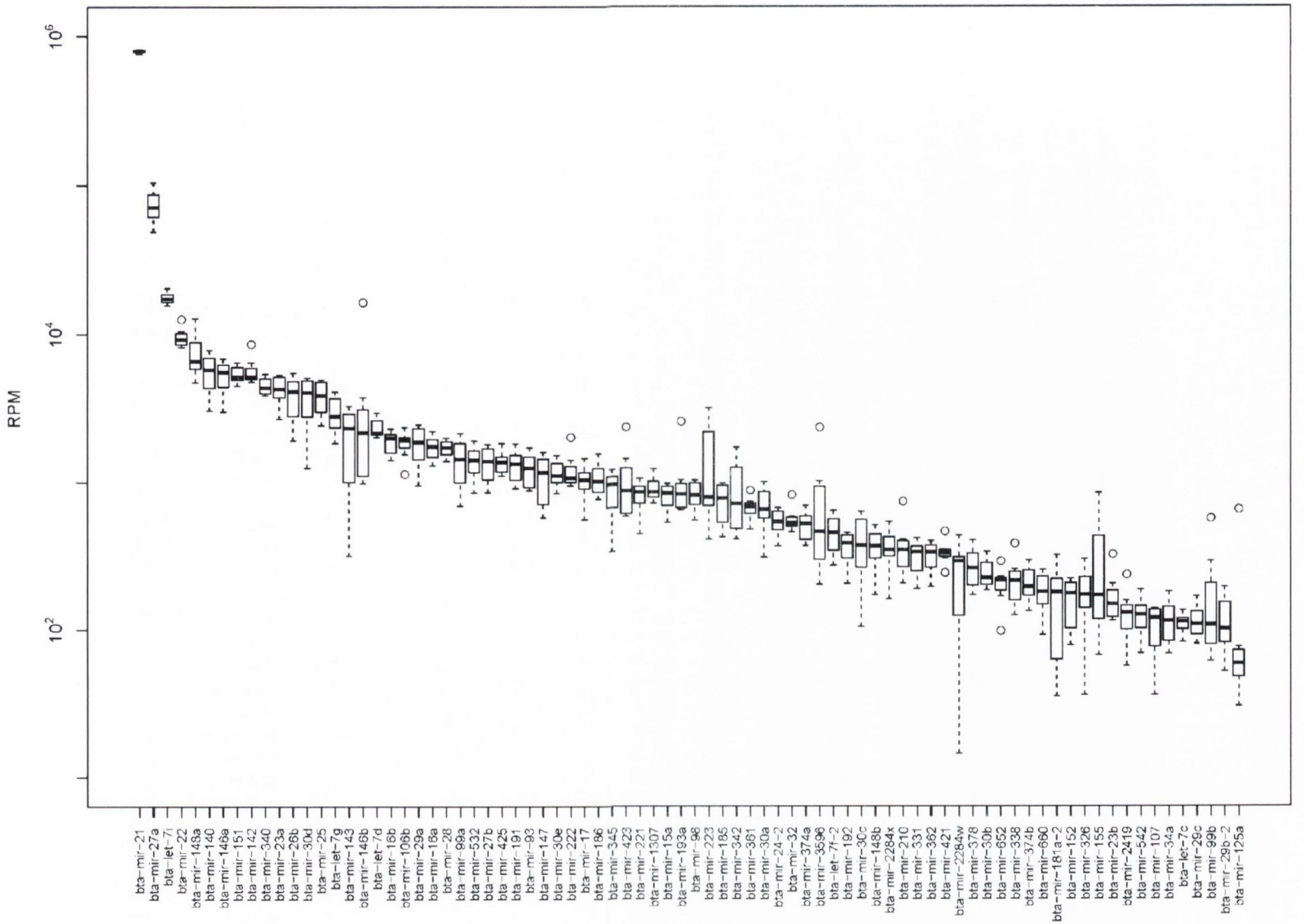

Figure 2-4 | Box plot of miRNAs expressed in AMs. RPM values are shown, for all miRNAs above a threshold of 100 RPM.

Several of the miRNAs which we identified as expressed in AMs (>100 RPM) have been shown to have regulatory roles in monocytes and macrophages of other species. The most highly expressed AM miRNA, miR-21, for example, regulates the expression of antimicrobial peptides and was found to be upregulated in *M. leprae* infected human monocytes (Liu *et al.*, 2012). miR-27, which was also found to be highly expressed in AMs, has been shown to be involved in the activation of human macrophages (Graff *et al.*, 2012, Cheng *et al.*, 2012). The third mostly highly AM-expressed miRNA, bta-let-7i, belongs to the let-7 family, a family of miRNAs that has several well-documented roles in immunity (Satoh *et al.*, 2012, Androulidaki *et al.*, 2009, Iliopoulos *et al.*, 2009). For example, several let-7 family members, including let-7i, were observed to be downregulated in murine macrophages during *Salmonella* infection (Schulte *et al.*, 2011). Other AM-expressed miRNAs identified in our study, including miR-21, miR-27b, miR-146, miR-147, miR-155, and miR-223, have all been found to be upregulated by TLR signalling in other studies (O'Neill *et al.*, 2011, Liu *et al.*, 2009, Ghorpade *et al.*, 2012). In addition to regulation by the host's immune system, miRNAs may also be regulated by pathogens to modulate the immune response in a way that is advantageous to the pathogen. For example, miR-99b, another AM-expressed miRNA, is upregulated by *M. tuberculosis* in infected murine DCs, and this inhibits the production of proinflammatory cytokines (Singh *et al.*, 2013b).

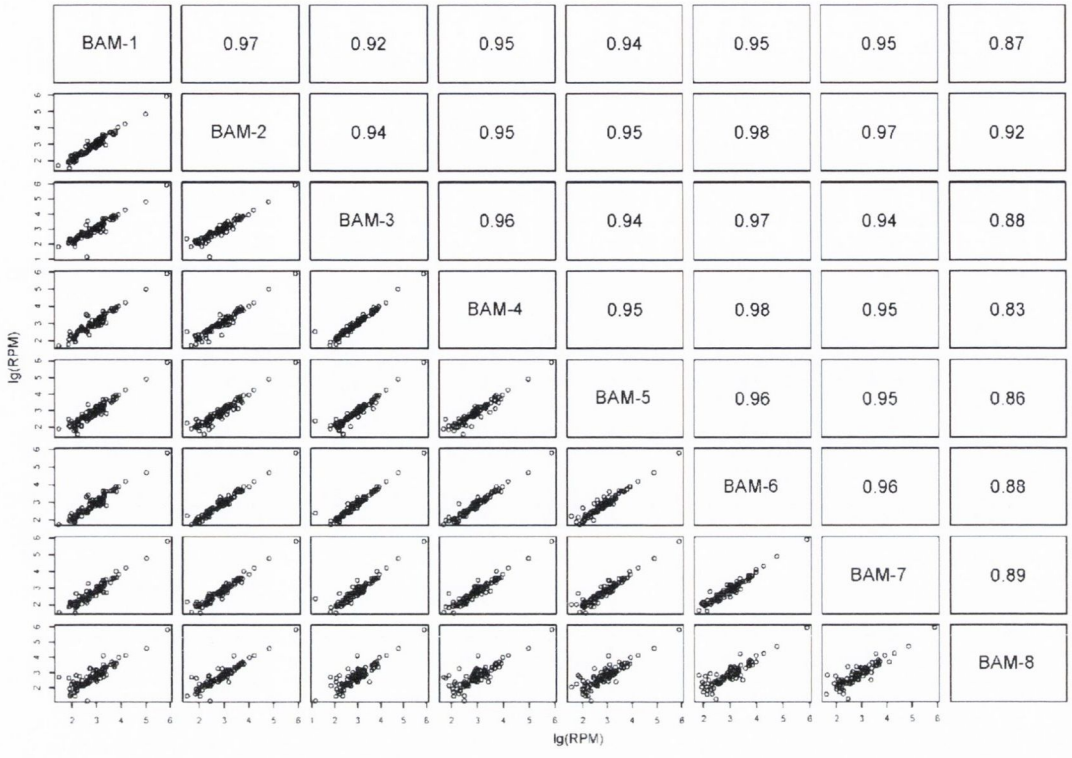

Figure 2-5 | Scatter plots of miRNAs expressed at a threshold above 100 RPM in AMs. Correlation coefficients are shown in the upper panel. Sample names are shown in the diagonal panels.

2.3.2 Relative expression of miR-21, miR-148a and miR-708

To assess reliability of the miRNAseq data presented in this study and to confirm that the high relative expression of miR-21 in AMs is not an artefact of the sequencing technology, we measured the relative expression of three miRNAs (miR-21, miR-148a, and miR-708) using RT-qPCR, in two samples (BAM-5 and BAM-7). We chose these miRNAs for the following reasons: according to our miRNAseq data, miR-21 was the highest expressed miRNA in AMs; miR-148a was expressed at a level approximately 100-fold less than miR-21; and miR-708 was expressed at a very low level (only a few reads mapped to it). RT-qPCR confirmed the same profile of expression of these miRNAs. miR-148a was found to be expressed two orders of magnitude less than miR-21 (C_q (quantification cycle) values for all four samples are shown in Table 2-2); while miR-708 was observed to be very lowly expressed compared to miR-21 ($\Delta C_q \approx 16$), which corresponds to the count numbers. These data were further confirmed using serial dilutions of the miRNA cDNA. We have found that

100× dilution of the miR-21 RT product cDNA used in the qPCR resulted in approximately the same C_q values as undiluted miR-148a ($\Delta C_q < 0.35$) in both samples. We had similar results for 1000× dilution of miR-21 and 10× dilution of miR-148a cDNA ($\Delta C_{qBAM\text{-}5} = -1$ and $\Delta C_{qBAM\text{-}7} = 0.1$).

Table 2-2 | The RT-qPCR results for miR-21, miR-148a and miR-708 in four samples. Means of C_q values of three wells are shown.

Sample	miR-21 (RPM)	miR-21 (Cq)	miR-21 (Cq) 1:100 dilution	miR-148a (RPM)	miR-148a (Cq)	miR-708 (RPM)	miR-708 (Cq)
BAM-5	796,997.0	19.23	26.92	8,045.3	26.98	0.0	35.78
BAM-7	792,298.7	18.73	26.10	12,734.4	25.78	0.7	34.38
BAM-3	798,223.6	17.56	N/A	6,909.3	25.06	0.3	N/A
BAM-4	759,240.9	19.03	N/A	5,540.9	26.80	0.7	N/A

2.3.3 Analysis of predicted miRNA target genes

To identify the genes and pathways that may be under miRNA control in AMs, we performed target prediction on the miRNAs which are expressed above 100 RPM. The targets that were predicted by both miRanda and TargetScan, are listed in Electronic Appendix 3. Using InnateDB, we found that innate immunity related genes were overrepresented (p-value = 0.049) among predicted targets of miRNAs. Pathway analysis of the predicted genes showed no pathways to be significantly overrepresented.

2.3.4 IsomiR expression in AMs

IsomiRs are isoforms of miRNAs that differ in a few nucleotides from the canonical sequence, and may have functional importance. Compared to the canonical sequence, isomiRs can be modified at either ends, with modifications at the 3' end being more common (Neilsen *et al.*, 2012). We have found that isomiRs are commonly expressed in AMs. More than 100 miRNAs had isomiRs that were expressed at >100 reads. Furthermore, over half of these miRNAs had an isomiR more highly expressed than the miRBase consensus sequence.

IsomiRs were generally a few nucleotides shorter than the consensus miRNAs; in agreement with earlier findings (Newman *et al.*, 2011, Lee *et al.*, 2010),

modifications at the 3' end were twice as common as at the 5' end (Table 2-3, Electronic Appendix 4). This is in concordance with observations that usually a short seed sequence at the 5' end is responsible for most of the miRNA target specificity (Brennecke *et al.*, 2005).

Table 2-3 | Summary of isomiR expression across samples. IsomiRs were found to be generally shorter than consensus sequences. Modifications at 3' ends were more common than at 5' ends. Several isomiRs were more highly expressed than their consensus sequences.

Sample	Strand	# miRs with isomiRs	# of isomiRs >100 reads	# isomiRs longer than consensus	# isomiRs shorter than consensus	# isomiRs 5' modified (first 5nt)	# isomiRs 3' modified (last 5nt)	# cases where isomiR expressed more highly than consensus
BAM-1	5p	54	456	65	344	183	418	31
	3p	39	352	100	136	167	268	27
BAM-2	5p	53	432	63	321	176	393	28
	3p	42	308	95	132	135	245	28
BAM-3	5p	49	435	59	327	180	395	26
	3p	41	303	99	117	132	241	25
BAM-4	5p	55	512	76	378	218	463	28
	3p	42	423	125	175	202	336	28
BAM-5	5p	56	463	74	333	198	409	29
	3p	39	377	119	136	177	290	25
BAM-6	5p	57	498	76	361	220	445	30
	3p	43	436	125	173	215	338	28
BAM-7	5p	55	479	63	362	183	435	32
	3p	42	389	104	164	181	298	27
BAM-8	5p	49	462	64	340	191	416	25
	3p	39	295	101	115	119	240	26

2.3.5 Prediction of novel bovine miRNAs expressed in AMs

In comparison with miRBase version 19, we also identified five putatively novel bovine miRNAs in the miRNA-seq data. Four of these were also recently discovered by us in bovine mammary epithelial cells (Lawless *et al.*, 2013). One putatively novel miRNA, bta-miR-6560, found on chromosome 7, with a predicted mature sequence 'caggcucuggaacacgggagc', is entirely novel and showed no homology to miRNAs in miRBase.

2.3.6 Conclusion

Here we have provided the first atlas of miRNA expression in unchallenged AMs, which will serve as a reference point for future functional studies or challenge experiments directed to uncover the role of miRNAs in these critical immune cells.

CHAPTER 3

MICRORNA PROFILING OF THE BOVINE ALVEOLAR MACROPHAGE RESPONSE TO MYCOBACTERIUM BOVIS INFECTION SUGGESTS PATHOGEN SURVIVAL IS ENHANCED BY MICRORNA REGULATION OF ENDOCYTOSIS AND LYSOSOME TRAFFICKING

3.1 Introduction

Tuberculosis is a major global health threat to both human and animal populations, which is caused by members of the intracellular *Mycobacterium* genus. Currently, one third of the human population world-wide is estimated to be infected with *Mycobacterium tuberculosis,* causing approximately nine million new cases and 1.3 million deaths every year (WHO, 2013). Bovine tuberculosis, caused by *M. bovis* is also a significant problem for global agriculture. Both *M. tuberculosis* and *M. bovis* are members of the *Mycobacterium tuberculosis* complex (MTBC), a group of highly related pathogens that are spread via an airborne route and are taken up by alveolar macrophages in their respective hosts. It is well established that *M. tuberculosis* and *M. bovis* can block the antimicrobial systems of the macrophage allowing them to replicate intracellularly and cause disease (Ehlers, 2009). There is increasing evidence for the role of the innate immune response in the outcome of MTBC pathogens (Subbian *et al.*, 2013). Macrophages are the first cells to encounter mycobacteria, and microarray (Magee *et al.*, 2012) and RNA-seq experiments (Nalpas *et al.*, 2013) have shown that mRNA expression is substantially altered in bovine monocyte-derived macrophages upon *M. bovis* infection *in vitro*. Changes in the expression of another type of RNA, microRNAs, however, are less well understood. MicroRNAs are short non-coding RNAs that post-transcriptionally regulate gene expression (Holley and Topkara, 2011) and are known to have roles in many aspects of immunity (Gantier, 2010). Several miRNAs have been found to be involved in mycobacterial infection (Singh *et al.*, 2013a). In mice infected with the vaccine strain *M. bovis* BCG, downregulated miR-29 expression in natural killer cells and T cells enhanced IFN-γ production, a cytokine important for immunity against intracellular pathogens (Ma *et al.*, 2011). Similarly, in human monocyte-derived macrophages infected with *M. avium*, caspase 3 and 7 are downregulated by miRNAs let-7e and miR-29a, thus inhibiting apoptosis, a defence mechanism against intracellular bacteria (Sharbati *et al.*, 2011).

In this project, we have built upon our previous work profiling miRNA expression in bovine AM using RNA-seq (Vegh *et al.*, 2013), and investigate which miRNAs are differentially expressed in primary bovine AM at several time-points post-infection with the genome-sequenced strain of *M. bovis* 2122/97 in comparison to paired uninfected controls.

3.2 Materials and methods

3.2.1 Ethical approval

All animal procedures were performed in accordance with the provisions of the Irish Cruelty to Animals Act, and ethical approval for the study was obtained from the University College Dublin Animal Ethics Committee (protocol number AREC-13-14-Gordon).

3.2.2 Animals

Ten unrelated age-matched (7-12 weeks) Holstein-Friesian male calves were used in the challenge experiment. All animals were maintained under uniform housing conditions and nutritional regimens at the UCD Lyons Research Farm (Newcastle, County Kildare, Ireland). The animals were selected from a herd without a recent history of bovine tuberculosis infection.

3.2.3 Alveolar macrophage in vitro infection

AM were harvested by pulmonary lavage of lungs obtained post-mortem from ten animals, and collected in cryovials as described before by Magee et al. (2014), and in Materials and methods, CHAPTER 2. The cryovials, containing 2.5×10^7 AM cells in 1 ml, were stored at −80°C for a period of 20 h after which they were removed from the freezing containers and transferred to −140°C freezer storage conditions until further use (Magee *et al.*, 2014).

Alveolar macrophage culture was prepared as described by Magee et al. (2014), and Materials and methods, CHAPTER 2. Briefly, cryovials were thawed by placing in a 37°C water bath for 1 min. Once thawed, cells were immediately transferred into 20 ml 37°C pre-warmed $R10^+$ media and centrifuged (200 × g for 5 min). The cell pellet was resuspended in 15 ml of $R10^+$ media and placed in a 75 cm^2 vented culture flask (Cellstar, Greiner Bio-One), and incubated for 24 h at 37°C, 5% CO_2. After incubation, alveolar macrophages were seeded in 24-flat well tissue culture plates (Sarstedt Ltd.) at a density of 5×10^5 cells/well, and incubated for a further 24 h at 37°C, 5% CO_2. Separate infected and control wells were maintained for each of the 4 time points (2 h, 6 h, 24 h, 48 h), in addition to the control (0 h). All *in vitro* infections were performed in a CL3 laboratory. For this, the media from all wells was removed and replaced with 1 ml R10 media containing *M. bovis* (5×10^6 cells/ml). The non-infected control alveolar

macrophage samples received 1 ml R10 media only. After infection, the tissue culture plates were incubated at 37°C, 5% CO_2 for 24 h and 48 h. After 2 h infection, the media from all wells of the 24 h and 48 h infection experiments was replaced with fresh R10 media (1 ml per well) and the plates were re-incubated at 37°C, 5% CO_2 until the cells were harvested (Magee *et al.*, 2014). Two samples (48 h infected and control for animal N1861) were excluded due to low cell numbers, therefore nine animals were used in the 48 h timepoint.

3.2.4 Small RNA preparation

In total, 88 RNA-seq libraries were prepared for sequencing. The small and total RNA fractions were prepared from the cells and assessed as described in Materials and methods, CHAPTER 2. The total RNA fractions had RIN values between 8.6 and 9.5. Small RNA concentrations were between 3,400 and 17,200 pg/µl, and miRNA concentrations were between 140 and 1,430 pg/µl (Appendix 2). The small RNA fractions were used for preparing RNA-seq libraries and for RT-qPCR.

3.2.5 RNA-seq library preparation

All 88 RNA-seq libraries were prepared with the Illumina Truseq Small RNA Sample Preparation Kit, according to the manufacturer's protocol, using 5 µl of the prepared small RNA. Libraries were sequenced (50 bp single-end) on 18 lanes of an Illumina HiSeq 2000 machine (BGI Hong Kong, China). Samples were randomised across the lanes as shown in Appendix 3. The RNA-seq fastq files have been uploaded to the NCBI GEO database (Barrett *et al.*, 2011) with experiment series accession number GSE58883.

3.2.6 Analysis of RNA-seq data

Reads were processed as described in CHAPTER 2. Shortly, Cutadapt (v1.2.1) (Martin, 2011) was used to trim 3' adapter sequences from reads. Reads which were less than 18 nt after trimming and all untrimmed reads were discarded. The remaining reads were then further filtered using FASTQ Quality Filter, and reads where at least 30% of the bases had a Phred score < 20 were removed. Finally, reads were also trimmed at their ends using FASTQ Quality Trimmer to remove low quality bases (Phred score < 20), and reads less than 18 nt after the trimming were discarded. The FASTQC results are shown in Electronic Appendix 5.

Reads that passed all quality control steps were aligned to the bovine genome (UMD3.1 assembly (Zimin *et al.*, 2009)) using Novoalign (v2.08.03) in 'miRNA' mode allowing one mismatch. Non-uniquely aligning reads were discarded. HTSeq-count in 'union' mode was then used to count aligned reads that overlapped with known miRBase (version 19, http://www.mirbase.org) (Kozomara and Griffiths-Jones, 2011) miRNA gene annotations. To investigate the proportion of reads sequenced from non-miRNA genes, HTSeq-count was also used separately to count reads that overlapped with all bovine gene annotations from Ensembl version 69. For a summary of the number of reads at each step, see Table 3-1 and Electronic Appendix 6.

Table 3-1 | Summary of number of reads at each data processing step.

Software	Number of reads
Cutadapt	
Processed	2,536,380,031
Untrimmed	9,387,842
Trimmed too short	450,945,626
Trimmed not short	2,076,046,563
Fastq filter	
Input	2,076,046,563
Output	2,073,837,300
Discarded	2,209,263
Fastq trimmer	
Input	2,073,837,300
Output	2,073,461,468
Discarded	375,832
Novoalign	
Total	2,073,461,468
Aligned	1,756,692,728
Unique	1,100,725,457

Potentially novel miRNAs were identified using miRDeep2, as described in CHAPTER 2, with the additional criteria that the mature sequence was expressed in at least ten samples and was expressed at a minimum of 100 reads per million. R (v3.0.1) was used to create the boxplots and the scatter plots. EdgeR (v3.2.4) (Robinson *et al.*, 2010) was used to identify statistically significant differentially expressed miRNAs with a paired test, using a generalized linear model method, with upper quartile normalization (Garmire and Subramaniam, 2012). Differentially expressed miRNAs were defined as those that had both an FDR ≤ 0.05 in the edgeR analysis and were

expressed above a threshold of 100 RPM, a level at which miRNAs are more likely to be functional (Mullokandov *et al.*, 2012). Results were robust for the normalization method used: all differentially expressed miRNAs were also detected with the other two normalization methods; TMM and RLE (relative log expression).

3.2.7 Co-expression and target analysis of miRNA and mRNA data

To identify mRNAs that were potentially regulated by differentially expressed (DE) miRNAs, Pearson correlations were calculated between DE miRNA expression and mRNA expression (also assayed by RNA-seq) from the same samples (Nalpas et al, manuscript submitted) using the Apache Commons Java Statistics Library (http://commons.apache.org/proper/commons-math). The resulting correlation matrix was then filtered to remove both non-significant correlations (critical value for Pearson's correlation for this matrix is r = -0.2483) and those inverse correlations that were not supported by miRanda (v3.3a) predicted miRNA-target pairs. Two-dimensional cluster analysis and visualization, using R (v3.0.1) *hclust* and *heatmap.plus* packages, was then applied to the filtered correlation matrix. The miRNA-mRNA interaction network was also visualized with Cytoscape (v3.0.0) (Cline *et al.*, 2007).

3.2.8 Pathway analysis of predicted miRNA target genes

The predicted target gene IDs of differentially expressed miRNAs were converted using 1:1 orthology annotation to human gene IDs and submitted to InnateDB (Lynn *et al.*, 2008) for pathway analysis. Genes were submitted in two groups; those that were targets of upregulated miRNAs, and those that were targets of downregulated miRNAs. Significant pathways were identified using the Hypergeometric test and were defined as having a Benjamini and Hochberg corrected p-value of ≤ 0.05 (Benjamini and Hochberg, 1995).

3.2.9 RT-qPCR validation of differentially expressed miRNA genes

The expression of four miRNAs identified as differentially expressed in the RNA-seq data (bta-miR-22, bta-miR-142-5p, bta-miR-146a, and bta-miR-423-3p) was investigated using RT-qPCR. Infected and control samples were compared for nine biological replicates. Based on the RNA-seq data, bta-miR-16b and bta-miR-26b were used as non-differentially expressed internal reference transcripts.

The Taqman MicroRNA Reverse Transcription Kit (Applied Biosystems) was used, according to the manufacturer's protocol, and using 5 µl of 10× diluted small RNA fraction, in 15 µl reverse transcription reaction (30 min 16°C, 30 min 42°C, 5 min at 85°C, and then maintained at 4°C). Taqman MicroRNA Assays (Applied Biosystems) with TaqMan Universal Master Mix II (no UNG) (Applied Biosystems), were used according to the manufacturer's protocol.

A 7500 Fast Real-Time PCR System (Applied Biosystems, software version 2.0.6) was used with MicroAmp Fast optical 96-well plates and Optical Adhesive Films (Applied Biosystems). Amplification was performed using 20 µl/well and the following thermal cycle: 95°C 10 min, and 40 cycles: 95°C for 15 s, 60°C for 1 min. Technical replication was performed in triplicate and results were corrected for amplification efficiency. No amplification was measured in the no template and the reverse transcription control wells. The one-tailed paired Student's *t*-test was performed with R (v3.0.1) on the normalized and efficiency-corrected ΔC_t (quantification cycle) values, with a significance level of 0.05. Using the Pfaffl method (Pfaffl, 2001), fold changes were calculated from the $\Delta\Delta C_t$ values ($FC = 2^{-\Delta\Delta Ct}$), using the negative reciprocal for downregulated genes ($-1 / FC$).

3.2.10 Transfection of Bomac cells with miRNA mimics

Bomac cells were a gift from Prof. Cliona O'Farrelly (Trinity College Dublin). Although Bomacs poorly replicate all the functions of primary macrophages (Sager *et al.*, 1999), the Bomac cell line is, to our knowledge, the only bovine macrophage cell-line available to undertake the miRNA mimic transfection studies and these experiments are largely independent of these functions. Cells were cultured in 150 cm^2 flasks (Cellstar, Greiner Bio-One) using RPMI 1640 medium (Sigma-Aldrich), supplemented with 10% FBS (Sigma-Aldrich), penicillin (50 unit/ml) and streptomycin (50 µg/ml) (Pen Strep, Gibco, Life Technologies). For the transfection, cells were seeded in 6 well flat bottom cell culture plates (Cellstar, Greiner Bio-One). Cells were transfected using Opti-MEM 1 (Gibco) and Lipofectamine RNAiMAX (Invitrogen), according to the manufacturer's protocol and using 75 pmol mimics (Ambion mirVana miRNA mimics, Life Technologies) per well. Based on the RNA-seq and RT-qPCR results, miR-146a and miR-146b were selected for the experiment. Additional wells were treated with negative (scrambled) control mimic, or the positive control (miR-1). Each well was treated with one miRNA only. As per the manufacturer's

recommendation, downregulation of miR-1's known target, *PTK-9,* was measured to confirm that transfection was successful. Experiments were performed in triplicate. After 24 hours, cells were washed with PBS (pH 7.4, Gibco) and then cells were lysed with the Ambion mirVana miRNA Isolation Kit. Total RNA was quantified with a Nanodrop ND-1000 and an Agilent 2100 Bioanalyzer, and all samples had RIN values above 9, and 28S/18S rRNA ratios between 1.8 and 2.3.

3.2.11 RT-qPCR analysis of target gene downregulation

The expression of two bovine genes, *IRAK1* and TGF-β receptor 2 *(TGFBR2),* was measured with RT-qPCR. Five genes, *ACTB, GAPDH, H3F3A, PPIA* and *RPS9,* were tested to find suitable internal reference genes. Three reference genes *(GAPDH, H3F3A, RPS9)* were selected with the Genorm algorithm (Vandesompele *et al.*, 2002), using the ReadqPCR and NormqPCR (version 1.8.0) R packages (Perkins *et al.*, 2012). The High-Capacity cDNA Reverse Transcription Kit (Invitrogen) was used, with 400 ng RNA in 20 µl reverse transcription reaction (10 min 25°C, 120 min 37°C, 5 min at 85°C, and then maintained at 4°C). The Fast SYBR Green Master Mix (Applied Biosystems) was used for assaying, using 1 µl of the cDNA. A 7500 Fast Real-Time PCR System was used as described above, using the following thermal cycling: 95°C 20 s, and 40 cycles: 95°C for 3 s, 60°C for 30 s. The no-template and reverse transcription control showed that preparations were free of contamination. For primer sequences see Table 3-2. Melt curve analysis confirmed specificity of primers. Treatments were compared to the scrambled mimic negative control. The two-tailed two-sample Student's *t*-test was performed on the normalized and efficiency-corrected ΔC_t values, with a significance level of 0.05. For the C_t values processed by NormqPCR, please see Electronic Appendix 7. Fold changes were calculated using the Pfaffl method, as described above.

Table 3-2 | Sequences of primers used in the RT-qPCR. Gene names, forward and reverse primer sequences are shown.

Gene	Forward	Reverse
PPIA	CCACCGTGTTCTTCGACAT	TCTGTGAAAGCAGGAACCTTT
H3F3A	CATGGCTCGTACAAAGCAGA	ACCAGGCCTGTAACGATGAG
GAPDH	CTCCCAACGTGTCTGTTGTG	TGAGCTTGACAAAGTGGTCG
ACTB	AGATGACCCAGATCATGTTCGA	TGACCCCGTCACCGGAGTCCATCACGAT
RPS9	GATTACATCCTGGGCCTGAA	ATGAAGGACGGGATGTTCAC
TGFBR2	CCCAAGTCGGTTAACAGCGA	AGGCAATCTTGGGGTCATGG
IRAK1	CCAATGACCCAGGTGTACCA	TAGGAGTTCTCTTGCGGGGA
PTK9	TGCAGCAACAAGAGCAACTC	ACGTCAGTCTGTACCTCATTAATTT

3.3 Results

A high-throughput sequencing approach was applied to monitor miRNA expression changes in bovine AM post-infection with *M. bovis* and in matched unchallenged control samples. In total, 2.5 billion reads were generated by sequencing, and approximately 2 billion reads remained for analysis after adapter removal and quality control. 93% of reads uniquely aligning to the genome aligned to annotated miRNAs in the bovine genome, 3.5% to snoRNAs, and the remainder mapped mainly to other types of RNAs (mRNAs, tRNAs, rRNAs, mtRNAs etc). miRNA expression was highly correlated across biological replicates (Figure 3-1). The most highly expressed miRNAs in unchallenged macrophages were bta-miR-21, bta-miR-22, bta-miR-27a, bta-let-7i and bta-miR-191 (Figure 3-2). The level of miRNA expression, however, varied over a wide range, with almost half of the reads aligning to bta-miR-21 (≈ 430,000 RPM), and the majority being more lowly expressed (1,000–10,000 RPM). For a full list of the read counts for all miRNAs at all time-points, see Electronic Appendix 8.

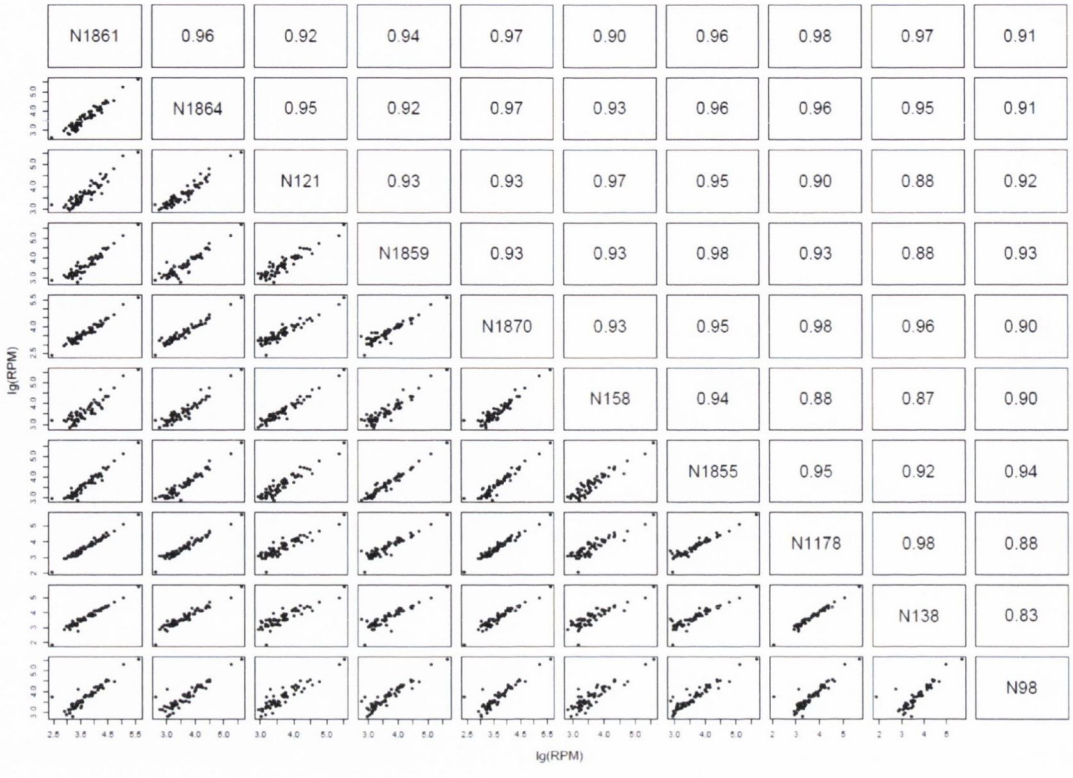

Figure 3-1 | Scatter plot of miRNAs expressed above 100 RPM in the ten 0 h control samples. Animal numbers are shown in the diagonal panels, and correlation coefficients are shown in the upper panel.

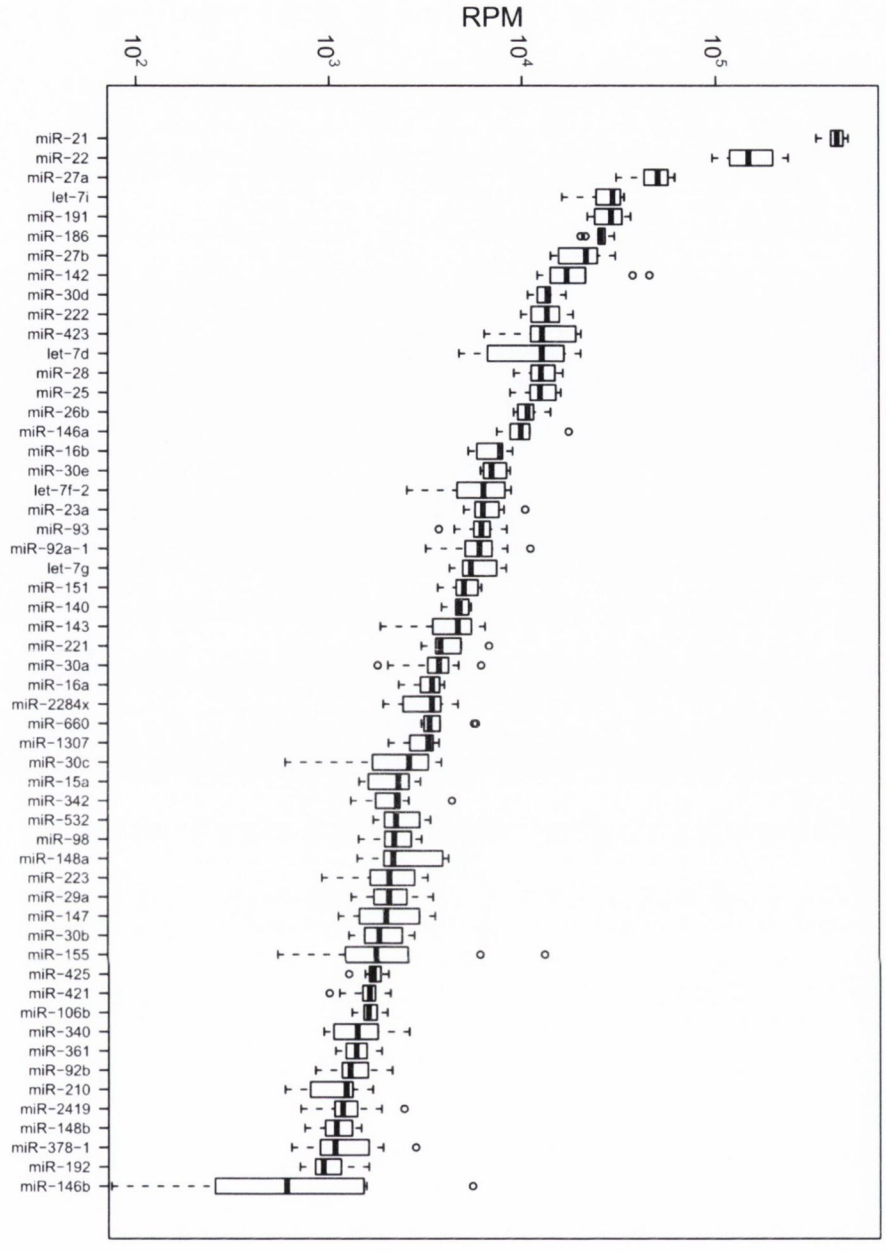

Figure 3-2 | MicroRNA expression in unchallenged bovine alveolar macrophages. Only those expressed above a threshold of 1,000 RPM are shown.

3.3.1 Multiple differentially expressed miRNAs were detected at 2, 24, and 48 hours post infection with M. bovis

The edgeR statistical package was used to determine miRNAs that were differentially expressed in response to *M. bovis* infection at 2, 6, 24, and 48 hours post infection (hpi). Only one miRNA, bta-miR-326, was identified as differentially expressed at 2 hpi (FDR ≤ 0.05) (Table 3-3), while no differentially expressed miRNAs were identified at 6 hpi. Six miRNAs were differentially expressed 24 hpi; of these, five (bta-miR-21-3p, bta-miR-27a-5p, bta-miR-146a, bta-miR-147, and bta-miR-149-5p) were upregulated and one (bta-miR-296) was downregulated (FDR ≤ 0.05). Forty differentially expressed miRNAs were identified at 48 hpi (Figure 3-3), of which 36 had a > 1.5 fold change difference in expression. All of the miRNAs that were differentially expressed at 24 hpi were also differentially expressed at 48 hpi. For the normalized count numbers for each differentially expressed miRNA, see Electronic Appendix 9. Among the upregulated miRNAs at 48 hpi, bta-miR-146b had the highest fold change (FC = 2.7), followed by bta-miR-146a (FC = 2.4). Seven members of the bta-let-7 family were found to be downregulated post-infection. Interestingly, two highly expressed miRNAs, bta-mir-423-3p, and bta-mir-423-5p, from the opposite arm of the same pre-miRNA, were both downregulated. The full list of differentially expressed miRNAs, their read counts and fold changes are listed in Table 3-3.

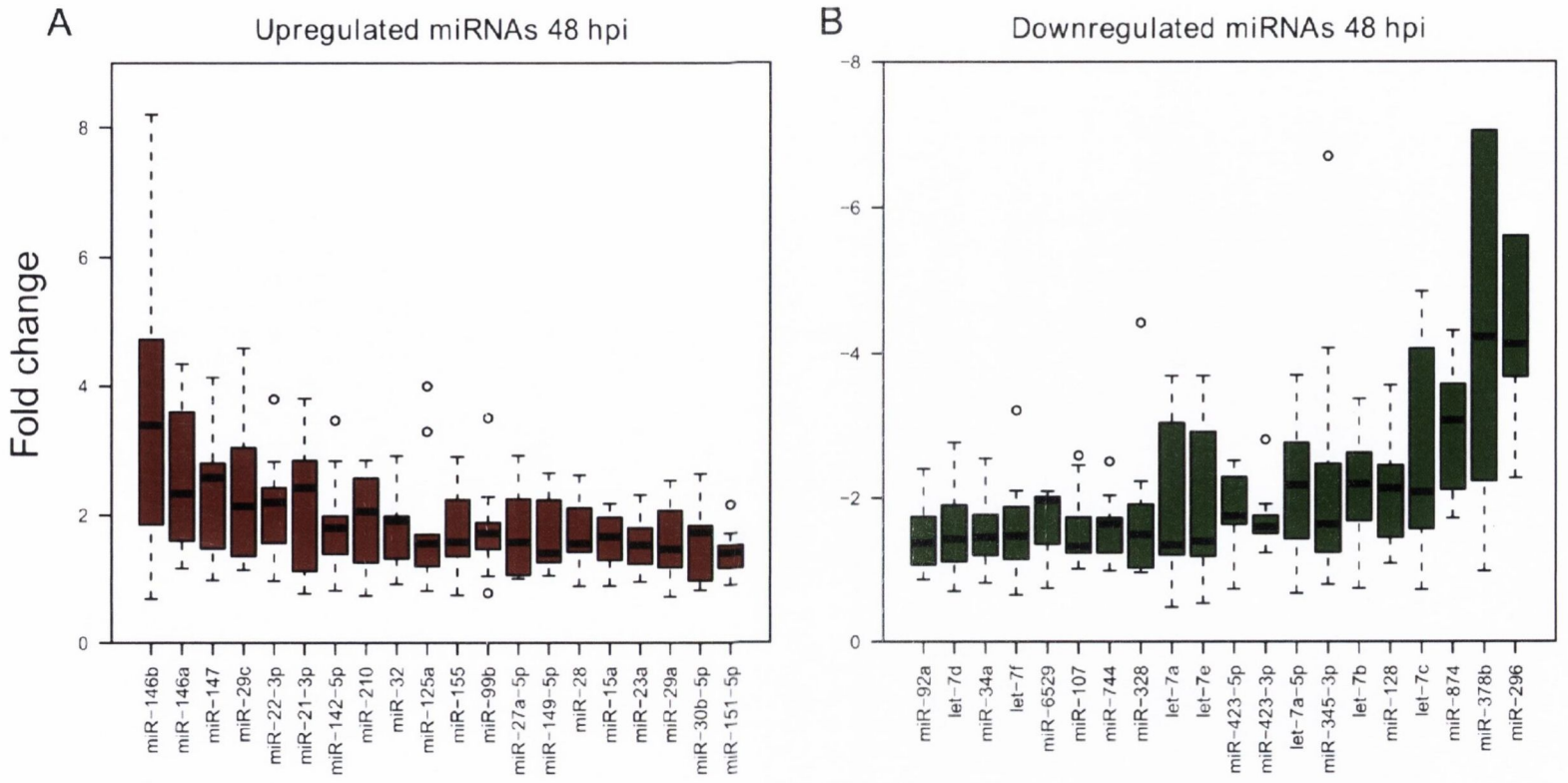

Figure 3-3 | Upregulated (A) and downregulated (B) miRNAs in bovine alveolar macrophages isolated from nine animals at 48 hours post infection with *M. bovis*. Fold changes are shown for all forty differentially expressed miRNAs.

Table 3-3 | Differentially expressed microRNAs in alveolar macrophages challenged with *M. bovis*. The results are sorted by time-point and fold-change.

miRNA	FC	RPM	p-value	FDR
2 hours post infection				
bta-miR-326	1.91	217.2	6.54×10^{-9}	2.09×10^{-6}
24 hours post infection				
bta-miR-149-5p	1.81	284.4	2.21×10^{-4}	1.15×10^{-2}
bta-miR-27a-5p	1.53	390.5	1.18×10^{-3}	2.94×10^{-2}
bta-miR-21-3p	1.52	7735.2	1.09×10^{-3}	2.94×10^{-2}
bta-miR-147	1.51	2332.4	8.22×10^{-4}	2.66×10^{-2}
bta-miR-146a	1.47	13481.5	1.00×10^{-3}	2.94×10^{-2}
bta-miR-296	−1.79	132	6.21×10^{-5}	5.03×10^{-3}
48 hours post infection				
bta-miR-146b	2.69	1526.5	3.95×10^{-6}	7.46×10^{-5}
bta-miR-146a	2.38	14030	7.36×10^{-9}	2.73×10^{-7}
bta-miR-147	2.17	2134.7	1.15×10^{-7}	3.84×10^{-6}
bta-miR-29c	2.12	381.3	1.35×10^{-6}	3.23×10^{-5}
bta-miR-22-3p/bta-miR-3600	1.96	152949.7	1.35×10^{-6}	3.23×10^{-5}
bta-miR-21-3p	1.79	5205.7	6.11×10^{-4}	4.30×10^{-3}
bta-miR-142-5p	1.76	15683.4	2.92×10^{-5}	4.65×10^{-4}
bta-miR-210	1.73	1324.4	3.70×10^{-4}	3.20×10^{-3}
bta-miR-32	1.69	604.6	1.34×10^{-4}	1.66×10^{-3}
bta-miR-125a	1.66	1824.2	8.30×10^{-4}	5.65×10^{-3}
bta-miR-155	1.65	3165.9	1.89×10^{-4}	2.11×10^{-3}
bta-miR-99b	1.63	1326.8	4.72×10^{-4}	3.50×10^{-3}
bta-miR-27a-5p	1.63	358.7	4.51×10^{-4}	3.43×10^{-3}
bta-miR-149-5p	1.61	366	3.01×10^{-4}	2.81×10^{-3}
bta-miR-28	1.6	1845.6	2.33×10^{-4}	2.43×10^{-3}
bta-miR-15a	1.54	1626.3	3.73×10^{-4}	3.20×10^{-3}
bta-miR-23a	1.51	5730.4	3.03×10^{-4}	2.81×10^{-3}
bta-miR-29a	1.49	1627.1	2.88×10^{-3}	1.66×10^{-2}
bta-miR-30b-5p	1.47	1671.1	4.06×10^{-3}	2.08×10^{-2}
bta-miR-151-5p	1.37	2640.2	5.83×10^{-3}	2.86×10^{-2}
bta-miR-92a	−1.36	6255.2	9.62×10^{-3}	4.07×10^{-2}

bta-let-7d	−1.43	12062.2	8.21×10^{-3}	3.61×10^{-2}
bta-miR-34a	−1.45	479.8	3.71×10^{-3}	1.97×10^{-2}
bta-let-7f	−1.46	7929	6.79×10^{-3}	3.19×10^{-2}
bta-miR-6529	−1.52	4179.4	2.18×10^{-3}	1.33×10^{-2}
bta-miR-107	−1.52	273.8	9.86×10^{-4}	6.46×10^{-3}
bta-miR-744	−1.55	330.4	4.21×10^{-4}	3.43×10^{-3}
bta-miR-328	−1.57	229.7	2.96×10^{-3}	1.68×10^{-2}
bta-let-7a	−1.58	186.8	1.13×10^{-2}	4.48×10^{-2}
bta-let-7e	−1.62	2038.4	4.38×10^{-3}	2.18×10^{-2}
bta-miR-423-5p	−1.64	9504.1	3.95×10^{-4}	3.30×10^{-3}
bta-miR-423-3p	−1.65	9898.1	4.45×10^{-6}	7.83×10^{-5}
bta-let-7a-5p	−1.84	120.9	2.74×10^{-4}	2.69×10^{-3}
bta-miR-345-3p	−1.89	996.2	4.31×10^{-4}	3.43×10^{-3}
bta-let-7b/bta-miR-3596	−1.91	239.4	5.51×10^{-5}	7.16×10^{-4}
bta-miR-128	−1.95	115.8	9.18×10^{-7}	2.55×10^{-5}
bta-let-7c	−2.25	808	4.02×10^{-6}	7.46×10^{-5}
bta-miR-874	−2.85	126	1.37×10^{-15}	2.29×10^{-13}
bta-miR-378b	−4.75	138.1	1.51×10^{-7}	4.60×10^{-6}
bta-miR-296	−4.93	191.8	4.54×10^{-20}	1.52×10^{-17}

3.3.2 Validation of three differentially expressed miRNAs using RT-qPCR

The differential expression of four miRNAs (bta-miR-22, bta-miR-142-5p, bta-miR-146a, and bta-miR-423-3p), found to be differentially expressed at 48 hpi using RNA-seq (Figure 3-4), was investigated using RT-qPCR in nine biological replicates. Differential expression was confirmed in three out of the four cases: miR-142-5p (FC = 1.3), miR-146a (FC = 3.0), and miR-423-3p (FC = −1.7). The upregulation of miR-22 (FC = 1.1) was not statistically significant (Figure 3-5). For the efficiency corrected C_t values for each sample, see Appendix 4. For fold changes across four timepoints for all differentially expressed miRNAs, see Figure 3-6.

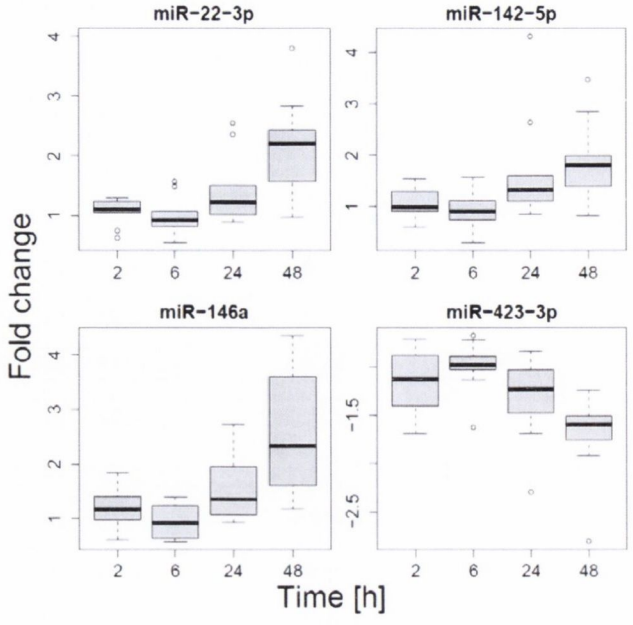

Figure 3-4 | Fold changes of four miRNAs across four time points. Differential expression of these miRNAs was tested with RT-qPCR.

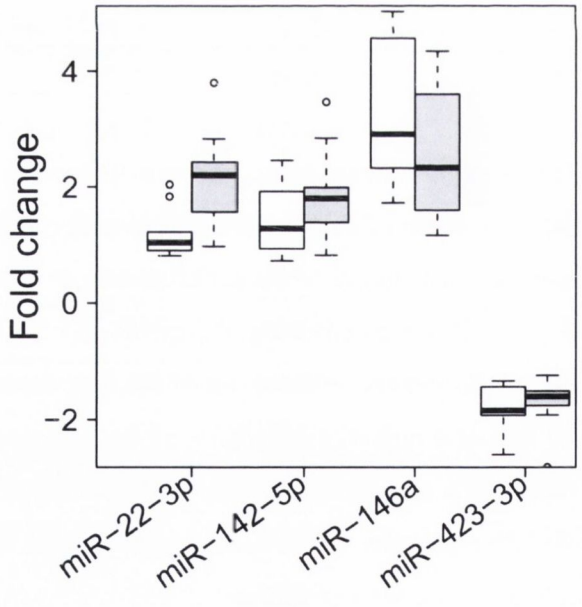

Figure 3-5 | The differential expression of three (bta-miR-142-5p, bta-miR-146a, and bta-miR-423-3p) out of four miRNAs for the nine animals at 48 hpi was confirmed with RT-qPCR (white). RNA-seq fold changes for these miRNAs are also shown (light grey).

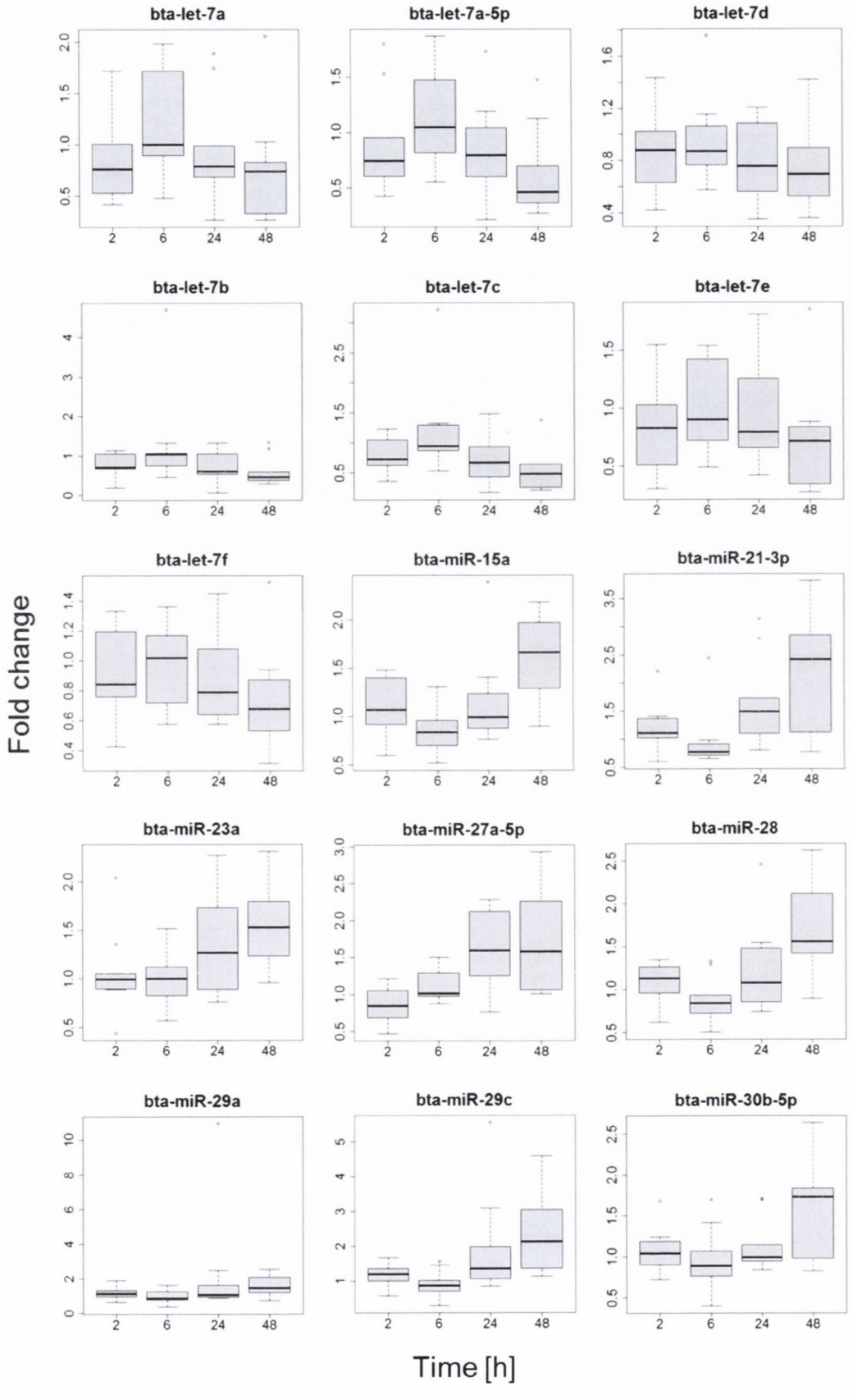
bta-let-7a
bta-let-7a-5p
bta-let-7d
bta-let-7b
bta-let-7c
bta-let-7e
bta-let-7f
bta-miR-15a
bta-miR-21-3p
bta-miR-23a
bta-miR-27a-5p
bta-miR-28
bta-miR-29a
bta-miR-29c
bta-miR-30b-5p
Fold change
Time [h]

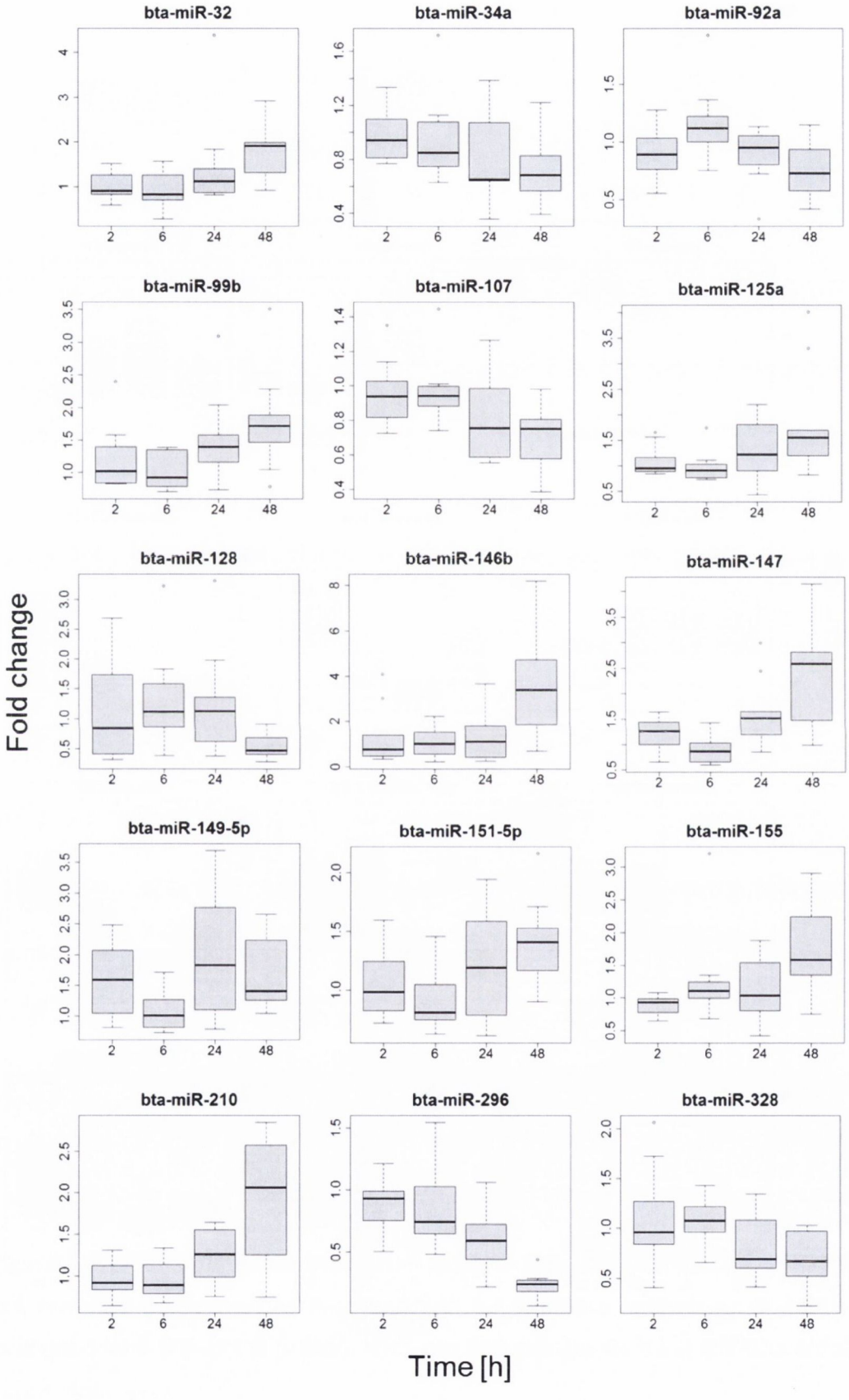
bta-miR-32
bta-miR-34a
bta-miR-92a
bta-miR-99b
bta-miR-107
bta-miR-125a
bta-miR-128
bta-miR-146b
bta-miR-147
bta-miR-149-5p
bta-miR-151-5p
bta-miR-155
bta-miR-210
bta-miR-296
bta-miR-328
Fold change
Time [h]

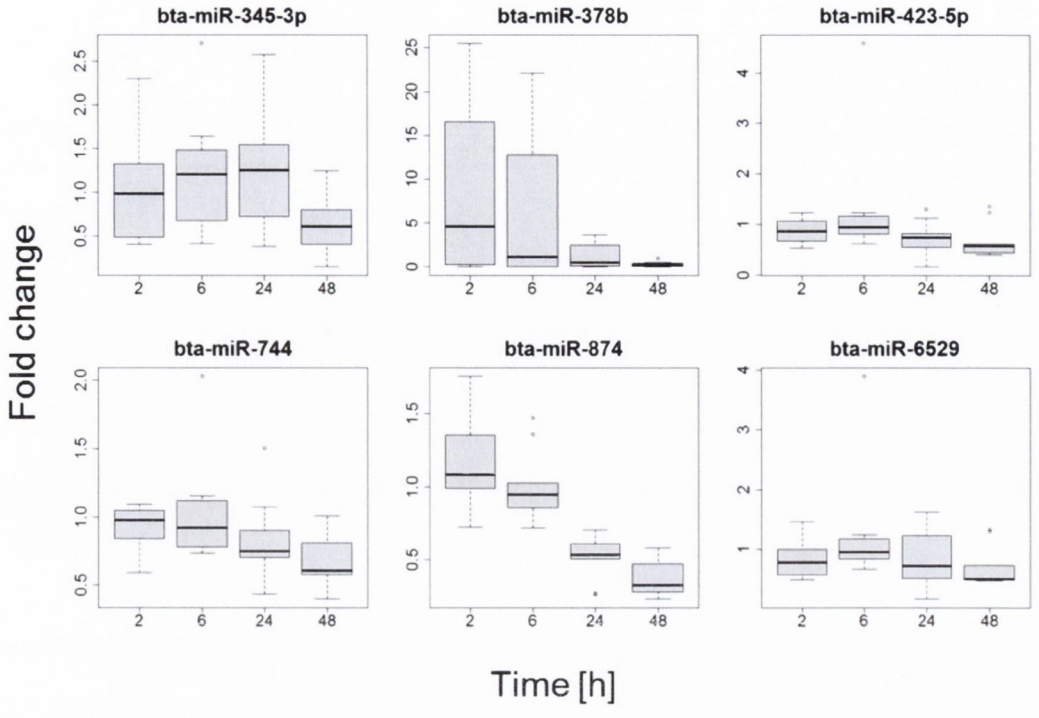

Figure 3-6 | Fold changes of differentially expressed miRNAs across four time points. For miRNAs tested with RT-qPCR (miR-22-3p, bta-miR-142-5p, bta-miR-146a, and bta-miR-423-3p) see Figure 3-4.

3.3.3 Two potentially novel bovine miRNAs are predicted from the sequencing data

Using miRDeep2, two putatively novel bovine miRNAs were identified from the sequencing data: bta-miR-8551 (mature sequence: ccgagccugacagaucacaca), located on chromosome 26, was found to be expressed in all animals (in 52 samples in total, with no preference for timepoint or infection status), with a mean expression of 1,890 RPM. A close homolog (with just one nucleotide mismatch) was also predicted in an adjacent genomic region (bta-miR-8552; mature sequence: ucgagccugacagaucacaca), and was detected in six animals (13 samples) with a mean expression of 950 RPM. There are several near-identical copies of these miRNAs in the same region.

3.3.4 The predicted targets of upregulated miRNAs are enriched for roles in endocytosis and lysosome function

To identify the potential mRNA targets of differentially expressed miRNAs, we identified those mRNAs with expression values (from Nalpas et al, manuscript submitted) significantly negatively correlated with miRNA expression. These predictions were further refined by removing those miRNA-target predicted relationships that were not supported by a predicted miRNA seed region match in the 3' UTR of the correlated mRNA (Figure 3-7, Electronic Appendix 10). This network of miRNA-mRNA interactions was visualized with Cytoscape (Figure 3-8). It is observable that miR-22-3p, miR-146a and b, miR-147, and miR-155 share many targets, suggesting they have a common role. Among the downregulated miRNAs, the let-7 family members, and miR-423-3p and -5p share most of their targets.

Analysis of the predicted target genes using InnateDB (www.innatedb.com) (Lynn *et al.*, 2008), revealed that the predicted targets of upregulated miRNAs were highly enriched for roles in the lysosome (FDR $\leq 3.2 \times 10^{-6}$) and in endocytosis (FDR $\leq$ 0.02). Key components of innate immunity signalling pathways, including the TLR pathway, transforming growth factor beta receptor signalling pathway, and the IL-10 anti-inflammatory signalling pathway, were also predicted to be preferentially targeted by upregulated miRNAs (Electronic Appendix 11).

In comparison, downregulated miRNAs were predicted to preferentially target IL-1 (FDR $\leq 5.4 \times 10^{-6}$) and MAPK signalling (FDR = 0.0001) pathways, as well as the tumour necrosis factor receptor 1 signalling pathway (FDR $\leq$ 0.03) and genes involved in bacterial invasion (Electronic Appendix 12). Additionally, the Toll-like receptor pathway was also targeted by downregulated miRNAs. Of the 22 TLR pathway genes predicted to be targeted, 11 were predicted to be targeted only by downregulated miRNAs, and 7 only by upregulated miRNAs.

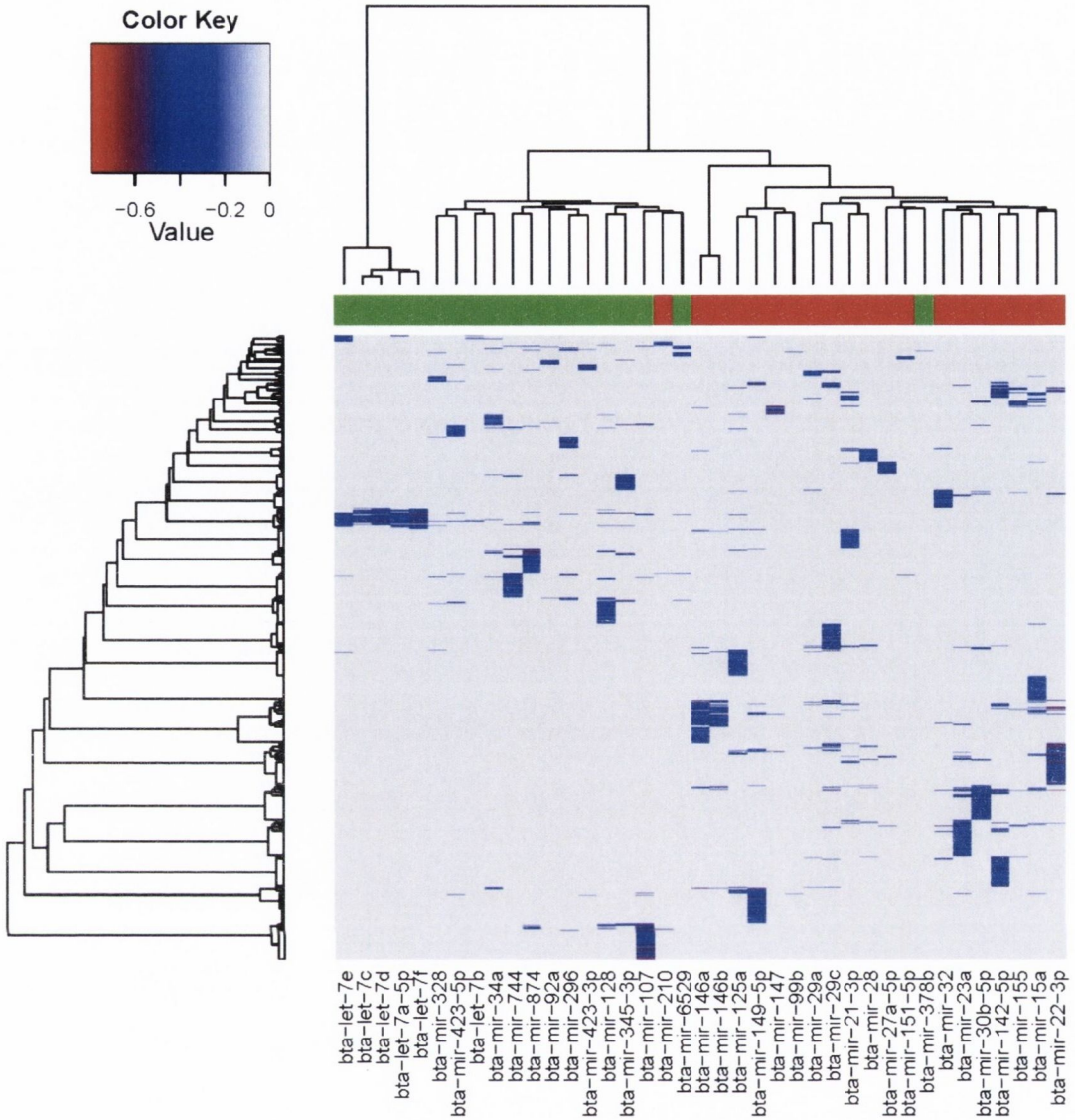

Figure 3-7 | Two-dimensional cluster analysis and heatmap visualization of significant correlations (shown as coloured lines) between miRNA and mRNA expression at 48 hpi. Non-significant correlations and those not supported by a 3' UTR miRNA seed match are shown in grey. Please see the colour key in the figure. The primary split in the upper hierarchical dendrogram largely aligns with the upregulated (red) and downregulated miRNAs (green).

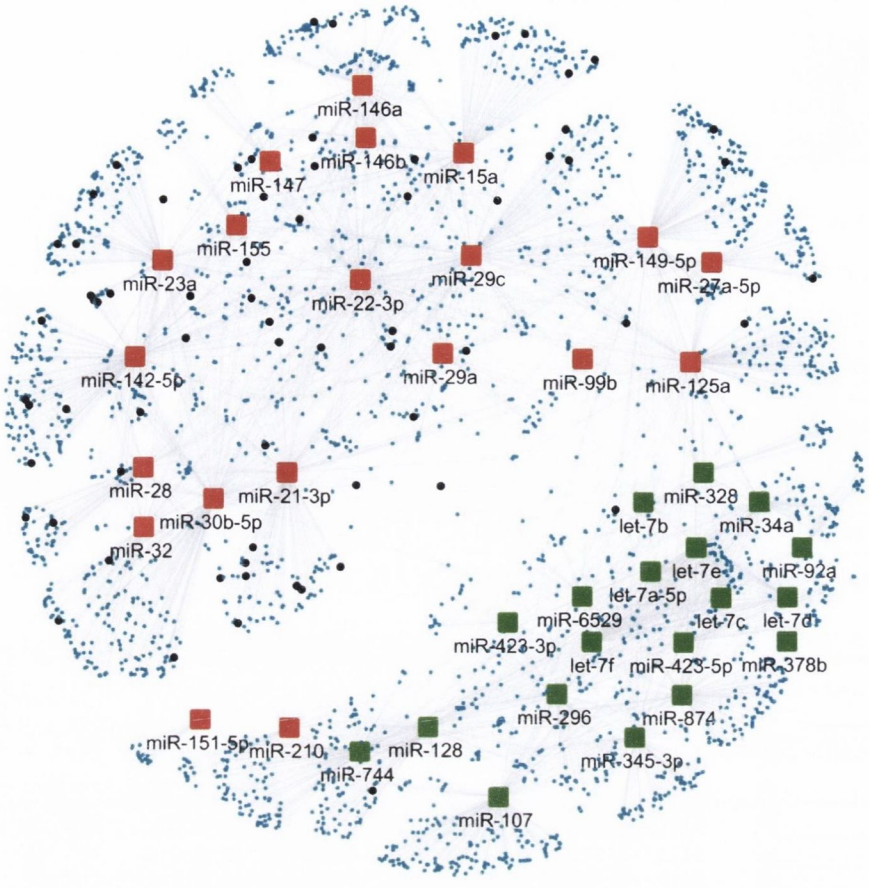

Figure 3-8 | A network of the predicted mRNA targets of differentially expressed miRNAs at 48 hpi with *M. bovis*. Targets are predicted based on a significant negative correlation between miRNA and mRNA expression and the presence of a miRanda seed match in the correlated mRNA. Squares = miRNAs; Circles = mRNAs. Red = upregulated; Green = downregulated. Lysosome and endocytosis pathway genes are shown as black circles. Please see Electronic Appendix 10 for details of targeted mRNAs.

3.3.5 Overexpression of miR-146 results in the transcriptional suppression of IRAK1 and TGFBR2

We have utilised a miRNA overexpression strategy to validate the predicted post-transcriptional regulation of two genes in these pathways by miR-146, a microRNA shown by RNA-seq and RT-qPCR to be upregulated in response to *M. bovis* infection. Successful transfection of miRNA mimics into a bovine macrophage cell line

(Bomac) was confirmed by the positive control miR-1, which was observed to three-fold downregulate its target, *PTK9*. In contrast, miR-1 did not alter the expression of *IRAK1*, and only marginally (1.2 fold upregulation) altered *TGFBR2* mRNA levels (Electronic Appendix 7). miR-146a or miR-146b was predicted from our computational analyses to downregulate *IRAK1*, and indeed, transfection (i.e. overexpression) of miRNA mimics for these miRNAs into Bomacs led to a more than three-fold decrease in *IRAK1* transcript levels (Figure 3-9), a central kinase in the TLR and IL-1 pathways (O'Neill, 2008). Another predicted target of bta-miR-146a and bta-miR-146b, *TGFBR2*, which is part of the TGF-β receptor pathway, was also downregulated 1.5 fold upon transfection with mimics (Figure 3-9).

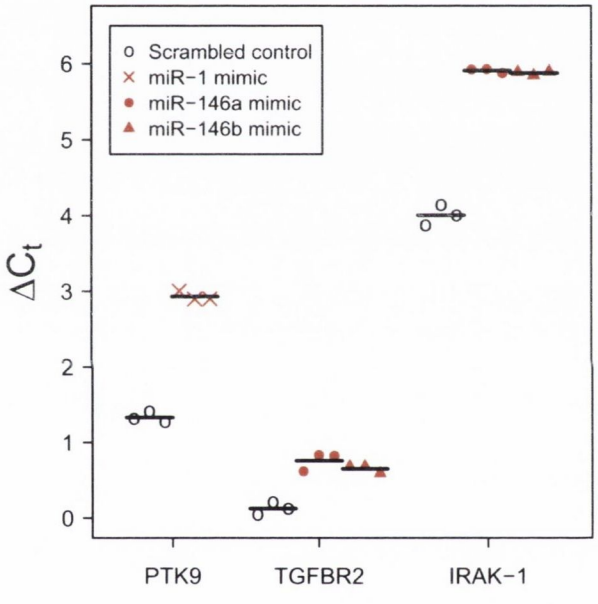

Figure 3-9 | Transfection of miRNA mimics for miR-146a or miR-146b into a bovine macrophage cell line (Bomac) led to a 3 fold decrease in *IRAK1* transcript levels, and a 1.5 fold downregulation of *TGFBR2* in comparison to a scrambled control miRNA, as measured by RT-qPCR. Successful transfection was confirmed by the positive control miR-1, which was observed to downregulate its target, *PTK9*, by 3 fold.

3.4 Discussion

In this study, we have used high-throughput sequencing to profile miRNA expression at multiple time-points, in primary bovine alveolar macrophages infected with *M. bovis*, the causative agent of bovine TB. Over the time-course, 41 miRNAs were identified as being significantly differentially expressed in response to *M. bovis* infection. The majority of miRNAs were differentially expressed only after 48 hpi. Several of the differentially expressed miRNAs have been shown to have regulatory roles in monocytes and macrophages and during infection. For example, miR-149-5p, which was upregulated in our study at 24 and 48 hpi, has also been shown to be upregulated in murine bone-marrow derived macrophages infected with *Listeria monocytogenes* (Schnitger *et al.*, 2011). Another highly expressed miRNA detected in our study, miR-27, has previously been shown to have a role in the activation of human macrophages (Cheng *et al.*, 2012, Graff *et al.*, 2012).

Many of the differentially expressed miRNAs have also been shown to have a role in other mycobacterial infections. The most highly expressed miRNA at 24 hpi, bta-miR-146a, was upregulated more than two-fold, and has also been found to be upregulated in human monocyte-derived macrophages after *M. avium* infection (Sharbati *et al.*, 2011). Another example at 24 hpi is bta-miR-21-3p. MiR-21 has a well-established role in immunity and has been shown to target the vitamin D-dependent antimicrobial pathway in *M. leprae* infected monocytes (Liu *et al.*, 2012, O'Neill *et al.*, 2011). MicroRNAs bta-mir-423-3p, and bta-mir-423-5p, which were downregulated in response to *M. bovis* infection in our study, have also been found to be downregulated in human monocyte-derived macrophages infected with *M. avium* (Sharbati *et al.*, 2011), and are involved in regulating chemokine expression and apoptosis related pathways. Although these findings show that not all observed changes are *M. bovis*-specific, the differentially expressed miRNAs may serve as potential biomarker candidates for *M. bovis* infection in cattle, for example, as was suggested for miR-155 (Golby *et al.*, 2014).

Pathway analysis of the predicted mRNA targets of DE miRNAs suggests that these miRNAs preferentially target several pathways that are functionally relevant for mycobacterial pathogenesis. The predicted targets of upregulated miRNAs at 48 hpi, for example, were statistically enriched for functions in the lysosome and in the endocytosis pathway. These pathways were predicted to be targeted by multiple miRNAs including bta-miR-15a, bta-miR-21-3p, bta-miR-22-3p, bta-miR-23a, bta-

miR-30b-5p and bta-miR-142-5p. A key feature of mycobacteria is their ability to survive and reproduce in the phagosome by retarding maturation of the phagosome along the endosomal-lysosomal pathway and blocking fusion with the lysosome (Clemens and Horwitz, 1995). Mycobacteria also enhance phagosome fusion with early endosomes, possibly providing access to host nutrients and secreted glycoproteins (Vergne *et al.*, 2004). In our analysis, the endocytosis pathway was predicted to be targeted mainly through several members of the membrane trafficking regulator Rab family, namely, RAB22A, RAB4A, RAB5B, RAB5C, and RAB7A, in addition to rabaptin (RABEP1) and the RAB11 family interacting protein 5 (RAB11FIP5). Autophagy is an effective innate defence mechanism for eliminating mycobacteria (Ni Cheallaigh *et al.*, 2011, Deretic *et al.*, 2009). Recently, the Rab protein family was found to be necessary for autophagic clearance of mycobacteria and the knockdown of Rab proteins resulted in increased *M. bovis*-BCG survival (Pilli *et al.*, 2012). Our results therefore suggest that *M. bovis* utilises host miRNAs as part of its strategy to manipulate these processes for its own benefit and survival.

We have also shown, that overexpression of miR-146a and miR-146b, which are upregulated during *M. bovis* infection, leads to a downregulation of *IRAK1,* a central kinase in IL-1 signal transduction (Liu *et al.*, 2008), TLR signalling and in the Type I Interferon Pathway (Pauls *et al.*, 2013). The targeting of IRAK1 by miR-146a/b has also been demonstrated in human (Taganov *et al.*, 2006) and mouse (Hou *et al.*, 2009). IL-1 receptor signalling is required for the innate response to *M. tuberculosis* and IL1R1-deficient mice display a dramatic defect of early control of MTB infection (Fremond *et al.*, 2007). Thus, this may be another example of *M. bovis* exploiting host miRNAs for its own benefit. Pathway analysis, however, has also revealed that despite the targeting of IRAK1 by upregulated miR-146a/b, many other members of this pathway were statistically enriched as targets of downregulated miRNAs, which would be predicted to transcriptionally upregulate these genes in the IL-1 pathway. This suggests that both the pathogen and the host are battling for the control of this central pro-inflammatory pathway at the post-transcriptional level.

The TGF-β pathway was also predicted to be significantly targeted by upregulated miRNAs and we have shown that the overexpression of miR-146a or miR-146b – two of the upregulated miRNAs – results in the downregulation of TGFBR2, one the receptors for the TGF-β pathway. TGF-β signalling has a well-established role in tuberculosis pathogenesis (Toossi and Ellner, 1998). Thus, the post-transcriptional

targeting of this pathway by upregulated miRNAs may be an example of the host immune response utilising miRNAs for the benefit of the host.

In conclusion, our work, which investigates the post-transcriptional regulation of the innate immune response by miRNAs in alveolar macrophages, the natural host cell-type for *M. bovis*, suggests that miRNAs play a key role in finely tuning the complex interplay and tightly controlled balance between pathogen survival strategies and the host immune response.

CHAPTER 4

TRANSCRIPTOMIC (RNA-SEQ) ANALYSIS OF BOMAC CELLS OVEREXPRESSING MIR-146A

4.1 Introduction

Gene silencing by microRNAs is an important regulator of gene expression in eukaryotes. As described in CHAPTER 1, miRNAs act by targeting mRNAs through base-pairing between the 5'-end of the miRNA called the 'seed region', and the 3' UTR of the mRNA. Identification of all targets of a miRNA, and conversely all miRNA-regulators of a gene is necessary for understanding the function of a miRNA or the regulation of a particular gene. As miRNAs can have a great number of targets, and an mRNA can be regulated by multiple miRNAs, the interaction network can be quite complex. The reliability of current *in silico* approaches for finding targets is limited, therefore experimentation is indispensable for finding the real targets of miRNAs (Thomson *et al.*, 2011).

There are several methods for studying mRNA targeted by miRNAs; RT-qPCR, luciferase reporter assays and western blot are commonly used for validation of predicted targets (Kuhn *et al.*, 2008). However, these assays can only usually be used to assess a small number of already predicted targets, and lack the ability to distinguish between direct and secondary effects (Thomson *et al.*, 2011). The two main transcript-level based approaches for experimental target screening of miRNAs are sequencing of RISC components isolated with immunoprecipitation, and gene expression analysis upon differential expression of a miRNA (Tarang and Weston, 2014). Overexpression can be achieved by transient transfection of a synthetic miRNA, or with a miRNA-expression vector (Jin *et al.*, 2010). Inhibition can be achieved with antisense oligonucleotides, such as anti-miRs, or miRNA sponges. An obstacle in identifying direct targets is the modest effect of miRNAs on the levels of some of their target mRNAs. Additionally, some miRNA-targeting occurs predominantly at the level of translational repression (Thomson *et al.*, 2011), although in mammals miRNAs act mostly by decreasing target mRNA abundance (Guo *et al.*, 2010).

In the first use of this method, vectors expressing miR-1 or miR-124 were transfected into HeLa cells, and using microarrays more than 100 mRNAs were identified as downregulated for each miRNA (Lim *et al.*, 2005). The first RNA-seq analysis of a miRNA targetome used a vector to achieve high miR-155 expression and identified 102 potential targets, downregulated genes with a 3' UTR 8-mer seed match to miR-155 (Xu *et al.*, 2010). Targets of miR-155 were enriched for members of the bone morphogenetic protein signalling pathway (Yin *et al.*, 2010).

Several studies have established the importance of miRNAs in the immune system including miR-146, a family comprising of miR-146a and miR-146b. The expression of miR-146a increases as HSCs mature and is thought to control development of HSCs into blood cells (Zhao and Starczynowski, 2014). Moreover, its expression is strongly induced by a wide range of infectious and inflammatory stimuli in accordance with its role in immune cell activation. It inhibits inflammation, mainly by negatively regulating NF-κB signalling through two of its targets, *TRAF6* and *IRAK1* (Zhao and Starczynowski, 2014). In macrophages, miR-146a has a dominant role in inducing differentiation and maturation (Montagner *et al.*, 2013). The mature sequence of bta-miR-146a, 'UGAGAACUGAAUUCCAUAGGUUGU' was predicted by the miRNAminer software (Artzi *et al.*, 2008), based on sequence identity with its mouse ortholog (Lagos-Quintana *et al.*, 2002). In previous Chapters, the expression level of this miRNA was found to be upregulated in bovine alveolar macrophages in response to infection with *M. bovis*. Moreover, we have validated the regulation of two genes, *IRAK1* and *TGFBR2* by miR-146a. Following up on this work, here we describe an RNA-seq transcriptomic analysis of a bovine macrophage cell line (Bomac) transfected with bta-miR-146a mimics, to gain insight into the wider targetome and the functions of miR-146a in cattle.

4.2 Materials and methods

4.2.1 Transfection of Bomac cells with bta-miR-146a mimics

Bomac cells were treated as described in CHAPTER 3. In brief, cultured cells were seeded in 6-well flat-bottom cell culture plates (Cellstar, Greiner Bio-One). Cells were transfected using Opti-MEM 1 (Gibco) and Lipofectamine RNAiMAX (Invitrogen), according to the manufacturer's protocol and using 75 pmol of bta-miR-146a mimics (Ambion mirVana miRNA mimics, Life Technologies) per well. Additional wells were treated with negative control mimics (scrambled sequence). In addition, untreated cells were used as secondary controls. Treatments were performed in triplicate. After 24 hours, cells were washed with PBS (pH 7.4, Gibco) and subsequently lysed with the Ambion mirVana miRNA Isolation Kit. Total RNA was quantified with an Agilent 2100 Bioanalyzer, and all samples had RIN values above

9.5, and 28S/18S rRNA ratios between 1.9 and 2.3, thus suitable for library preparation (Appendix 5).

4.2.2 RNA-seq library preparation

Nine RNA-seq libraries were prepared using the Illumina Truseq RNA Sample Prep Kit (v2), according to the manufacturer's instructions, and different index barcode sequences were used for each library. The quality and size of the prepared libraries were checked with an Agilent 2100 Bioanalyzer, and library sizes were found to be approximately 270 bp. After quantification with a Qubit Fluorometer, all nine libraries were pooled in equal amounts, with a final concentration of 39.7 ng/uL. The pooled libraries were sequenced on three flowcell lanes, using an Illumina HiSeq 2000 machine (BGI Hong Kong), to obtain 90 bp paired-end reads.

4.2.3 RNA-seq data analysis

FastQC (v0.10.0, http://www.bioinformatics.bbsrc.ac.uk/projects/fastqc) was used to assess quality of sequencing reads. Trim Galore (v0.3.7, http://www.bioinformatics.babraham.ac.uk/projects/trim_galore) with Cutadapt (v1.6) (Martin, 2011) was used to trim Illumina adapters, and remove bases with a Phred score less than 20. Trimmed reads were mapped to the bovine genome (UMD3.1 assembly, version 77) (Zimin *et al.*, 2009) with Tophat (v2.0.13) (Kim *et al.*, 2013). The counts of uniquely aligning read-pairs were assigned to genes (Ensembl v77 annotation), using featureCounts, part of the Subread package (v1.4.6) (Liao *et al.*, 2014). Only unambiguously aligning reads were used in further analysis.

The R (v3.1.1) package edgeR (v3.6.7) (Robinson *et al.*, 2010), was used to prepare the MDS (multi-dimensional scaling) and volcano plots and to test for differential expression of genes. Genes with low expression (one read per million in at least three samples) were removed. TMM normalisation was used to compensate for library composition (Robinson and Oshlack, 2010). The software models count data with binomial distribution, and uses a modified version of Fisher's exact test to identify differentially expressed genes between groups. The Benjamini and Hochberg method was used to correct for multiple testing (Benjamini and Hochberg, 1995). Differentially expressed genes were defined as having absolute fold change > 2 between treatments and an adjusted p-value <0.05.

Experimentally validated targets (in other species) for miR-146a were identified using their human orthologs in miRTarBase (version 4.5) (Hsu *et al.*, 2014). Additionally, differentially expressed genes with a predicted seed match to miR-146a were identified using TargetScan v6.2 (Friedman *et al.*, 2009).

Overrepresented KEGG pathways (Kanehisa *et al.*, 2012) among human orthologs of the differentially expressed bovine genes were identified with the Bioconductor package GOseq (v1.18.0) (Young *et al.*, 2010), which uses the Wallenius non-central hypergeometric distribution for overrepresentation analysis. GOseq corrects for highly expressed or long genes as they are more likely to be detected as differentially expressed. Upregulated and downregulated genes were analysed separately. Ingenuity Pathway Analysis (IPA, version 21249400, Ingenuity Systems, Qiagen) was also used to identify pathways and cellular functions associated with the differentially expressed genes. IPA uses an overrepresentation analysis of categories (pathways, processes) in the Ingenuity Knowledge Base, a large manually curated database of experimentally validated interactions (Kramer *et al.*, 2014). P-values were adjusted for multiple testing using the Benjamini-Hochberg method. The IPA upstream regulator analysis identifies transcriptional regulators that can explain the observed gene expression changes. The calculated 'overlap p-value' measures whether there is a statistically significant overlap between a user-supplied gene-set and the known targets of a transcriptional regulator.

4.3 Results and discussion

Here, we report an RNA-seq approach to profile gene expression in a bovine macrophage cell line (Bomac) transfected with a synthetic miR-146a mimic. Our goal was to find gene expression changes induced by bta-miR-146a overexpression, in comparison with a negative control (scrambled sequence) miRNA mimic. Additionally, untreated cells were also transcriptionally profiled as a further control. Nine RNA-seq libraries were prepared, with three replicates for each condition.

4.3.1 Sequencing data

Almost 580 million raw sequencing reads were generated from the nine RNA-seq libraries, with approximately 65 million reads in each library. In total, 430 million reads (or 75% of all reads) aligned unambiguously to the genome, and with assigned features. The rest of the reads aligned ambiguously, or had no annotation. The library

sequencing depth ranged from 43 million to 54 million reads. Table 4-1 summarizes the number of reads at each data processing step.

Table 4-1 | Summary of read counts. For each sample the input count numbers for each program used in the data processing are shown.

Sample	Trim Galore	Tophat (aligned pairs)	Featurecounts (input)	Featurecounts (output)
Untreated cells 1	62,493,079	56,863,176	61,335,753	46,685,732
Untreated cells 2	61,583,066	55,926,679	60,437,378	45,750,541
Untreated cells 3	56,854,497	51,301,343	55,751,269	42,953,343
Negative control mimic 1	72,459,581	65,795,376	71,043,819	54,298,199
Negative control mimic 2	66,669,426	60,032,488	65,265,312	50,716,288
Negative control mimic 3	56,168,673	50,797,569	55,016,334	42,029,244
miR-146a mimic 1	62,312,592	56,382,357	61,028,837	45,627,048
miR-146a mimic 2	69,497,691	62,945,092	68,096,091	51,295,252
miR-146a mimic 3	70,060,713	63,192,276	68,602,006	51,800,244

After filtering for low numbers of reads and normalization, a correlation plot of genes (above 10 RPM) was prepared with edgeR, which shows that expression profiles were highly correlated across replicates (Figure 4-1). Similarly, an MDS plot was prepared to visualize the level of similarity between samples, based on $\log_2$ fold changes in expression of genes (Figure 4-2). Samples were clearly differentiated and grouped according to treatment status (i.e. untreated versus scrambled miRNA-transfected versus miR-146a- transfected samples), indicating a distinct gene expression profile in each case.

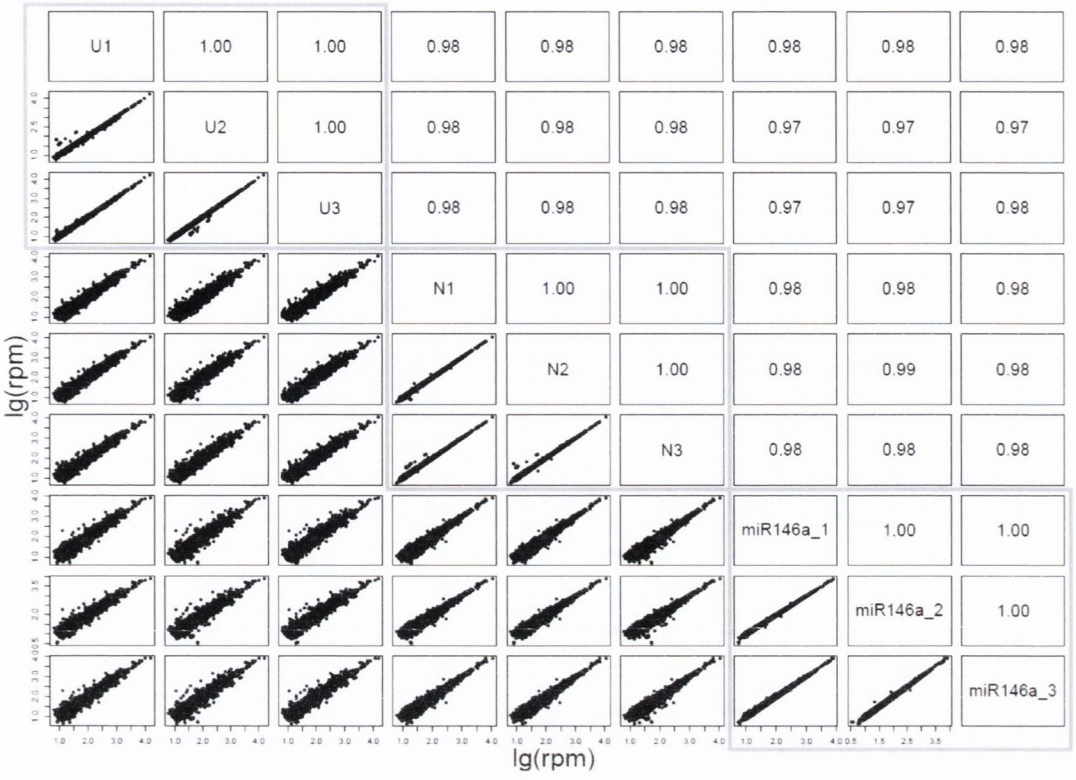

Figure 4-1 | Scatter plot of genes expressed above 10 RPM in all samples. Comparisons within one treatment are in grey rectangles. Treatment conditions and replicate numbers are shown in the diagonal panels, and correlation coefficients are shown in the upper panel. Expression profiles were highly correlated across replicates. U: untreated cells, N: negative control, miR146a: miR-146a mimic treated cells.

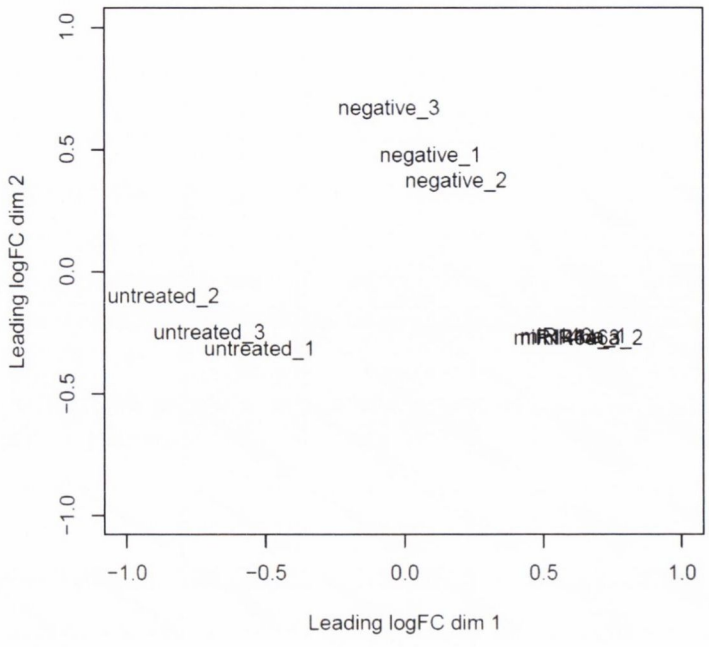

Figure 4-2 | Multi-dimensional scaling (MDS) plots comparing transcriptomic profiles of untreated and miRNA-mimic treated cells. The three replicates for untreated Bomac cells ("untreated"), scrambled control mimic-transfected cells ("negative"), and miR-146a-transfected cells ("miR-146a") are shown. Samples were differentiated and grouped according to treatment status.

4.3.2 Upregulated genes in the negative control miRNA treated cells

There were 108 upregulated and 70 downregulated genes in the negative control miRNA treated cells, in comparison with untreated cells (Appendix 6). Among the most highly upregulated genes (Table 4-2) were interferon beta 2 (*IFNB2 / IL6,* FC = 11.7, p-value = 1.82×10^{-15}) and interferon beta 3 (*IFNB3,* FC = 9.4, p-value = 2.86×10^{-42}). Interferon beta 2, also known as IL-6, is a pro-inflammatory cytokine produced by T cells and macrophages in response to recognition of pathogen-associated molecular patterns (PAMPs) (Tanaka and Kishimoto, 2014). The bovine *IFNB3* is annotated as a member of the GO category 'Defence response to virus'. Other highly upregulated genes were interleukin 8 (*CXCL8 / IL8,* FC = 8.8, p-value = 4.85×10^{-44}) and the chemokine (C-X-C motif) ligand 1 (*CXCL1 / GRO1,* FC = 6.7, p-value = 1.59×10^{-26}). IL-8 is

secreted by multiple cell types, including macrophages, and its function is to recruit neutrophil granulocytes, and other immune cells (Zarogoulidis *et al.*, 2014). Upregulation of these and other cytokines, the CCL2 and CCL5, suggests that the RNA transfection was interpreted by the cell as a viral infection. Several PRRs recognize intracellular RNA; RIG-I (retinoic acid-inducible gene 1), PKR (protein kinase R), and TLR3 directly bind to double-stranded RNA, meanwhile, TLR7 and TLR8 are receptors for single-stranded RNA (Mogensen, 2009).

An alternative explanation for the response observed to transfection with the scrambled negative control miRNA is that overexpression leads to saturation of RISC complexes and displaces other endogenous miRNAs (Khan *et al.*, 2009). The displacement of endogenous miRNAs from the RISC complex can lead to increased expression of their target genes, which are now relieved from suppression by these miRNAs (Khan *et al.*, 2009). This explanation is less likely, however, given that up-regulated genes were enriched for roles in innate immunity and anti-viral responses (the top 20 genes contains many interferon or interferon inducible genes) (Table 4-3) suggesting that this is a specific immune response to transfection and not due to a dysregulation of endogenous miRNA responses which would result in a wide range of pathways and processes being affected. In either case, the results highlight the importance of using negative control mimics in miRNA overexpression experiments.

Table 4-2 | Upregulated genes in Bomac cells treated with scrambled negative control miRNA mimic, in comparison with untreated cells.

Top 20 genes are shown, sorted by fold-change.

Ensembl gene ID	Gene name	Description	Fold change	p-value (FDR)
ENSBTAG00000033695	*IFNB2*	Interferon beta-2	11.7	1.82×10^{-15}
ENSBTAG00000046324		Uncharacterized protein	9.6	6.22×10^{-9}
ENSBTAG00000046849	*IFNB3*	Interferon beta-3	9.4	2.86×10^{-42}
ENSBTAG00000019716	*CXCL8*	Bos taurus interleukin 8 (IL8), mRNA.	8.8	4.85×10^{-44}
ENSBTAG00000046456	*IL6*	Bos taurus interleukin 6 (interferon, beta 2) (IL6), mRNA.	7.6	2.59×10^{-22}
ENSBTAG00000037558	*GRO1*	Bos taurus chemokine (C-X-C motif) ligand 1 (melanoma growth stimulating activity, alpha) (GRO1), mRNA.	6.7	1.59×10^{-26}
ENSBTAG00000037811	*CCL2*	Bos taurus chemokine (C-C motif) ligand 2 (CCL2), mRNA.	6.2	7.59×10^{-22}
ENSBTAG00000015060	*GBP5*	Bos taurus guanylate binding protein 5 (GBP5), mRNA.	6.0	1.29×10^{-11}
ENSBTAG00000007191	*CCL5*	Bos taurus chemokine (C-C motif) ligand 5 (CCL5), mRNA.	5.4	2.63×10^{-249}
ENSBTAG00000005990	*S1PR1*	Bos taurus sphingosine-1-phosphate receptor 1 (S1PR1), mRNA.	5.2	5.34×10^{-81}
ENSBTAG00000046336	*RNPS1*	RNA binding protein S1, serine-rich domain	5.1	3.77×10^{-11}
ENSBTAG00000009768	*IFIT3*	Bos taurus interferon-induced protein with tetratricopeptide repeats 3 (IFIT3), mRNA.	5.1	1.79×10^{-79}
ENSBTAG00000034918	*IFIT2*	interferon-induced protein with tetratricopeptide repeats 2	4.8	5.11×10^{-46}
ENSBTAG00000030921	*FAM3B*	family with sequence similarity 3, member B	4.6	2.81×10^{-43}
ENSBTAG00000018366	*SLC15A3*	Solute carrier family 15, member 3	4.6	6.19×10^{-15}
ENSBTAG00000008471	*MX2*	MX dynamin-like GTPase 2	4.5	1.02×10^{-46}
ENSBTAG00000015727	*IFI47*	Bos taurus interferon gamma inducible protein 47 (IFI47), mRNA.	4.5	1.15×10^{-31}
ENSBTAG00000004381	*TACSTD2*	tumour-associated calcium signal transducer 2	4.4	4.07×10^{-19}
ENSBTAG00000022396	*SAA3*	Bos taurus serum amyloid A 3 (SAA3), mRNA.	4.3	2.04×10^{-11}
ENSBTAG00000039035	*HSPA6*	heat shock 70kDa protein 6 (HSP70B')	4.2	4.91×10^{-44}

Table 4-3 | Overrepresented KEGG pathways among upregulated genes. Pathways with a corrected p-value < 0.05 are shown.

Pathway	KEGG number	p-value (FDR)
Cytokine-cytokine receptor interaction	04060	3.47×10^{-5}
Rheumatoid arthritis	05323	3.47×10^{-5}
NOD-like receptor signalling pathway	04621	2.33×10^{-4}
Chemokine signalling pathway	04062	4.42×10^{-3}
Staphylococcus aureus infection	05150	2.91×10^{-2}

*Rheumatoid arthritis is an autoimmune joint disease characterized by persistent inflammation. IL-6 and other proinflammatory cytokines play a key role in this disease, which explains the presence of the KEGG pathway 'Rheumatoid arthritis' (Yoshida and Tanaka, 2014).

**Similarly, IL-6 and IL-8, among other cytokines, are induced by *Staphylococcus aureus* infection (Bishayi *et al.*, 2014).

4.3.3 Downregulated genes in the negative control miRNA treated cells

The number of downregulated genes (Table 4-4) was less than the number of upregulated, which is consistent with the assumption that the transfected miRNA mimic negative control does not function as a true miRNA. It is a randomised miRNA sequence that has been tested and shown to not produce effects similar to known miRNAs, thus should not be capable of gene silencing. The most highly downregulated genes were a new mitochondrial tRNA gene (FC = -3.6, p-value = 1.55×10^{-57}) and *CXCL9* (FC = -3.2, p-value = 1.20×10^{-11}).

Pathway overrepresentation analysis returned only two significant pathways (Table 4-5). The overrepresentation of genes in 'Oxidative phosphorylation' is also evident from the list of upregulated genes, and may be due to dysregulation of gene expression by the transfection. Another plausible explanation is that cytokine production shuts down oxidative phosphorylation in a negative feedback. Activated immune cells prefer to use glycolysis, as it is faster than oxidative phosphorylation (Delmastro-Greenwood and Piganelli, 2013). For example, activated lymphocytes switch the source of ATP from oxidative phosphorylation to glycolysis, and macrophages activated by proinflammatory cytokines, such as IL-6, are known to use glycolysis (Delmastro-Greenwood and Piganelli, 2013). Similarly, IL-6 enhances production of reactive oxygen species (ROS), which in turn impair oxidative

phosphorylation through oxidation of mitochondrial lipids and respiratory enzymes (Ouyang *et al.*, 2015). Oxidative stress is thought to contribute to the development of Parkinson's disease, which may explain the overrepresentation of the KEGG pathway 'Parkinson's disease' (Chen and Zhong, 2014).

It may be concluded from these results that transfection of cells with short double stranded RNA – miRNA mimics – induces extensive changes in the transcriptome. These underline the importance of using scrambled miRNAs – as opposed to untreated cells – as the appropriate negative control. More work is needed to decipher the consequences of miRNA transfection or overexpression, and the exact cause and mechanism of subsequent gene dysregulation.

Table 4-4 | Downregulated genes in Bomac cells treated with scrambled negative control miRNA mimic, in comparison with untreated cells. Top 20 genes are shown, sorted by fold-change.

Ensembl gene ID	Gene name	Description	Fold change	p-value (FDR)
ENSBTAG00000043583		Novel Mt tRNA	-3.6	1.55×10^{-57}
ENSBTAG00000038639	*CXCL9*	Bos taurus chemokine (C-X-C motif) ligand 9 (CXCL9), mRNA.	-3.2	1.20×10^{-11}
ENSBTAG00000033160	*FAM114A1*	family with sequence similarity 114, member A1	-3.2	1.74×10^{-129}
ENSBTAG00000006326	*ALDH1L2*	Bos taurus aldehyde dehydrogenase 1 family, member L2 (ALDH1L2), mRNA.	-2.9	1.23×10^{-136}
ENSBTAG00000015441	*ACTB*	Actin, cytoplasmic 1	-2.8	4.98×10^{-10}
ENSBTAG00000006037	*WISP2*	WNT1 inducible signalling pathway protein 2	-2.8	1.73×10^{-26}
ENSBTAG00000043550	*MT-CYB*	Cytochrome b	-2.7	9.39×10^{-126}
ENSBTAG00000003791	*LPAR3*	lysophosphatidic acid receptor 3	-2.7	4.97×10^{-60}
ENSBTAG00000018400	*BRMS1L*	Bos taurus breast cancer metastasis-suppressor 1-like (BRMS1L), mRNA.	-2.7	3.05×10^{-94}
ENSBTAG00000007962	*ATP9A*	ATPase, class II, type 9A	-2.7	3.30×10^{-124}
ENSBTAG00000005871	*MECOM*	MDS1 and EVI1 complex locus	-2.7	7.61×10^{-9}
ENSBTAG00000007444	*C1H21ORF7*	C1H21ORF7 protein; Uncharacterized protein	-2.6	3.19×10^{-12}
ENSBTAG00000043559	*MT-ND4L*	NADH-ubiquinone oxidoreductase chain 4L	-2.5	4.59×10^{-123}
ENSBTAG00000034075	*SLC7A11*	Solute carrier family 7 member 11	-2.5	3.08×10^{-21}
ENSBTAG00000001745	*LUM*	Bos taurus lumican (LUM), mRNA.	-2.5	1.35×10^{-42}
ENSBTAG00000015214	*CA3*	Bos taurus carbonic anhydrase III, muscle specific (CA3), mRNA.	-2.5	4.79×10^{-16}
ENSBTAG00000018829	*SPRYD7*	Bos taurus SPRY domain containing 7 (SPRYD7), mRNA.	-2.5	1.78×10^{-49}
ENSBTAG00000012693		Novel protein coding gene	-2.5	1.58×10^{-20}
ENSBTAG00000043577	*MT-ND4*	NADH-ubiquinone oxidoreductase chain 4	-2.4	3.46×10^{-111}
ENSBTAG00000006599	*INHBE*	Bos taurus inhibin, beta E (INHBE), mRNA.	-2.4	4.77×10^{-37}

Table 4-5 | Overrepresented KEGG pathways among downregulated genes.
Pathways with a corrected p-value < 0.05 are shown are shown.

Pathway	KEGG number	p-value (FDR)
Oxidative phosphorylation	00190	7.07×10^{-6}
Parkinson's disease	05012	6.95×10^{-5}

4.3.4 Differentially expressed genes in miR-146a mimic transfected cells, in comparison to the negative control mimic

In total, there were 79 downregulated and 46 upregulated genes (Figure 4-3, Appendix 7). Among the most highly downregulated genes (Table 4-6) were the genes encoding Metazoan signal recognition particle RNA, Nuclear RNase P, 5S and 5.8S ribosomal RNAs, U1 spliceosomal RNA. Another gene, *RAB7L1* (RAB7, member RAS oncogene family-like 1) is a member of the Rab family, which regulates membrane traffic. In CHAPTER 3, several members of this family, including RAB7A, were predicted to be targeted by miRNAs upregulated in alveolar macrophages response to *Mycobacterium* infection. Notably, several novel miRNA genes, and bta-mir-2904-1 – which has no orthologs, and no known function – were also found to be downregulated.

Although miRNAs act primarily by gene silencing, there are a few ways through which they can cause upregulation of a gene: for example, by targeting a transcription factor that negatively regulates gene expression. The number of upregulated genes (Table 4-7) was less than the number of downregulated genes. This may be due to the fact that increase of mRNA stability via miRNA targeting is less frequent than causing downregulation (Vasudevan, 2012). The most highly upregulated gene was a yet uncharacterized protein, composed of 212 amino acids (Ensembl ID: ENSBTAG00000046324), followed by *TNFRSF11B,* a cytokine receptor. The exact role of *TNFRSF11B* and other upregulated genes here is yet to be clarified.

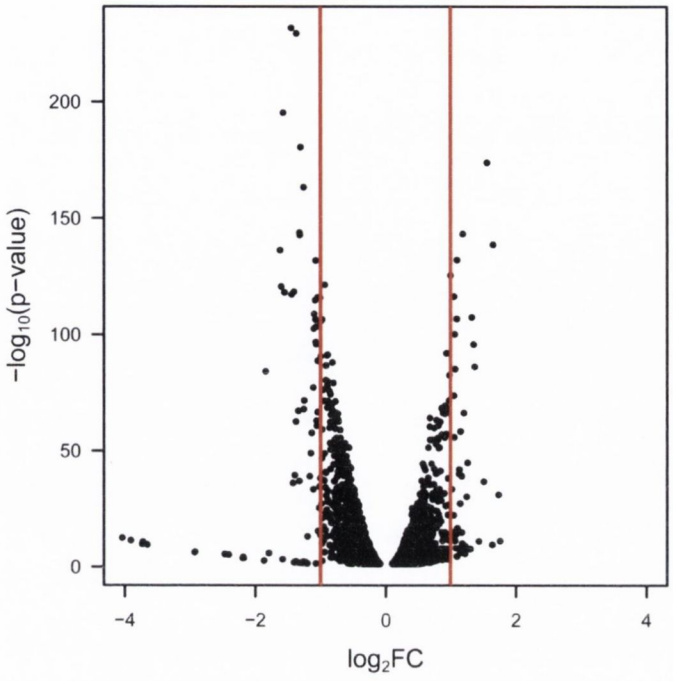

Figure 4-3 | Volcano plot of differentially expressed genes. Genes with corrected p-value <0.05 are shown. The threshold of fold change 2 is marked with a red line.

Table 4-6 | Downregulated genes in miR-146a overexpressed Bomac cells, in comparison with scrambled negative control miRNA mimic treated cells. Top 20 genes are shown, sorted by fold-change.

Ensembl gene ID	Gene name	Description	Fold change	p-value (FDR)
ENSBTAG00000045661	Metazoa_SRP	Metazoan signal recognition particle RNA	-16.5	3.06×10^{-13}
ENSBTAG00000046912	Metazoa_SRP	Metazoan signal recognition particle RNA	-15.0	3.63×10^{-12}
ENSBTAG00000042458	RNase_MRP	RNase MRP	-13.3	1.35×10^{-10}
ENSBTAG00000047908	Metazoa_SRP	Metazoan signal recognition particle RNA	-13.2	1.35×10^{-11}
ENSBTAG00000044427	RNaseP_nuc	Nuclear RNase P	-12.6	2.22×10^{-10}
ENSBTAG00000038155	U1	U1 spliceosomal RNA	-7.6	4.09×10^{-7}
ENSBTAG00000047122	5S_rRNA	5S ribosomal RNA	-7.6	2.58×10^{-7}
ENSBTAG00000048148	5_8S_rRNA	5.8S ribosomal RNA	-5.5	2.56×10^{-6}
ENSBTAG00000047401	5_8S_rRNA	5.8S ribosomal RNA	-5.5	2.71×10^{-6}
ENSBTAG00000045825	5_8S_rRNA	5.8S ribosomal RNA	-5.3	4.49×10^{-6}
ENSBTAG00000046797	NRAS	Bos taurus neuroblastoma RAS viral (v-ras) oncogene homolog (NRAS), mRNA.	-5.1	0
ENSBTAG00000046304	U1	U1 spliceosomal RNA	-4.6	1.12×10^{-4}
ENSBTAG00000043250	7SK	7SK RNA	-4.6	4.26×10^{-5}
ENSBTAG00000045741	U1	U1 spliceosomal RNA	-4.5	1.18×10^{-4}
ENSBTAG00000003836	ADAM19	ADAM metallopeptidase domain 19	-4.3	0
ENSBTAG00000046695		Novel miRNA	-3.6	1.67×10^{-3}
ENSBTAG00000013168	RPA3	Bos taurus replication protein A3, 14kDa (RPA3), mRNA.	-3.6	6.21×10^{-85}
ENSBTAG00000045952	5_8S_rRNA	5.8S ribosomal RNA	-3.5	9.70×10^{-7}
ENSBTAG00000003232	RAB7L1	Bos taurus RAB7, member RAS oncogene family-like 1 (RAB7L1), mRNA.	-3.1	5.39×10^{-137}
ENSBTAG00000010984	CDKN2AIPNL	CDKN2A interacting protein N-terminal like	-3.0	2.23×10^{-121}

Table 4-7 | Upregulated genes in miR-146a overexpressed Bomac cells, in comparison with scrambled negative control miRNA mimic treated cells. Top 20 genes are shown, sorted by fold-change.

Ensembl gene ID	Gene name	Description	Fold change	p-value (FDR)
ENSBTAG00000046324		Uncharacterized protein	3.4	5.49×10^{-12}
ENSBTAG00000007423	TNFRSF11B	Bos taurus tumour necrosis factor receptor superfamily, member 11b (TNFRSF11B), mRNA.	3.3	6.43×10^{-32}
ENSBTAG00000007191	CCL5	Bos taurus chemokine (C-C motif) ligand 5 (CCL5), mRNA.	3.1	2.16×10^{-139}
ENSBTAG00000037539	VCAM1	Bos taurus vascular cell adhesion molecule 1 (VCAM1), mRNA.	3.1	2.20×10^{-10}
ENSBTAG00000046054	RHOB	Bos taurus ras homolog gene family, member B (RHOB), mRNA.	2.9	1.12×10^{-174}
ENSBTAG00000008612	C1R	Bos taurus complement component 1, r subcomponent (C1R), mRNA.	2.8	1.34×10^{-37}
ENSBTAG00000009153	MLXIPL	MLX interacting protein-like	2.7	7.59×10^{-12}
ENSBTAG00000018400	BRMS1L	Bos taurus breast cancer metastasis-suppressor 1-like (BRMS1L), mRNA.	2.6	5.57×10^{-87}
ENSBTAG00000009984	SGPL1	Bos taurus sphingosine-1-phosphate lyase 1 (SGPL1), mRNA.	2.5	1.52×10^{-96}
ENSBTAG00000007962	ATP9A	ATPase, class II, type 9A	2.5	3.31×10^{-108}
ENSBTAG00000001785	TGM3	Bos taurus transglutaminase 3 (E polypeptide, protein-glutamine-gamma-glutamyltransferase) (TGM3), mRNA.	2.5	1.44×10^{-8}
ENSBTAG00000006048	DCAKD	Dephospho-CoA kinase domain-containing protein	2.4	1.09×10^{-45}
ENSBTAG00000008105	RBM38	RNA binding motif protein 38	2.4	4.33×10^{-31}
ENSBTAG00000033695	IFNB2	Interferon beta-2	2.3	4.86×10^{-8}
ENSBTAG00000004840	C1S	Bos taurus complement component 1, s subcomponent (C1S), mRNA.	2.3	8.29×10^{-10}
ENSBTAG00000005871	MECOM	MDS1 and EVI1 complex locus	2.3	1.52×10^{-6}
ENSBTAG00000018948	HIF3A	Bos taurus hypoxia inducible factor 3, alpha subunit (HIF3A), mRNA.	2.3	4.47×10^{-7}
ENSBTAG00000033160	FAM114A1	family with sequence similarity 114, member A1	2.3	4.26×10^{-67}
ENSBTAG00000004438	XPNPEP1	Bos taurus X-prolyl aminopeptidase (aminopeptidase P) 1, soluble (XPNPEP1), mRNA.	2.3	5.30×10^{-144}
ENSBTAG00000002850	HEATR9	HEAT repeat containing 9	2.3	7.10×10^{-11}

4.3.5 Differentially expressed genes with seed match to miR-146a

Comparison of miR-146a targets in miRTarBase with downregulated genes, confirms targeting of *IRAK1* (FC = -2.7, p-value = 3.74×10^{-119}), which was investigated in CHAPTER 3. Similarly, *TGFBR2,* another gene studied in CHAPTER 3, was also significantly downregulated (FC = -1.28, p-value = 3.39×10^{-19}), but did not meet the threshold for fold change. *IRAK1* also has a seed match with miR-146a, as predicted by TargetScan. Six other down-regulated genes were identified with a seed match to miR-146a. These genes are the most likely to be directly targeted by miR-146a (Table 4-8). DCP1A (DCP1 decapping enzyme homolog A) is involved in mRNA decay and also in the TGF-β pathway through an interaction with SMAD4 (Dougherty *et al.*, 2014). Importantly, none of the upregulated genes had a seed match with miR-146a as predicted in TargetScan, and also none of them were annotated in miRTarBase as targets of miR-146a, supporting our conclusion that the upregulated genes are indirectly regulated by this miRNA.

Table 4-8 | Downregulated genes with seed match to miR-146a.

Ensembl ID	Gene name	Fold change	p-value (FDR)
ENSBTAG00000010863	DCP1 decapping enzyme homolog A *(DCP1A)*	-2.4	4.32×10^{-164}
ENSBTAG00000014151	RCSD domain containing 1 *(RCSD1)*	-2.1	4.25×10^{-104}
ENSBTAG00000016085	Interleukin-1 receptor-associated kinase 1 *(IRAK1)*	-2.7	3.74×10^{-119}
ENSBTAG00000001754	Adenosylhomocysteinase-like 2 *(AHCYL2)*	-2.0	5.05×10^{-39}
ENSBTAG00000014333	Solute carrier family 1, member 3 *(SLC10A3)*	-2.5	1.52×10^{-143}
ENSBTAG00000010984	CDKN2A interacting protein N-terminal like *(CDKN2AIPNL)*	-3.0	2.23×10^{-121}
ENSBTAG00000046797	Neuroblastoma RAS viral (v-ras) oncogene homolog *(NRAS)*	-5.1	0

4.3.6 Pathway analysis of differentially expressed genes

Pathway analysis of differentially expressed genes using IPA, identified several statistically enriched pathways and biological processes (Table 4-9). The top canonical pathways together draw a picture of miR-146a having a role in initiating the immune response through macrophage activation and mobilization. The acute phase response is a rapid inflammatory response that provides protection against microorganisms. The

overrepresentation of the pathway 'Acute Phase Response Signalling' is consistent with the role of miR-146a as a negative feedback regulator of inflammation (So *et al.*, 2013). Similarly, HMGB1 (High-mobility group protein B1), a nuclear protein, and its signalling pathway mediate the activation of innate immune response and promotes inflammation (Figure 4-4) (Andersson and Tracey, 2011) (Harris *et al.*, 2012). The overrepresentation of the pathway 'Role of Macrophages, Fibroblasts and Endothelial Cells in Rheumatoid Arthritis' is explained by the fact that the autoimmune disease, rheumatoid arthritis, is characterized by inflammation and upregulation of miR-146a in humans (Chan *et al.*, 2013).

A list of putative molecules that could be upstream regulators of the differentially expressed genes, as predicted by IPA, is shown in Table 4-9. Among these was miR-21, which would suggest that miR-21 and miR-146a has similar or complementing functions. Indeed, miR-21 has been described, along with miR-155, miR-146a, as upregulated in the macrophage inflammatory response to infection (Rusca and Monticelli, 2011). Another upstream regulator, IFI16 (Interferon gamma inducible protein 16) has been described as having a role in differentiation and maturation of the myelomonocytic lineage (Luan *et al.*, 2008). More recently, its role as an intracellular (viral) DNA sensor was identified (Unterholzner *et al.*, 2010). Another upstream regulator, lymphotoxin-α1-β2 (LT-α1-β2), a heterotrimer of LT-α and -β, mediates a large variety of inflammatory, immunostimulatory, and antiviral responses (Upadhyay and Fu, 2013). TGFB1 was also indicated as potential cause of differential expression, which agrees with the observation that miR-146a targets SMAD4, a member of the TGF-β signalling pathway (Kamato *et al.*, 2013). Additionally, in CHAPTER 3 we have shown the downregulation of TGFBR2 by miR-146a, which may act as negative feedback.

Table 4-9 | IPA analysis of downregulated and upregulated genes. Top canonical pathways and potential upstream regulators (p-value of overlap) are shown.

Ingenuity Canonical Pathways	p-value	Molecules
Acute Phase Response Signalling	7.41×10^{-5}	C1R, NRAS, C1S, C2, TNFRSF11B, IRAK1
HMGB1 Signalling	1.45×10^{-4}	VCAM1, NRAS, RHOB, TNFRSF11B, PLAT
Complement System	3.47×10^{-4}	C1R, C1S, C2
Granulocyte Adhesion and Diapedesis	8.71×10^{-4}	VCAM1, CCL5, TNFRSF11B, MMP19, IL18RAP
Role of Macrophages, Fibroblasts and Endothelial Cells in Rheumatoid Arthritis	1.55×10^{-3}	VCAM1, NRAS, CCL5, TNFRSF11B, IL18RAP, IRAK1

Upstream regulator	Molecule type	p-value	Target molecules in dataset
mir-21	microRNA	1.96×10^{-7}	C1R, GBP5, HMGA2, IFNB1, IRAK1, PLAT, RHOB, VCAM1
IFI16	transcription regulator	8.03×10^{-6}	CCL5, CYP1A1, IFNB1, RPA3, VCAM1
genistein	chemical drug	1.76×10^{-5}	CCL5, CD74, CYP1A1, IFNB1, PLAT, PXMP4, TNFRSF11B, VCAM1
lymphotoxin-α1-β2	complex	2.03×10^{-5}	CCL5, IFNB1, VCAM1
TGFB1	growth factor	4.07×10^{-5}	ACTC1, ADAM19, C1S, C2, CCL5, CDC42SE1, FGF5, HMGA2, MLXIPL, OSTF1, PLAT, RHOB, ROR1, SLC39A14, TGIF1, TNFRSF11B, TRIM2, VCAM1

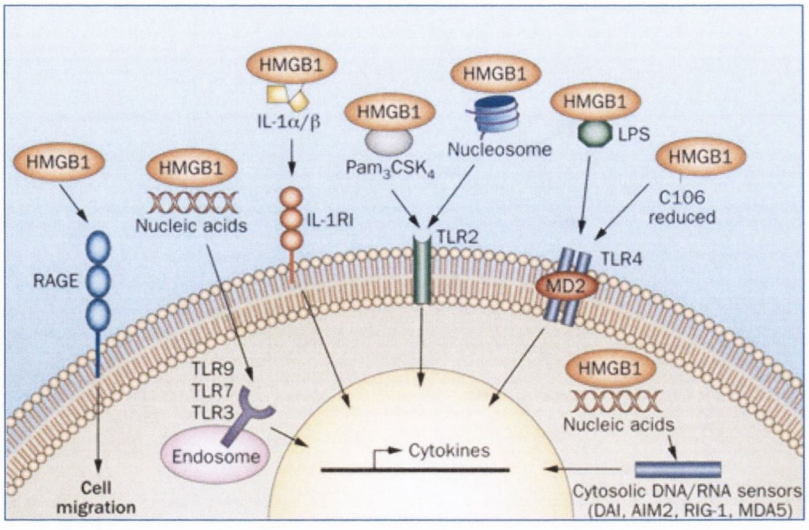

Figure 4-4 | Signalling by HMGB1. Extracellular HMGB1 (High-mobility group protein B1) induces cytokine production, cell migration, proliferation and differentiation by interaction with TLR2, TLR4, TLR9 and RAGE (Receptor for Advanced Glycation End products). Source: Harris et al., 2012, *Nat. Rev. Rheumatol. 8(4), pp. 195-202.*

4.3.7 Conclusion

The work in this Chapter shows that transfection of Bomacs with miRNA mimics appears to induce an antiviral immune response, which highlights the importance of using appropriate controls, i.e. the negative control (scrambled) sequences as opposed to untreated cells. Transfection with miR-146a identified more than 100 genes that were differentially expressed in comparison to negative control. These genes were enriched for roles in the acute phase response, HMGB1 signalling and complement system, all part of the early innate immune and inflammatory response. Relatively few – seven out of seventy-nine – downregulated genes had a seed match with miR-146a, which reflects the high false rate of computational approaches to predict genes regulated by a miRNA. Other explanations include the fact that many of the DE genes were not direct targets of miR-146a (Thomson *et al.*, 2011), or that the seed targets are not in the 3' UTR region. A limitation of this technology is the dependence on approach used; expression and CLIP (crosslinking and immunoprecipitation)-based approaches were found to return different miRNA-target

sets (Wen *et al.*, 2011). This concern is somewhat alleviated by the fact that the RNA-seq approach confirmed the targeting of *IRAK1* and *TGFBR2* as was found using SYBR Green RT-qPCR in CHAPTER 3. Overexpression experiments are commonly performed in cells that do not express the miRNA, which could skew results, although most miRNA-target interactions are not affected by the cell type (Nam *et al.*, 2014). In this study there is no such concern as macrophages express miR-146a.

This work confirmed roles of miR-146a described in the literature and identified several potentially interesting target genes for future studies. One of the advantages of RNA-seq is the possible re-analysis of data in light of more knowledge. Future work may reconsider the fold change threshold for differentially expressed genes or other parameters, or use better annotation of the bovine genome, leading to more conclusions from this dataset.

CHAPTER 5

MICRORNA-SEQ PROFILING OF PBMCS OF *MYCOBACTERIUM BOVIS* INFECTED CATTLE SHOWS REGULATION OF CELL CYCLE AND TGF-β RECEPTOR SIGNALLING BY DIFFERENTIALLY EXPRESSED MIRNAS

5.1 Introduction

Bovine tuberculosis is an infectious disease of cattle, which is caused by *Mycobacterium bovis*, and is a significant problem for global agriculture. Currently, the single intradermal comparative cervical tuberculin test (SICCT) is used for the diagnosis of this disease, which measures response to mycobacterial antigens (de la Rua-Domenech *et al.*, 2006). This test has high specificity (>99%), but lower sensitivity (70–90%), which leads to undetected animals in the herd, contributing to the spread of infection (Goodchild and Clifton-Hadley, 2001). A more sensitive (82–100%) and similarly specific (94–100%) test, the IFN-γ release assay (IGRA) is also used (Wood and Jones, 2001). However, improved diagnostic tests would help in controlling the disease. Investigating blood gene and miRNA expression profiles in TB infected animals – in comparison to uninfected – may identify new more accurate diagnostics, and will also contribute to the understanding of the molecular mechanisms underlying the disease. Gene expression studies in PBMCs from *M. bovis* infected cattle suggest that immune genes are repressed in long-term infections (MacHugh *et al.*, 2009). Decreased expression of the *IL8* cytokine gene and genes involved TLR signalling, among others, have been identified in TB-infected animals (Meade *et al.*, 2007). In contrast, stimulation of PBMCs with PPDb led to the induction of several genes associated with innate and adaptive immune responses, including those involved in antigen presentation and interferon signalling (Meade *et al.*, 2008). In humans, miRNA microarray experiments have identified that several miRNAs are differentially expressed in PBMCs from patients with active or latent tuberculosis (Wang *et al.*, 2011). The diagnostic potential of these miRNAs for human TB is being actively investigated and a recent study has identified three miRNAs in the serum of patients which distinguishes TB infected patients from healthy controls (Qi *et al.*, 2012). MicroRNAs have many properties that make them suitable as non-invasive biomarkers: miRNAs are abundantly expressed, in a stable form, in a range of extracellular fluids, are easily measured, and in many cases exhibit temporal and spatial specificity (Chen *et al.*, 2010, Hata *et al.*, 2010, De Guire *et al.*, 2013). The potential of using miRNAs to diagnose bovine TB is also being investigated. A recent study (published after our study was completed) has used a microarray approach to investigate the expression of miRNAs in bovine PBMCs isolated from *M. bovis*-challenged BCG vaccinated and unvaccinated animals. miR-155 was found to be significantly up-regulated both at week 2 and week 11 post-infection in unvaccinated cattle, but only at week 11 in BCG

vaccinated animals. No differential expression of miR-155 was observed in pre-infection samples from unvaccinated and vaccinated cattle, suggesting that miR-155 could be exploited as a marker distinguishing vaccinated from infected animals (Golby *et al.*, 2014).

Here, I report a next-generation sequencing based approach to profile miRNA expression in PBMCs isolated from healthy and TB-infected cattle. As discussed previously, next-generation sequencing has several advantages over microarrays, including its broad dynamic range and high sensitivity.

5.2 Materials and methods

5.2.1 Animals

All animal procedures were carried out according to the provisions of the Irish Cruelty to Animals Act. Blood samples from nine animals were used in the experiment. Five *M. bovis*-infected Holstein-Friesian bullocks were selected from a herd maintained for ongoing disease surveillance at the Irish Department of Agriculture, Fisheries and Food (Co. Kildare, Ireland). The animals had a positive tuberculin test (SICCT) result, and were also tested by the whole-blood IFN-γ based BoviGAM assay (Prionics AG, Switzerland). High levels of IFN-γ were detected in all infected blood samples tested in response to PPD stimulation. Four non-infected age, breed, and sex matched control animals were selected from a herd with no recent history of *M. bovis* infection. The control animals tested negative for the IFN-γ test.

5.2.2 Haematological analysis and PBMC isolation

Blood (30 mL) was collected in Vacuette Lithium-Heparin tubes (Greiner Bio-One, Germany) from each of the nine animals. Haematology analysis was carried out using an automated analyser (Advia 2120, Bayer Healthcare, Siemens, UK). PBMCs were isolated using Leucosep tubes (Greiner Bio-One) and 15 mL Histopaque 1077 (Sigma-Aldrich, Ireland) as a separation medium. To separate PBMCs, the blood was centrifuged at 1200 × g for 20 min and the buffy coat was transferred with a Pasteur pipet to a new 50 mL falcon tube. Cells were then washed in 15 mL PBS and centrifuged at 400 × g for 10 min. The supernatant was removed and the pellet was resuspended in 0.25% NaCl, in order to lyse any red blood cells carried over during the

separation procedure. Cells were then washed with PBS and centrifuged at 400 × g for 10 min to pellet. After washing (400 × g, 10 min in 15 mL PBS), cells were counted using a haemocytometer and 10 × 10^6 cells were pelleted in an eppendorf (400 × g, 5min). Pellet was loosened, then lysed with 1 mL TRIzol reagent (Invitrogen, UK), and stored at −80°C until further use.

5.2.3 Small RNA preparation

Total and small RNA fractions were extracted from TRIzol using the Qiagen RNeasy Plus Mini kit (Qiagen, UK). Total RNA and miRNA quantity and quality was determined using the Agilent 2100 Bioanalyzer (Agilent Technologies, Ireland) with the 6000 Nano and small RNA LabChip kits (Agilent Technologies). The prepared RNA was stored at −80°C until further use.

5.2.4 RNA-seq library preparation and sequencing data analysis

Nine RNA-seq libraries were prepared using the Illumina Truseq Small RNA Sample Preparation Kit (Illumina, USA), according to the manufacturer's protocol. Libraries were sequenced (50 bp single-end) on two flowcell lanes of an Illumina HiSeq 2000 machine (BGI Hong Kong, China), and more than 300 million raw reads were generated.

The quality and number of the reads for each sample were assessed using FASTQC (v0.10.0, http://www.bioinformatics.bbsrc.ac.uk/projects/fastqc/). The FASTQC results are shown in Electronic Appendix 14. Cutadapt (v1.2.1) (Martin, 2011) was used to trim 3' Illumina adapter sequences from reads. Reads which were less than 18 nt after trimming and all untrimmed reads were discarded. The remaining reads were then further filtered using FASTQ Quality Filter (FASTX Toolkit v0.0.13; http://hannonlab.cshl.edu/fastx_toolkit/). Reads where at least 30% of the bases had a Phred score < 20 were removed. Finally, reads passing all the above filters were also trimmed at their ends using FASTQ Quality Trimmer (FASTX Toolkit v0.0.13) to remove low quality bases (Phred score < 20), and reads less than 18 nt after the trimming were discarded.

After the quality control steps, the remaining reads were aligned to the bovine genome (UMD3.1 assembly (Zimin *et al.*, 2009)) using Novoalign (v2.08.03) in 'miRNA' mode, allowing one mismatch. Non-uniquely aligning reads were discarded. HTSeq-count in 'union' mode was then used to count aligned reads that overlapped

with known miRBase (version 19, http://www.mirbase.org) (Kozomara and Griffiths-Jones, 2011) miRNA gene annotations. To investigate the proportion of reads sequenced from non-miRNA genes, HTSeq-count was also used separately to count reads that overlapped with all bovine gene annotations from Ensembl version 69.

R (v3.1.1) was used to create the correlation plot, the dot plots and the volcano plots, and to perform the statistical analysis. EdgeR (v3.6.7) (Robinson *et al.*, 2010) was used to identify differentially expressed miRNAs, using upperquartile normalization. Differentially expressed miRNAs were defined as those that had a fold change > 1.5 and an FDR ≤ 0.05 in the edgeR analysis, and were expressed above a threshold of 100 read per million. All miRNAs were found differentially expressed using the other two normalization methods (TMM or RLE), therefore results are robust to using different normalization methods.

5.2.5 Target prediction and pathway analysis

The experimentally validated targets of differentially expressed miRNAs were obtained from miRTarBase (version 4.5) (Hsu *et al.*, 2014). The targets of down-regulated miRNAs and the targets of up-regulated miRNAs were analysed separately. Pathway annotations for all experimentally validated targets in miRTarBase were downloaded from InnateDB (www.innatedb.com) (Lynn *et al.*, 2008) for pathway analysis. Multiple genes from five gene families *(EIF, HNRNP, RPL, RPS, ZNF)* were predicted to be targeted by the same differentially expressed miRNAs. These genes also tended to be annotated to the same pathways, which could bias pathway analysis results. To correct for this bias, only one representative gene per family was used for subsequent pathway analysis. Overrepresented pathways were identified using the hypergeometric test, using pathway annotations for all experimentally validated miRNA targets as the background. Results were corrected for multiple testing using the Benjamini and Hochberg correction for the false discovery rate (Benjamini and Hochberg, 1995). Pathways with a Benjamini and Hochberg corrected p-value < 0.05 were considered statistically significant.

5.2.6 RT-qPCR validation of differentially expressed miRNA genes

The differential expression of two miRNAs, miR-222, miR-423, was tested using RT-qPCR. Three control and five infected samples were tested. One sample (Control 1) was omitted as it had insufficient RNA. Based on the RNA-seq data, bta-miR-16b and bta-miR-26b were used as non-differentially expressed internal reference genes.

The Applied Biosystems Taqman MicroRNA Reverse Transcription Kit was used, according to the manufacturer's protocol, and 5 µl of 10× diluted small RNA fraction was used in 15 µl reverse transcription reaction (30 min 16°C, 30 min 42°C, 5 min at 85°C, and then maintained at 4°C). Taqman MicroRNA Assays (Applied Biosystems) with TaqMan Universal Master Mix II (no UNG) (Applied Biosystems), were used according to the manufacturer's protocol.

A 7500 Fast Real-Time PCR System (Applied Biosystems, software version 2.0.6) was used with MicroAmp Fast optical 96-well plates and Optical Adhesive Films (Applied Biosystems). Amplification was performed using 20 µl/well and the following thermal cycle: 95°C 10 min, and 40 cycles: 95°C for 15 s, 60°C for 1 min. Technical replication was performed in triplicate and results were corrected for amplification efficiency. No amplification was measured in the no template and the reverse transcription control wells. The one-tailed paired Student's t-test was performed with R (v3.0.1) on the normalized and efficiency-corrected ΔC_t (quantification cycle) values, with a significance level of 0.05. Using the Pfaffl method (Pfaffl, 2001), fold changes were calculated from the $\Delta\Delta C_t$ values ($FC = 2^{-\Delta\Delta Ct}$), using the negative reciprocal for downregulated genes ($-1 / FC$).

5.3 Results and discussion

5.3.1 IFN-γ testing

High levels of IFN-γ were detected in all infected blood samples tested, in response to PPD stimulation. This confirms that the animals were tuberculosis positive. IFN-γ testing results are shown in Table 5-1. The healthy animals did not show substantial IFN-γ production.

Table 5-1 | IFN-γ release assay results for all animals. The concentration of IFN-γ (pg/mL) produced in response to avian PPD and bovine PPD are shown.

Animal ID	Control	Avian PPD	Bovine PPD
Control 1	29	109	157
Control 2	34	136	81
Control 3	36	55	78
Control 4	24	262	285
Infected 1	32	2345	3927
Infected 2	51	1977	3931
Infected 3	20	1165	2808
Infected 4	62	575	3933
Infected 5	140	805	3940

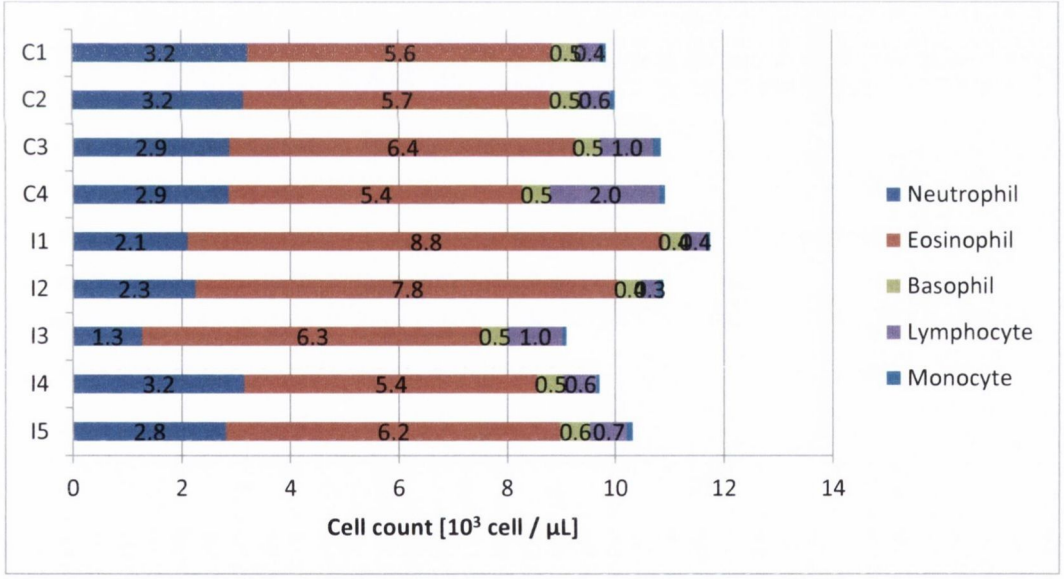

Figure 5-1 | Whole blood cell counts for infected and control samples. There was no statistically significant difference in the whole blood cell counts between infected and healthy control animals. C: control, I: infected.

5.3.2 Haematological analysis

The whole blood cell counts from tuberculosis infected animals were compared to those of the healthy control animals. The proportions of basophil, eosinophil and neutrophil granulocytes, lymphocytes, and monocytes in both groups are shown in Figure 5-1. There was no statistically significant difference in the whole blood cell counts (cell/μL) between infected and healthy control animals.

5.3.3 Small RNA

Total RNA concentration was between 110 and 460 ng/μL, and the range of miRNA concentration in the small RNA fraction was 1433–9123 pg/μL (Table 5-2).

Table 5-2 | Sample RNA concentrations.

Sample	Small RNA [pg/μl]	miRNA [pg/μl]
Control 1	153624	4258
Control 2	62741	2385
Control 3	59208	3575
Control 4	88793	8387
Infected 1	165044	9123
Infected 2	31848	1968
Infected 3	96354	4331
Infected 4	24094	1433
Infected 5	22427	2666

5.3.4 The miRNA-seq profile of healthy animals

In total, more than 300 million reads were generated from the nine libraries, with approximately 30–40 million reads in each library. After the processing steps, 53–59% aligned uniquely to the bovine genome, resulting in 16–23 million reads for each library. The rest of the reads were low quality reads, adapter sequences, and reads aligning to multiple places in the genome. For the read numbers at each step, see Table 5-3.

Table 5-3 | Read numbers at each data processing step. Input count numbers are shown for each program used in the pipeline. For Novoalign, the output reads are shown. Majority of the reads aligned to the genome (Novoalign / Aligned), and around 55% aligned uniquely to one location, (i.e. without ambiguity).

Sample	Cutadapt	Fastq filter	Fastq trimmer	Novoalign	Aligned	Unique alignment	Aligned / Processed	Unique alignment / Processed
Control 1	31,338,680	29,759,206	29,713,466	29,710,164	28,755,279	18,295,947	92%	58%
Control 2	34,622,088	30,767,894	30,719,771	30,716,226	29,947,017	19,008,681	86%	55%
Control 3	39,346,406	36,416,348	36,371,742	36,368,583	35,320,968	23,293,373	90%	59%
Control 4	35,772,629	32,207,811	32,169,230	32,166,838	31,333,778	20,609,791	88%	58%
Infected 1	40,120,991	36,588,626	36,544,049	36,541,043	34,692,138	21,379,986	86%	53%
Infected 2	29,574,778	27,262,220	27,218,060	27,214,629	24,943,089	16,051,924	84%	54%
Infected 3	31,312,005	28,964,153	28,917,646	28,913,252	28,081,995	17,628,240	90%	56%
Infected 4	32,498,038	28,617,397	28,572,631	28,568,667	27,786,801	17,687,782	86%	54%
Infected 5	34,810,316	32,310,976	32,272,559	32,269,889	31,417,014	19,143,036	90%	55%

In total, 90.1% of reads aligning to known gene annotations from Ensembl (v69) aligned to miRNAs, 7.8% to snoRNAs, 1% to mitochondrial RNAs, 0.6% to mRNAs, and the rest to other RNA types, including small nuclear RNAs, ribosomal RNAs (Figure 5-2). In healthy animals, 127 miRNAs were expressed above 100 RPM, a level below which miRNAs are less likely to be functional (Mullokandov *et al.*, 2012). The correlation plots show high correlation between the healthy samples and also between the infected samples, with slightly less correlation between healthy and infected samples, due to differentially expressed genes (Figure 5-3).

The PBMC miRNA profile of healthy animals is shown in Figure 5-4. The most highly expressed, miR-21-5p, was also found as most highly expressed in other bovine immune cell types, including alveolar macrophages, as found by us in CHAPTER 2, monocytes (Lawless *et al.*, 2014), and mammary epithelial cells (Lawless *et al.*, 2013), and has been shown to be important in vitamin D dependent defence in *Mycobacterium leprae*-infected human monocytes (Liu *et al.*, 2012). Other top expressed miRNAs also have functions in the immune system, for example, miR-150 has important roles in haematopoiesis and B or T cell differentiation (Undi *et al.*, 2013), and is expressed in mature B and T cells (He *et al.*, 2014). The miRNA read counts for all samples are shown in Electronic Appendix 15.

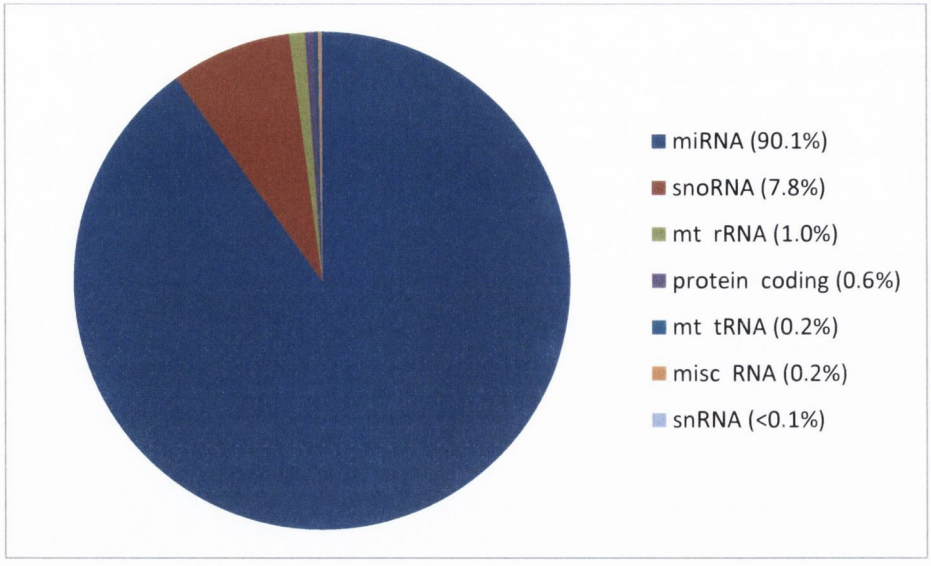

Figure 5-2 | The proportion of reads aligning uniquely to annotated bovine genes. Average of the nine samples is shown. 90.1% of annotated reads aligned to known miRNAs. snoRNA: small nucleolar RNA; mt: mitochondrial; snRNA: small nuclear RNA. Ribosomal RNA (rRNA) constituted less than 0.01% of reads (not shown).

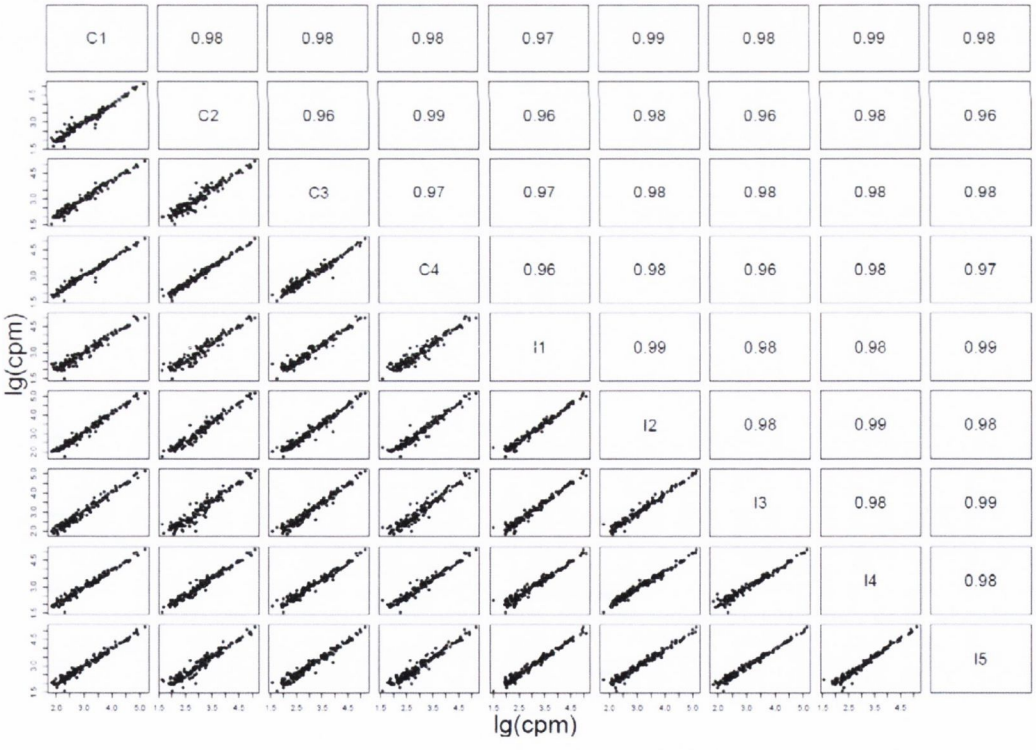

Figure 5-3 | Scatter plot of miRNAs expressed above 100 reads per million in healthy (C) and the infected (I) samples. Animal IDs are shown in the diagonal panels, and correlation coefficients are shown in the upper panel.

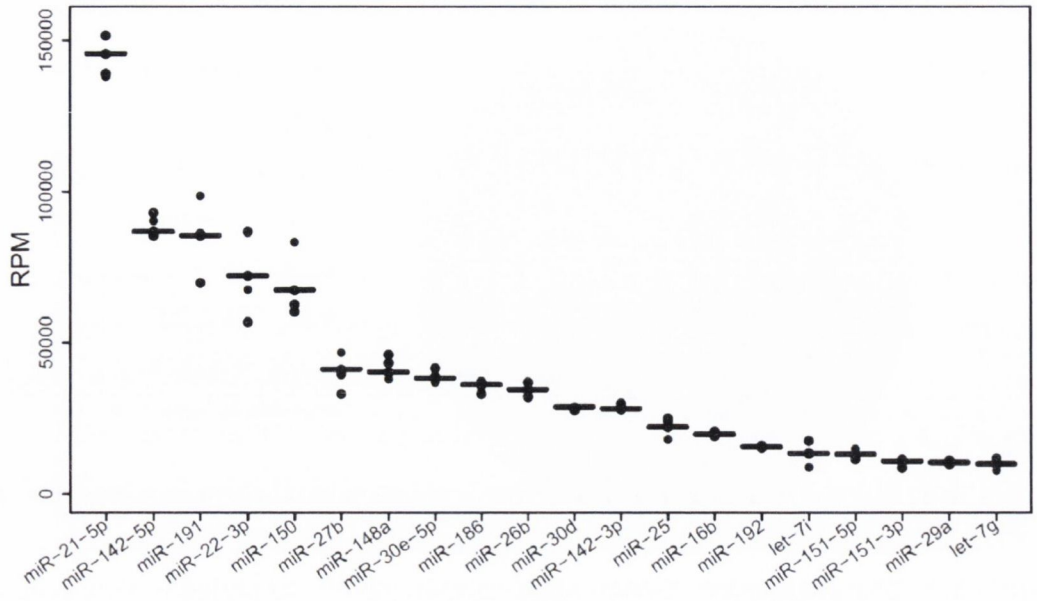

Figure 5-4 | The miRNA expression profile of PBMCs of healthy animals. The read per million values for the four healthy animals are shown.

5.3.5 Nine miRNAs are differentially expressed miRNAs between PBMCs of healthy and infected cattle

A multidimensional scaling plot was prepared to visualize the relative similarity of the expression profiles. The MDS plot readily separates infected and control samples (Figure 5-5), thus suggesting that miRNA profiles are specific for the infection status.

In total, nine miRNAs were found differentially expressed in PBMCs of *M. bovis* infected cattle, which represent 7% of the miRNAs expressed above 100 RPM in the animals (Figure 5-6). For full details of edgeR output for each tested miRNA see Electronic Appendix 16, and for the normalized count numbers for each differentially expressed miRNA, see Appendix 8. Among the upregulated miRNAs, miR-423, which was first described in cattle by Coutinho et al. (Coutinho *et al.*, 2007), had the highest read count (7500 RPM), and both miRNA arms were differentially expressed (miR-423-5p: 3600 RPM). It was also selected as promising biomarker of pulmonary tuberculosis infection using the TaqMan low-density array, however, the results were not confirmed in the subsequent RT-qPCR analysis (Qi *et al.*, 2012). Another upregulated miRNA, miR-31, targets MyD88, an adaptor protein of TLR2 signalling in mouse macrophages, and leads to suppression of TLR2 responses. Recently, miR-31 was found upregulated, in spleen, lymph nodes and peritoneal macrophages of BCG-

treated mice, showing that this miRNA regulates the TLR2 responses (Ghorpade *et al.*, 2013).

In contrast to our results, the homolog hsa-miR-222 was downregulated in human THP-1 cells, in response to *M. tuberculosis* challenge, meanwhile hsa-miR-18a was found upregulated (Das *et al.*, 2013). The differential expression of miRNAs above a threshold of 100 RPM is shown in Table 5-4. All miRNAs have a fold change above 1.5.

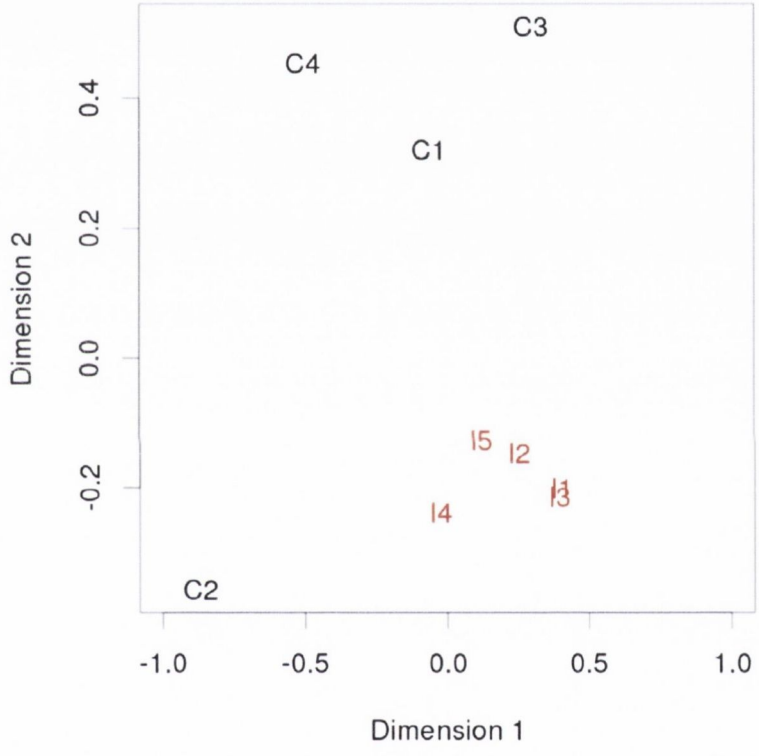

Figure 5-5 | Multidimensional scaling (MDS) plot comparing samples in the healthy (C) and infected (I) groups. Infected and control samples are separated, suggesting that miRNA profiles are specific for the infection status.

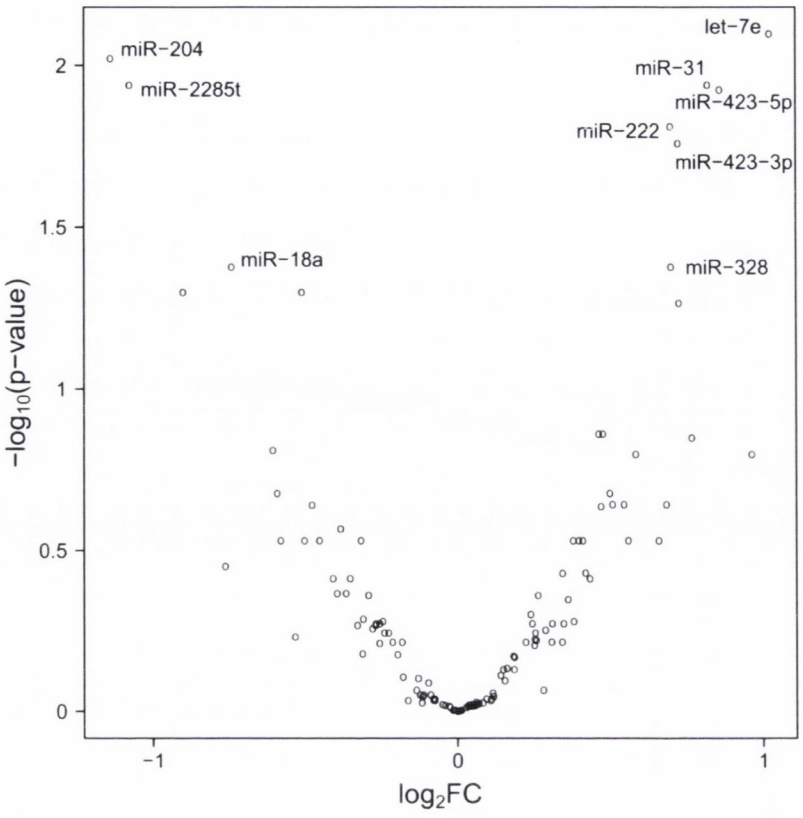

Figure 5-6 | Volcano plot showing edgeR results. The differentially expressed miRNAs are labelled.

Table 5-4 | Differentially expressed miRNAs in PBMCs of TB reactor animals. The results are sorted by expression levels. RPM: read per million; FDR: false discovery rate (corrected p-value).

miRNA	p-value	FDR	RPM	Fold change
bta-miR-423-3p	8.89×10^{-4}	1.75×10^{-2}	7521.7	1.65
bta-miR-423-5p	3.90×10^{-4}	1.19×10^{-2}	3634.3	1.81
bta-miR-222	6.29×10^{-4}	1.55×10^{-2}	1732.2	1.62
bta-miR-2285t	3.35×10^{-4}	1.15×10^{-2}	689.8	-2.13
bta-miR-204	1.73×10^{-4}	9.53×10^{-3}	354.8	-2.22
bta-miR-31	3.29×10^{-4}	1.15×10^{-2}	299.3	1.76
bta-miR-18a	3.05×10^{-3}	4.20×10^{-2}	266.7	-1.67
bta-let-7e	1.16×10^{-4}	8.00×10^{-3}	137.6	2.03
bta-miR-328	3.06×10^{-3}	4.20×10^{-2}	107.2	1.62

5.3.6 Differentially expressed miRNAs target cell cycle regulation and TGF-β receptor signalling

Pathway analysis of experimentally validated targets of the human homologs of upregulated miRNAs (miR-423-3p, miR-423-5p, miR-222, miR-31, let-7e, and miR-328) show overrepresentation of cell cycle related pathways (Table 5-5). The full list of targets is shown in Appendix 9, and the pathway analysis results are shown in Electronic Appendix 17. Three genes that are commonly targeted in these pathways are the cyclin dependent kinase inhibitor *(CDKN)* 1A, 1B and 2A, which act as cell cycle inhibitors. In humans, miR-423-3p has been experimentally verified to target *CDKN1A* (p21) (Lin *et al.*, 2011). miR-222 has also been experimentally validated to target *CDKN1B* (p27) and *CDKN1C* (p57), genes which act as cell cycle suppressors (Medina *et al.*, 2008, le Sage *et al.*, 2007, Kim *et al.*, 2009). Upregulation of miR-423-3p and miR-222 leads to downregulation of these cell cycle inhibitors, thus possibly promoting cell growth and proliferation of PBMCs. The human miR-222 has also been found to be partially responsible for monocyte differentiation in a myeloid leukemia cell line (Forrest *et al.*, 2010), and for monocyte function in response to infection (Sharbati *et al.*, 2012).

Table 5-5 | Pathway overrepresentation analysis of targets of upregulated miRNAs. Pathways with a corrected p-value < 0.05 are shown are shown.

Pathway Name	Pathway p-value (corrected)
C-MYB transcription factor network	0.028
Cell cycle, mitotic	0.028
Cell cycle	0.028
Cellular responses to stress	0.028

Pathway analysis of the targets of downregulated miRNAs (bta-miR-2285t, bta-miR-204, and bta-miR-18a) suggests that transforming growth factor beta receptor (TGFBR) signalling is preferentially targeted (p-value = 3.62×10^{-3}) by these miRNAs, which target TGFBR1/2 and TGF-β signal transducer proteins (SMAD) (Table 5-6). TGF-β regulates proliferation, differentiation and apoptosis (Kang *et al.*, 2009), and functions as a monocyte activator (Ashcroft, 1999). It also has a role in human macrophage deactivation and suppression of T cell responses to *M. tuberculosis,* thus leading to bacterium growth (Toossi and Ellner, 1998). Human miR-18a has been

experimentally validated to target *SMAD3, SMAD4* and *TGFBR2* (Dews *et al.*, 2010). Inhibition of SMAD3 has been shown to reduce *M. tuberculosis* induced signalling by TGF-β in human mononuclear phagocytes (Wu *et al.*, 2012b).

The human homolog of bta-miR-204 has also been shown to directly regulate several TGF-β pathway members, including TGFBR1 and 2 (Wang *et al.*, 2010). Other confirmed targets are *RAB22A* (Adijanto *et al.*, 2012) and *RAB40B* (Li *et al.*, 2011a). The Rab family of proteins have been shown to be necessary for clearance of mycobacteria and that the blockade of phagosome maturation by *M. tuberculosis* depends on Rab22A (Roberts *et al.*, 2006). These findings are also in agreement with earlier findings presented in this thesis, where I found that the TGF-β pathway and *RAB22A* was predicted to be targeted by miRNAs upregulated in *M. bovis* infected bovine alveolar macrophages.

Table 5-6 | Pathway overrepresentation analysis of targets of downregulated miRNAs. Pathways with corrected p-values less than 0.05 are shown.

Pathway Name	Pathway p-value (corrected)
TGFBR2 Kinase Domain Mutants in Cancer	3.62×10^{-3}
Signalling by TGF-beta Receptor Complex	3.62×10^{-3}
SMAD2/3 Phosphorylation Motif Mutants in Cancer	3.62×10^{-3}
SMAD2/3 MH2 Domain Mutants in Cancer	3.62×10^{-3}
Loss of Function of TGFBR2 in Cancer	3.62×10^{-3}
TGFBR1 KD Mutants in Cancer	3.62×10^{-3}
Loss of Function of TGFBR1 in Cancer	3.62×10^{-3}
TGFBR1 LBD Mutants in Cancer	3.62×10^{-3}
Signalling by TGF-beta Receptor Complex in Cancer	3.62×10^{-3}
Loss of Function of SMAD4 in Cancer	3.62×10^{-3}
Loss of Function of SMAD2/3 in Cancer	3.62×10^{-3}
TGFBR2 MSI Frameshift Mutants in Cancer	3.62×10^{-3}
SMAD4 MH2 Domain Mutants in Cancer	3.62×10^{-3}
NFkB activation by nontypeable *Haemophilus influenzae*	3.62×10^{-3}
SMAD2/SMAD3:SMAD4 heterotrimer regulates transcription	6.91×10^{-3}
TGF-beta receptor signalling activates SMADs	8.00×10^{-3}
Downregulation of TGF-beta receptor signalling	3.04×10^{-2}
Transcriptional activity of SMAD2/SMAD3:SMAD4 heterotrimer	4.57×10^{-2}

5.3.7 Validation of three miRNAs using RT-qPCR

The differential expression of two miRNAs, bta-miR-222 and bta-miR-423-3p was investigated using RT-qPCR, in order to validate the RNA-seq results using a complementary technology (Figure 5-7). Unexpectedly, differential expression of these miRNAs was not validated by this method (cf. CHAPTER 3, where differential expression of bta-miR-423-3p was confirmed by this method). Variability between RNA-seq and RT-qPCR results has been described in the literature. In the first systematic comparison of the three methods used to measure expression levels of miRNAs – RT-qPCR, microarray hybridization, and next-generation sequencing – RNA-seq showed good consistency with the other platforms tested (Git *et al.*, 2010). However, while RT-qPCR shows good correlation with RNA-seq results, expression levels and thus fold changes for individual data points (miRNA genes) can differ greatly – including having opposite fold change signs. Based on correlation analysis of the three methodologies, the authors of this review concluded that RT-qPCR is "not an infallible validation method" (Git *et al.*, 2010). These findings were confirmed in a more recent comparison of NGS with microarrays and qPCR, which compared five pairs of cell lines. It concluded that "NGS had the greatest detection sensitivity, largest dynamic range of detection and highest accuracy in differential expression analysis," and that the concordance across miRNA profiling technologies is moderate and NGS technologies have better sensitivity, accuracy and robustness for miRNA profiling (Tam *et al.*, 2014). Similarly to the above report, individual data points were found to greatly differ between any two platforms. Additionally, the technical reproducibility of NGS was found to be high, with intra-sample correlations of at least 0.95 in all cases (Tam *et al.*, 2014). This agrees with our correlation analysis shown in Figure 3. The correlation plot and correlation coefficients confirm that our RNA-seq data is consistent across replicates. The normalized RNA-seq count numbers for these two miRNAs are shown in Figure 5-8. In spite of the variation, the data suggest a consistent upregulation of bta-miR-222 and bta-miR-423-3p in PBMCs of the infected group.

Future work should further test differential expression of these miRNAs, possibly with another supplier or technology, such as SYBR Green, to ensure that the negative results are not a peculiarity of this particular RT-qPCR kit or primer design. For example, in these Taqman assays reverse transcription is performed in separate reaction tubes for each miRNA, which may lead to high variation. As another possible explanation, RNA degradation or other differences arising from storage or the freeze-

thaw cycles cannot be excluded. The choice of reference genes in qPCR is also important. In these experiments, two non-differentially expressed miRNAs were chosen based on the RNA-seq data. Their human orthologs, hsa-miR-16 and hsa-miR-26a, were also validated as suitable reference transcripts in human colorectal tissues (Chang *et al.*, 2010). However, additional or other reference genes may increase accuracy of the measurement. Finally, future work should also test other differentially expressed miRNAs. In this project, the insufficient amount of RNA left after quality check, library preparation and RT-qPCR prevented further investigation of this question.

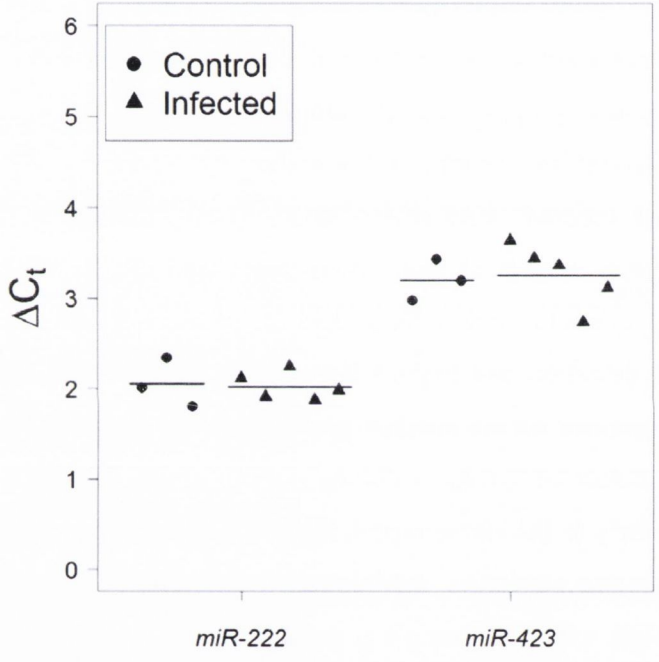

Figure 5-7 | Dotplot of ΔC_t results for infected and control samples. There were no statistically significant changes in miRNA expression according to RT-qPCR.

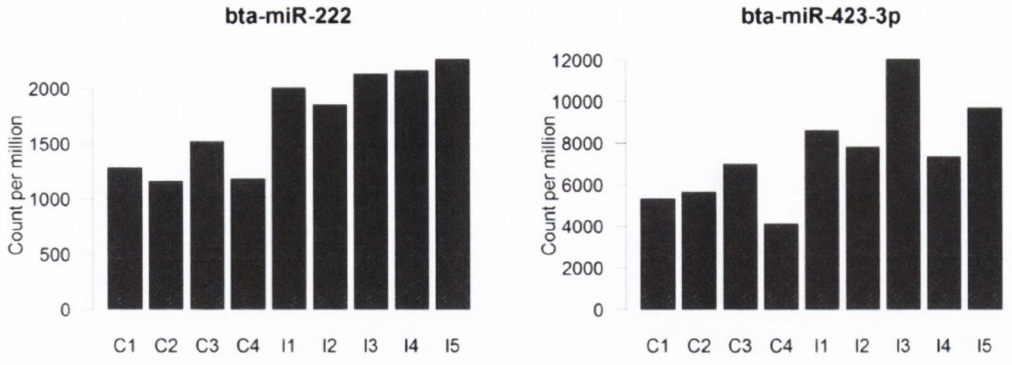

Figure 5-8 | RNA-seq count numbers for miR-222 and miR-423-3p. Normalized count numbers for four healthy (C) and five TB infected (I) samples are shown. The data suggest a consistent upregulation of these miRNAs in the infected group.

5.3.8 Conclusion

In this Chapter, I have determined the miRNA expression profile of bovine PBMCs in healthy and TB infected animals using next-generation sequencing. These profiles provide guidance for further studies on which miRNAs are the major players in posttranscriptional regulation in these cells. In this RNA-seq project, a relatively high number of unpooled samples (9) were used. We have determined that nine miRNAs are differentially expressed in PBMCs of infected animals compared to age, breed, and sex matched healthy animals, which shows that the miRNA profile of circulating cells may reflect infection status and underlying processes. Six miRNAs (bta-miR-423-3p, bta-miR-423-5p, bta-miR-222, bta-miR-31, bta-let-7e, and bta-miR-328) were found upregulated, and three miRNAs (bta-miR-2285t, bta-miR-204, and bta-miR-18a) were downregulated. Pathway analysis suggested that differentially expressed miRNAs are involved in controlling cell proliferation and immune functions in response to infection. Two of these differentially expressed miRNAs, miR-423-3p and miR-222, were also tested with RT-qPCR, but their upregulation was not confirmed. Further studies are needed to understand the role of miRNAs in more detail and to verify our results. This work was partly aimed at finding miRNA biomarkers in blood of TB infected cattle. Our measurements come from a mixed cell population, therefore miRNAs may remain undetected due to averaging. The design of future experiments, focusing only on disease biology, can be improved by isolating specific immune cell subsets, such as

$CD4^+$ T cells. It will also be important to determine whether the miRNA expression profiles reported in this study are specific for *M. bovis* infection or whether they are also differentially regulated in response to other unrelated infections. Nevertheless, it can be concluded that the miRNAs in PBMCs of TB infected cattle are likely to differentially regulate cell cycle and TGF-β receptor signalling, and these results warrant the study of more specific cell types.

CHAPTER 6

GENERAL DISCUSSION

6.1 General discussion

Bovine tuberculosis is one of the most important infectious diseases in cattle, resulting in significant economic losses to agriculture throughout the world. The causative agent is *Mycobacterium bovis,* a rod-shaped acid-fast bacterium that is a member of the *Mycobacterium tuberculosis* complex (MTBC), a group of highly related pathogens. Alveolar macrophages are the primary host cells for the bacteria, which spread via an airborne route. Transcriptional profiling studies have shown changes in expression of several thousand mRNA transcripts in bovine monocyte-derived macrophages upon infection *in vitro* with live *M. bovis* (Magee *et al.*, 2012, Nalpas *et al.*, 2013). However, the role that microRNAs, a type short non-coding RNAs which regulate gene expression, play in the pathogenesis of the disease has been poorly investigated.

This work aimed to characterise miRNA expression, using next-generation sequencing (RNA-seq), in several bovine immune cell types that are important mediators of the host response to *M. bovis* infection. The thesis was organized into four research projects. Firstly, we have determined miRNA expression in bovine alveolar macrophages isolated from eight healthy animals. Building upon this, an RNA-seq approach was implemented to temporally profile miRNA expression in primary bovine AMs post-infection with *M. bovis,* and more than 40 miRNAs were identified as differentially expressed at several time-points in the early innate immune response to bovine tuberculosis. Based on these results, we have further studied the function of two key miRNAs, miR-146a and miR-146b, in a mimic-transfection (overexpression) model using a bovine macrophage cell line (Bomac), and confirmed the predicted targeting of two key genes, *IRAK1* and *TGFBR2* by miR-146. Additionally, the genes regulated by miR-146a were further studied on a transcriptome-wide scale, and 125 differentially expressed genes were identified following transfection. Finally, we have also profiled miRNA expression in bovine peripheral blood mononuclear cells isolated from five healthy and four naturally-infected tuberculosis animals. Nine miRNAs were found to be differentially expressed between healthy and infected animals, and the differentially expressed miRNAs were found to preferentially target cell cycle regulation and TGF-β receptor signalling. These findings described in the thesis confirmed our hypothesis that miRNAs have an important role in regulating bovine alveolar macrophage response to *Mycobacterium.*

6.1.1 MicroRNA expression studies in cattle

In the first project, a high-throughput sequencing approach, RNA-seq, was utilised to profile miRNA expression on a genome-wide scale in unchallenged bovine alveolar macrophages isolated from lung lavages of eight different healthy Holstein-Friesian male calves. The first studies demonstrating miRNA expression in bovine tissues were published in 2007 (Coutinho *et al.*, 2007). Since then, 793 mature miRNAs have been identified in the *Bos taurus* genome, and one of these was discovered by work in CHAPTER 1. Eighty miRNAs were identified as being expressed in AMs at a threshold of at least 100 reads per million. The expression levels of miRNAs varied over a large dynamic range, with a few miRNAs expressed at very high levels, and the majority lowly expressed. Many of the most highly expressed miRNAs, including the top, miR-21, have known roles in regulating immunity in other species, as miRNAs often share significant functional and sequence similarities between species, indicating evolutionary conservation and, putatively, conservation of function. The human miR-155, for example, is a perfect homolog to its bovine counterpart, bta-miR-155. In humans, this miRNA acts as an anti-inflammatory agent targeting the TLR/IL-1 receptor inflammatory pathway (Ceppi *et al.*, 2009). While there is significant conservation of miRNAs between species, there are also notable differences that very likely have functional consequences. There are numerous cases, for example, of miRNAs found in the human genome that are absent in the bovine genome annotation. Some of these differences may be due to better annotation of the human miRNAome but clearly there are real differences too. The human miRNA, hsa-miR-198, for example, has a role in human immunity and has no homolog in the bovine genome. This miRNA targets the Cyclin T1 gene (CCNT1), which acts as a co-factor for HIV-1 (Sung and Rice, 2009). In addition to single-miRNA differences in the bovine and other genomes, there are also several cases where entire families or clusters of miRNAs that have yet to be discovered or do not exist in the bovine genome, and are present in one species. There are also miRNA families that are specific to the bovine genome, such as the bta-miR-2284 family. This miRNA family has been shown to be expressed in a number of bovine immune-relevant tissues including $CD14^{+}$ monocytes, mammary epithelial cells, including as shown in thesis in AMs, however, the genes targeted by the miRNAs in this family are currently unknown (Lawless *et al.*, 2014, Lawless *et al.*, 2013). These issues point to the importance of performing miRNA profiling experiments in all model species. Altogether, miRNA expression has now been

demonstrated in ten immune related bovine tissues (bovine embryo, thymus, small intestine, mesenteric lymph node, abomasum lymph node, $CD14^+$ blood isolated monocytes, $CD14^+$ milk isolated monocytes, mammary epithelial cells, mammary tissue, and the MDBK cell line) and alveolar macrophages (Jin *et al.*, 2014, Coutinho *et al.*, 2007, Dilda *et al.*, 2011, Lawless *et al.*, 2013, Lawless *et al.*, 2014, Naeem *et al.*, 2012, Glazov *et al.*, 2009). Importantly, annotated miRNAs are much fewer in the bovine genome than in murine or human genomes, and a bovine miRNA expression atlas across bovine tissues and cells is needed to bridge this gap. Gene expression and regulation studies in multiple cell types and tissues, and connecting multiple kinds of 'omics' data will allow systems-level analysis of the organism. One such endeavour, the Genotype-Tissue Expression (GTEx) Project seeks to map gene expression in all human tissues (GTEx Consortium, 2013). Eventual conclusions from this and similar projects will inform on the merit of implementing such approaches in cattle and other agriculturally important species. Among its many uses, better annotation of non-coding RNAs would aid in the interpretation of bovine genome-wide association study (GWAS) data. A previously unannotated small non-coding RNA, for example, was recently identified as the only gene in a novel genome-wide significant QTL for somatic cell score, a mastitis indicator trait (Meredith *et al.*, 2013).

MicroRNA expression is tissue-specific and reflects the role of the cell, which was confirmed in our data, where the predicted target genes of miRNAs expressed by AMs were found to be statistically enriched for roles in innate immunity. Additionally, this work established the protocol for further projects. We confirmed that good quality total RNA and miRNA-containing small RNA fractions can simultaneously be isolated from bovine alveolar macrophages, and the sequencing of eight bovine alveolar macrophage miRNA libraries validated the next-generation sequencing protocol.

6.1.2 Role of microRNAs in regulating host responses to infection in cattle

Several studies have examined whether miRNA expression is altered in response to bacterial infections in cattle. Early studies investigated only a small number of miRNAs (Naeem *et al.*, 2012, Dilda *et al.*, 2011), but more recent studies have employed high-throughput sequencing approaches to temporally profile transcriptome-wide changes in miRNA expression in different cell-types, in response to challenge with pathogens such as the mastitis-causing *Escherichia coli*, *S. aureus* or *S. uberis*.

Lawless et al. identified twenty-one miRNAs that were differentially expressed in bovine mammary epithelial cells challenged *in vitro* with live *S. uberis*, a Gram-positive bacterium (Lawless *et al.*, 2013). Subsequently, Jin et al. also reported notable differences in miRNA expression profiles in MAC-T cells challenged with either heat-killed *E. coli* or *S. aureus* (Jin *et al.*, 2014). In the first NGS-based study to temporally profile infection-induced miRNA responses in cattle *in vivo*, Lawless et al. simultaneously profiled genome-wide mRNA and miRNA expression at multiple time-points in both milk and blood FACS-isolated $CD14^{+}$ monocytes from cattle infected with *S. uberis* (Lawless *et al.*, 2014). Twenty-six miRNAs and more than 3500 genes were identified as being significantly differentially expressed over the 48 hour time-course. Pathway analysis results suggested that during *S. uberis* infection miRNAs are key regulators of monocyte inflammatory response networks and repressors of several metabolic pathways.

The work described in CHAPTER 2 is the first RNA-seq experiment to temporally profile miRNA expression in primary bovine AMs, isolated from ten different healthy Holstein-Friesian male calves, post-infection with *M. bovis*. Macrophages were challenged with *M. bovis*, and miRNA expression was measured with RNA-seq at four timepoints. In total, 2.5 billion sequencing reads were generated. One common issue in RNA-seq studies is the low number of replicates, partly due to the high cost of library preparation and sequencing. In comparison to the vast majority of other studies, our approach is exceptional in terms of depth of sequencing, the number of replicates used, the fact that the replicates were not pooled and the fact that miRNA expression was examined across multiple time-points.

One, six, and forty miRNAs were identified as significantly differentially expressed at 2, 24 and 48 h post-infection, respectively. The differential expression of three of four tested miRNAs (bta-miR-142-5p, bta-miR-146a, and bta-miR-423-3p) was confirmed by RT-qPCR. Several of the differentially expressed miRNAs have been shown to have roles in mycobacterial infection, such as bta-miR-146a (Sharbati *et al.*, 2011). Another example is miR-21, which has been shown to target the vitamin D-dependent antimicrobial pathway in *M. leprae* infected monocytes (Liu *et al.*, 2012, O'Neill *et al.*, 2011). Other miRNAs include bta-mir-423-3p and bta-mir-423-5p, which regulate chemokine expression and apoptosis related pathways. As reported in our study, these miRNAs have also been shown to be downregulated in human monocyte-derived macrophages infected with *M. avium* (Sharbati *et al.*, 2011).

Pathway analysis of the predicted mRNA targets of differentially expressed miRNAs in AMs post-infection with *M. bovis,* suggested that these miRNAs preferentially target several pathways that are functionally relevant for mycobacterial pathogenesis, including endocytosis and lysosome trafficking, IL-1 signalling and the TGF-β pathway. IL-1 receptor signals are indispensable for the control of *Mycobacterium* infection (Fremond *et al.*, 2007), and TGF-β receptor 2 signalling has been shown to promote the anti-inflammatory macrophage phenotype (M2) activation in mice (Gong *et al.*, 2012). The role and behaviour of macrophages is critical to the outcome of the disease. Macrophages of cattle naturally resistant to tuberculosis show a stronger proinflammatory response against mycobacteria than those from susceptible animals (Castillo-Velazquez *et al.*, 2013). Macrophage regulatory factors that alter mycobacterium growth include pattern recognition receptors, cytokines, lipid metabolism, and miRNAs (Rajaram *et al.*, 2014). MicroRNAs, together with this network of factors have a role in deciding the path of macrophage activation (Kaufmann and Dorhoi, 2013). Taken together, our study identified the key roles miRNAs play in this complex interaction between *M. bovis* survival strategies and the host immune response.

6.1.3 Validating miRNA targets

A current limitation of many miRNA studies both in cattle and in other species is the lack of validated targets for miRNAs, and in cattle only a handful of studies to date have functionally validated predicted miRNA targets (Li *et al.*, 2012, Wang *et al.*, 2014). Computationally, hundreds of putative miRNA targets can be predicted, and experimental validation is a costly and labour-intensive procedure. Methods which integrate and correlate miRNA expression with mRNA expression in the same sample can refine computational predictions and increase the validation hit rate, as was employed by us in CHAPTER 3. Nevertheless, the reliability of current *in silico* approaches is limited, therefore experimental validation is indispensable for finding true miRNA targets (Thomson *et al.*, 2011). A direct approach to validate miRNA targets is to use a reporter assay, where the miRNA binding site of the predicted target gene is cloned upstream of a luciferase or green fluorescent protein (GFP) reporter gene, and the reduced level of reporter protein demonstrates a direct silencing effect of the miRNA on the gene (Kuhn *et al.*, 2008). This approach is limited however to those

targets that are predicted *a priori*. A less biased genome-wide approach involves gene expression analysis upon differential expression of a miRNA (Tarang and Weston, 2014). This approach provides evidence that a given miRNA can alter the expression of a target gene but does not prove direct regulation (Martinez-Sanchez and Murphy, 2013). The miRNA could, for example, regulate a transcription factor which subsequently regulates the putative target gene.

In this thesis, we sought to identify the targets of bta-miR-146a, a miRNA that is differentially expressed in AMs infected with *M. bovis*, by transfecting a synthetic mimic of miR-146a into a bovine macrophage cell line (Bomac). RT-qPCR revealed the down-regulation of two key genes in the innate immune response to *M. bovis,* IL-1 receptor-associated kinase 1 *(IRAK1)* and TGF-β receptor 2 *(TGFBR2)*, following transfection of the miR-146a synthetic mimic. Subsequently, we have utilised an RNA-seq approach to identify targets of this miRNA on a genome-wide scale. Comparison of mRNA expression of untreated cells to negative control mimic treated cells uncovered considerable changes in mRNA levels, likely due to a cellular response to double-stranded RNA, which resulted in production of proinflammatory cytokines, such as IL-6 and IL-8, and interferon-induced genes. The results uncovered that transfection of cells with short double stranded RNA – miRNA mimics – induces significant changes in the transcriptome, and highlight the importance of using scrambled miRNAs as negative controls. Comparison of miR-146a transfected cells to cells transfected with the negative control mimic identified 46 and 79 genes that were up- or down-regulated more than 2-fold, respectively. Seven genes also had a predicted seed match with miR-146a, among them *IRAK1*.

Several studies have examined the function of miR-146. The expression of miR-146a increases as HSCs mature and is thought to control development of HSCs into blood cells (Zhao and Starczynowski, 2014). Moreover, a wide range of infectious and inflammatory stimuli induce expression of miR-146a, which in turn provides important negative feedback of inflammation (So *et al.*, 2013). miR-146a inhibits inflammation mainly by negatively regulating NF-κB signalling via two of its targets, *TRAF6* and *IRAK1* (Zhao and Starczynowski, 2014). In macrophages, miR-146a has a key role in inducing differentiation and maturation (Montagner *et al.*, 2013). Pathway analysis revealed that miR-146a preferentially targets genes involved in macrophage activation and the immune response in Bomacs and identified several potentially interesting target genes for future studies.

A limitation of this approach, however, is the difficulty in separate direct from indirect targets. In future, new technologies, such as sequencing of RISC (RNA-induced silencing complex) components isolated by crosslinking immunoprecipitation (CLIP-seq) or a variation of this technique, photoactivable-ribonucleoside-enhanced cross linking and immunoprecipitation (PAR-CLIP), can be used to identify miRNA direct targets on a genome-wide scale (Darnell, 2010). Other exciting approaches label the miRNA and analyse the associated transcripts. The labelled miRNA pull-down assay (LAMP) involves transfection of a biotin or digoxygenin tagged-miRNA and isolating the miRNA–mRNA complex (Tarang and Weston, 2014).

6.1.4 MicroRNAs as novel biomarkers

Aside from understanding the important basic biology of how miRNAs regulate bovine gene expression, miRNAs could also potentially be of significant utility as biomarkers of specific diseases in cattle. In humans, miRNAs have been evaluated for use as biomarkers of TB, including miR-155-3p and miR-155-5p in stimulated PBMCs, and miR-29a in serum (Wu *et al.*, 2012a, Fu *et al.*, 2011). Recently, hsa-miR-196b and hsa-miR-376c were identified as potential markers of active TB disease in the serum of patients (Zhang *et al.*, 2014). In cattle, improved diagnostic tests would help in controlling the disease; the currently used single intradermal comparative cervical tuberculin test and the IFN-γ release assay have high specificity (>95%), but lower sensitivity (70–100%) (de la Rua-Domenech *et al.*, 2006), which leads to undetected animals in the herd, contributing to the spread of infection (Goodchild and Clifton-Hadley, 2001).

We have investigated miRNA expression in peripheral blood mononuclear cells in the context of a natural *M. bovis* infection. In a pilot study, blood was taken from five *M. bovis*-infected and four healthy age, breed and sex matched animals. Subsequently, the miRNA expression profile of PBMCs was determined. Six miRNAs (bta-miR-423-3p, bta-miR-423-5p, bta-miR-222, bta-miR-31, bta-let-7e, and bta-miR-328) were upregulated, and three miRNAs (bta-miR-2285t, bta-miR-204, and bta-miR-18a) were downregulated in comparison to healthy controls. A recent study – published after our study was completed – has used a microarray approach to investigate the expression of miRNAs in bovine PBMCs isolated from *M. bovis*-challenged BCG vaccinated and unvaccinated animals. miR-155 was found to be significantly up-regulated both at week

2 and week 11 post-infection in unvaccinated cattle, but only at week 11 in BCG vaccinated animals. No differential expression of miR-155 was observed in pre-infection samples from unvaccinated and vaccinated cattle, suggesting that miR-155 could be exploited as a marker distinguishing vaccinated from infected animals (Golby *et al.*, 2014). In our data, miR-155 was not differentially expressed, which may be due to the different stages of the disease, and shows that more work is needed to find reliable biomarkers of TB. The differentially expressed miRNAs in our work preferentially targeted cell cycle regulation and TGF-β receptor signalling, suggesting that proliferation of blood cells in response to infection is under control of these miRNAs. High levels and excessive TGF-β activity is a feature of active pulmonary TB, which is consistent with the targeting of its signalling by downregulated miRNAs (Wu *et al.*, 2012b). However, TGF-β signalling pathway and its regulation by miRNAs is a complex network, and uncovering the exact mechanism and consequences of miRNA targeting requires more detailed work (Butz *et al.*, 2012).

Surprisingly, RT-qPCR did not confirm differential expression of two of the tested miRNAs. Several studies have now reported that despite being highly correlated, RT-qPCR and RNA-seq results can diverge substantially for individual genes (Git *et al.*, 2010). Future work should study these miRNAs in a larger number of animals, preferably together with other differentially expressed miRNAs, and possibly using a different technology.

6.1.5 Future directions

Mycobacteria are a step ahead of their host in the evolutionary arms race, and the adaptive immune system is often not capable of producing sterilizing immunity, as the bacteria are adept at influencing the host immune system. A successful intervention therefore requires *immunomodulatory* treatment approaches, to complement conventional drug treatment regimens targeting the pathogen. This 'host-directed therapeutic' approach is also preferable because bacteria can, and will, evolve resistance against many drugs, as the emergence of multi-drug-resistant (MDR), extensively drug-resistant (XDR), and more recently the totally drug resistant tuberculosis (TDR-TB) strains has demonstrated. Innate immunity has a critical role in TB pathogenesis, and this thesis provides insight into the role miRNAs play in this first line of defence. MicroRNAs have significant potential as therapeutic targets or agents,

and several miRNAs are currently in preclinical and clinical trials in humans (van Rooij and Kauppinen, 2014). Human miR-208, for example, has been shown to have an important role in modulating cardiac function and remodelling (van Rooij *et al.*, 2007), and, interestingly from a bovine perspective, this miRNA also has a big impact on metabolism. This and other therapeutic miRNAs have orthologs in cattle, which clearly suggest that there is a potential for the application of miRNA-based therapeutic strategies to combat disease and regulate metabolism in cattle in order to influence important economic traits, such as tuberculosis resistance. Even individual miRNAs can have a profound effect, such as in the case of let-7f, whose upregulation was shown to diminish *M. tuberculosis* survival in murine macrophages (Kumar *et al.*, 2015).

However, likely a combination of approaches will be necessary for fast and efficient treatment and prevention. Several challenges need to be overcome to achieve this, and in all these miRNAs play a defining role. It needs to be understood how the antimicrobial innate immunity pathways (such as phagocytosis, antimicrobial peptides, oxidative stress, apoptosis, and autophagy) integrate into a bactericidal network, and also what constitutes of protective immunity, as no single cell or function can be linearly correlated to protection (Ottenhoff, 2012). Another challenge is to understand the adaptive response and how it cooperates with innate immunity to inhibit mycobacterium replication inside macrophages, and how these processes can be utilized to provide protective immunity (Shaler *et al.*, 2012). These issues are further complicated by the fact that each disease stage has different characteristics, as described in CHAPTER 1.

New technologies, such as third-generation RNA-seq or single-cell sequencing, may accelerate discoveries, and eliminate shortcomings of current approaches. Third-generation sequencing, real-time sequencing of single DNA molecules by synthesis or ligation, does not require PCR amplification, thus eliminates PCR amplification bias and simplifies library construction (Kawaji *et al.*, 2014). In these experiments, we are studying populations of cells; however, differences between individual cells may be important, and cells also influence each other. One example is a report of antimicrobial interactions between naive and infected murine macrophages, which reduced *M. tuberculosis* viability (Hartman and Kornfeld, 2011). Application of single-cell sequencing in transcriptomics and epigenomics will allow examination of cell subpopulations and taking other functional states into consideration, with unprecedented resolution (Shapiro *et al.*, 2013). Finally, high-throughput

experimentation (screening) has already been applied in TB research, for example, for finding new antitubercular drugs (Stanley *et al.*, 2012). The combination of this approach with high-throughput data collection will bring unprecedented amount of data with great number of replicates and treatment conditions. These advancements will hopefully help us to draw a more accurate model of tuberculosis pathogenesis, which will be indispensable to efficiently modulate the immune response to combat and eradicate this ancient disease.

6.1.6 Conclusion

In conclusion, the work presented in this thesis has profiled miRNA expression in bovine alveolar macrophages using next-generation sequencing and identified the differential expression of more than 40 miRNAs in AMs at several time-points following infection with *M. bovis*. These miRNAs play important roles in targeting genes that are functionally relevant for mycobacterial pathogenesis, suggesting that miRNAs play a key role in tuning the complex interaction between *M. bovis* survival strategies and the host immune response.

References

Adijanto, J., Castorino, J. J., Wang, Z. X., Maminishkis, A., Grunwald, G. B. and Philp, N. J. (2012) 'Microphthalmia-associated transcription factor (MITF) promotes differentiation of human retinal pigment epithelium (RPE) by regulating microRNAs-204/211 expression', *The Journal of Biological Chemistry,* 287(24), pp. 20491-503.

Alam, M. M. and O'Neill, L. A. (2011) 'MicroRNAs and the resolution phase of inflammation in macrophages', *European Journal of Immunology,* 41(9), pp. 2482-5.

Alvarez-Garcia, I. and Miska, E. A. (2005) 'MicroRNA functions in animal development and human disease', *Development,* 132(21), pp. 4653-62.

Anders, S. and Huber, W. (2010) 'Differential expression analysis for sequence count data', *Genome Biology,* 11(10), pp. R106.

Anders, S., Pyl, P. T. and Huber, W. (2015) 'HTSeq--a Python framework to work with high-throughput sequencing data', *Bioinformatics,* 31(2), pp. 166-9.

Andersson, U. and Tracey, K. J. (2011) 'HMGB1 is a therapeutic target for sterile inflammation and infection', *Annu Rev Immunol,* 29, pp. 139-62.

Androulidaki, A., Iliopoulos, D., Arranz, A., Doxaki, C., Schworer, S., Zacharioudaki, V., Margioris, A. N., Tsichlis, P. N. and Tsatsanis, C. (2009) 'The kinase Akt1 controls macrophage response to lipopolysaccharide by regulating microRNAs', *Immunity,* 31(2), pp. 220-31.

Apt, A. and Kondratieva, T. K. (2008) 'Tuberculosis: Pathogenesis, immune response, and host genetics', *Molecular Biology,* 42(5), pp. 784-793.

Arnvig, K. B., Comas, I., Thomson, N. R., Houghton, J., Boshoff, H. I., Croucher, N. J., Rose, G., Perkins, T. T., Parkhill, J., Dougan, G. and Young, D. B. (2011) 'Sequence-based analysis uncovers an abundance of non-coding RNA in the total transcriptome of Mycobacterium tuberculosis', *PLoS Pathogens,* 7(11), pp. e1002342.

Artzi, S., Kiezun, A. and Shomron, N. (2008) 'miRNAminer: a tool for homologous microRNA gene search', *BMC Bioinformatics,* 9, pp. 39.

Ashcroft, G. S. (1999) 'Bidirectional regulation of macrophage function by TGF-beta', *Microbes and Infection,* 1(15), pp. 1275-82.

Ayele, W. Y., Neill, S. D., Zinsstag, J., Weiss, M. G. and Pavlik, I. (2004) 'Bovine tuberculosis: an old disease but a new threat to Africa', *International Journal of Tuberculosis and Lung Disease,* 8(8), pp. 924-37.

Azad, A. K., Sadee, W. and Schlesinger, L. S. (2012) 'Innate immune gene polymorphisms in tuberculosis', *Infection and Immunity,* 80(10), pp. 3343-59.

Barrett, T., Troup, D. B., Wilhite, S. E., Ledoux, P., Evangelista, C., Kim, I. F., Tomashevsky, M., Marshall, K. A., Phillippy, K. H., Sherman, P. M., Muertter, R. N., Holko, M., Ayanbule, O., Yefanov, A. and Soboleva, A. (2011) 'NCBI GEO: archive for functional genomics data sets--10 years on', *Nucleic Acids Research,* 39(Database issue), pp. D1005-10.

Bartel, D. P. (2009) 'MicroRNAs: target recognition and regulatory functions', *Cell,* 136(2), pp. 215-233.

Belver, L., Papavasiliou, F. N. and Ramiro, A. R. (2011) 'MicroRNA control of lymphocyte differentiation and function', *Current Opinion in Immunology,* 23(3), pp. 368-73.

Benjamini, Y. and Hochberg, Y. (1995) 'Controlling the False Discovery Rate: a practical and powerful approach to multiple testing', *Journal of the Royal Statistical Society. Series B (Methodological),* 57(1), pp. 289-300.

Betel, D., Wilson, M., Gabow, A., Marks, D. S. and Sander, C. (2008) 'The microRNA.org resource: targets and expression', *Nucleic Acids Research,* 36(Database issue), pp. 149-53.

Bhatt, K. and Salgame, P. (2007) 'Host innate immune response to *Mycobacterium tuberculosis*', *Journal of Clinical Immunology,* 27(4), pp. 347-62.

Bishayi, B., Bandyopadhyay, D., Majhi, A. and Adhikary, R. (2014) 'Expression of CXCR1 (Interleukin-8 Receptor) in murine macrophages after *Staphylococcus aureus* infection and its possible implication on intracellular survival correlating with cytokines and bacterial anti-oxidant enzymes', *Inflammation.*

Blair, K. (2013) 'A brief history of massively parallel cDNA sequencing', *Retrieved from http://blog.sbgenomics.com/history-of-rna-seq/, accessed on 2015.01.15.*

Bradfute, S. B., Castillo, E. F., Arko-Mensah, J., Chauhan, S., Jiang, S., Mandell, M. and Deretic, V. (2013) 'Autophagy as an immune effector against tuberculosis', *Current Opinion in Microbiology,* 16(3), pp. 355-65.

Brennecke, J., Stark, A., Russell, R. B. and Cohen, S. M. (2005) 'Principles of microRNA-target recognition', *PLoS Biology,* 3(3), pp. e85.

Brooks-Pollock, E., Roberts, G. O. and Keeling, M. J. (2014) 'A dynamic model of bovine tuberculosis spread and control in Great Britain', *Nature,* 511(7508), pp. 228-31.

Bushati, N. and Cohen, S. M. (2007) 'microRNA functions', *Annual Review of Cell and Developmental Biology,* 23, pp. 175-205.

Butz, H., Racz, K., Hunyady, L. and Patocs, A. (2012) 'Crosstalk between TGF-beta signaling and the microRNA machinery', *Trends Pharmacol Sci,* 33(7), pp. 382-93.

Castillo-Velazquez, U., Gomez-Flores, R., Tamez-Guerra, R., Tamez-Guerra, P. and Rodriguez-Padilla, C. (2013) 'Differential responses of macrophages from bovines naturally resistant or susceptible to *Mycobacterium bovis* after classical and alternative activation', *Veterinary Immunology and Immunopathology,* 154(1-2), pp. 8-16.

Castillo, E. F., Dekonenko, A., Arko-Mensah, J., Mandell, M. A., Dupont, N., Jiang, S., Delgado-Vargas, M., Timmins, G. S., Bhattacharya, D., Yang, H., Hutt, J., Lyons, C. R., Dobos, K. M. and Deretic, V. (2012) 'Autophagy protects against active tuberculosis by suppressing bacterial burden and inflammation', *Proceedings of the National Academy of Sciences of the United States of America,* 109(46), pp. 3168-76.

Ceppi, M., Pereira, P. M., Dunand-Sauthier, I., Barras, E., Reith, W., Santos, M. A. and Pierre, P. (2009) 'MicroRNA-155 modulates the interleukin-1 signaling pathway in activated human monocyte-derived dendritic cells', *Proceedings of the National Academy of Sciences of the United States of America,* 106(8), pp. 2735-40.

Chan, E. K., Ceribelli, A. and Satoh, M. (2013) 'MicroRNA-146a in autoimmunity and innate immune responses', *Ann Rheum Dis,* 72 Suppl 2, pp. ii90-5.

Chang, K. H., Mestdagh, P., Vandesompele, J., Kerin, M. J. and Miller, N. (2010) 'MicroRNA expression profiling to identify and validate reference genes for relative quantification in colorectal cancer', *BMC Cancer,* 10, pp. 173.

Chen, X., Gao, C., Li, H., Huang, L., Sun, Q., Dong, Y., Tian, C., Gao, S., Dong, H., Guan, D., Hu, X., Zhao, S., Li, L., Zhu, L., Yan, Q., Zhang, J., Zen, K. and Zhang, C. Y. (2010) 'Identification and characterization of microRNAs in raw milk during different periods of lactation, commercial fluid, and powdered milk products', *Cell Research,* 20(10), pp. 1128-37.

Chen, Z. and Zhong, C. (2014) 'Oxidative stress in Alzheimer's disease', *Neurosci Bull,* 30(2), pp. 271-81.

Cheng, Y., Kuang, W., Hao, Y., Zhang, D., Lei, M., Du, L., Jiao, H., Zhang, X. and Wang, F. (2012) 'Downregulation of miR-27a* and miR-532-5p and upregulation of miR-146a and miR-155 in LPS-induced RAW264.7 macrophage cells', *Inflammation,* 35(4), pp. 1308-13.

Clemens, D. L. and Horwitz, M. A. (1995) 'Characterization of the *Mycobacterium tuberculosis* phagosome and evidence that phagosomal maturation is inhibited', *The Journal of Experimental Medicine,* 181(1), pp. 257-70.

Cline, M. S., Smoot, M., Cerami, E., Kuchinsky, A., Landys, N., Workman, C., Christmas, R., Avila-Campilo, I., Creech, M., Gross, B., Hanspers, K., Isserlin, R., Kelley, R., Killcoyne, S., Lotia, S., Maere, S., Morris, J., Ono, K., Pavlovic, V., Pico, A. R., Vailaya, A., Wang, P. L., Adler, A., Conklin, B. R., Hood, L., Kuiper, M., Sander, C., Schmulevich, I., Schwikowski, B., Warner, G. J., Ideker, T. and Bader, G. D. (2007) 'Integration of biological networks and gene expression data using Cytoscape', *Nature Protocols,* 2(10), pp. 2366-82.

Cock, P. J., Fields, C. J., Goto, N., Heuer, M. L. and Rice, P. M. (2010) 'The Sanger FASTQ file format for sequences with quality scores, and the Solexa/Illumina FASTQ variants', *Nucleic Acids Research,* 38(6), pp. 1767-71.

Coutinho, L. L., Matukumalli, L. K., Sonstegard, T. S., Van Tassell, C. P., Gasbarre, L. C., Capuco, A. V. and Smith, T. P. (2007) 'Discovery and profiling of bovine microRNAs from immune-related and embryonic tissues', *Physiological Genomics,* 29(1), pp. 35-43.

Curtis, H. J., Sibley, C. R. and Wood, M. J. (2012) 'Mirtrons, an emerging class of atypical miRNA', *Wiley Interdisciplinary Reviews. RNA,* 3(5), pp. 617-32.

Cyktor, J. C., Carruthers, B., Kominsky, R. A., Beamer, G. L., Stromberg, P. and Turner, J. (2013) 'IL-10 inhibits mature fibrotic granuloma formation during *Mycobacterium tuberculosis* infection', *Journal of Immunology,* 190(6), pp. 2778-90.

Dannenberg, A. M. (2006) *Pathogenesis of human pulmonary tuberculosis: insights from the rabbit model.* ASM Press.

Darnell, R. B. (2010) 'HITS-CLIP: panoramic views of protein-RNA regulation in living cells', *Wiley Interdisciplinary Reviews. RNA,* 1(2), pp. 266-86.

Das, K., Saikolappan, S. and Dhandayuthapani, S. (2013) 'Differential expression of miRNAs by macrophages infected with virulent and avirulent *Mycobacterium tuberculosis*', *Tuberculosis,* 93, pp. S47-S50.

De Guire, V., Robitaille, R., Tetreault, N., Guerin, R., Menard, C., Bambace, N. and Sapieha, P. (2013) 'Circulating miRNAs as sensitive and specific biomarkers for the diagnosis and monitoring of human diseases: promises and challenges', *Clinical Biochemistry,* 46(10-11), pp. 846-60.

de la Rua-Domenech, R., Goodchild, A. T., Vordermeier, H. M., Hewinson, R. G., Christiansen, K. H. and Clifton-Hadley, R. S. (2006) 'Ante mortem diagnosis of tuberculosis in cattle: a review of the tuberculin tests, gamma-interferon assay and other ancillary diagnostic techniques', *Research in Veterinary Science,* 81(2), pp. 190-210.

Delmastro-Greenwood, M. M. and Piganelli, J. D. (2013) 'Changing the energy of an immune response', *Am J Clin Exp Immunol,* 2(1), pp. 30-54.

Deretic, V., Delgado, M., Vergne, I., Master, S., De Haro, S., Ponpuak, M. and Singh, S. (2009) 'Autophagy in immunity against *Mycobacterium tuberculosis:* a model system to dissect immunological roles of autophagy', *Current Topics in Microbiology and Immunology,* 335, pp. 169-88.

Dews, M., Fox, J. L., Hultine, S., Sundaram, P., Wang, W., Liu, Y. Y., Furth, E., Enders, G. H., El-Deiry, W., Schelter, J. M., Cleary, M. A. and Thomas-Tikhonenko, A. (2010) 'The myc-miR-17~92 axis blunts TGF-beta signaling and production of multiple TGF-beta-dependent antiangiogenic factors', *Cancer Research,* 70(20), pp. 8233-46.

Dilda, F., Gioia, G., Pisani, L., Restelli, L., Lecchi, C., Albonico, F., Bronzo, V., Mortarino, M. and Ceciliani, F. (2011) '*Escherichia coli* lipopolysaccharides and *Staphylococcus aureus* enterotoxin B differentially modulate inflammatory microRNAs in bovine monocytes', *Veterinary Journal,* 192(3), pp. 514-516.

Doherty, G. J. and McMahon, H. T. (2009) 'Mechanisms of endocytosis', *Annual Review of Biochemistry,* 78, pp. 857-902.

Dougherty, J. D., Reineke, L. C. and Lloyd, R. E. (2014) 'mRNA decapping enzyme 1a (Dcp1a)-induced translational arrest through protein kinase R (PKR) activation requires the N-terminal enabled vasodilator-stimulated protein homology 1 (EVH1) domain', *J Biol Chem,* 289(7), pp. 3936-49.

Ehlers, S. (2009) 'Lazy, dynamic or minimally recrudescent? On the elusive nature and location of the mycobacterium responsible for latent tuberculosis', *Infection,* 37(2), pp. 87-95.

Ernst, J. D. (2012) 'The immunological life cycle of tuberculosis', *Nature Reviews. Immunology,* 12(8), pp. 581-91.

Eulalio, A., Schulte, L. and Vogel, J. (2012) 'The mammalian microRNA response to bacterial infections', *RNA Biol,* 9(6), pp. 742-50.

Fabbri, M., Paone, A., Calore, F., Galli, R., Gaudio, E., Santhanam, R., Lovat, F., Fadda, P., Mao, C., Nuovo, G. J., Zanesi, N., Crawford, M., Ozer, G. H., Wernicke, D., Alder, H., Caligiuri, M. A., Nana-Sinkam, P., Perrotti, D. and Croce, C. M. (2012) 'MicroRNAs bind to Toll-like receptors to induce prometastatic inflammatory response', *Proceedings of the National Academy of Sciences of the United States of America,* 109(31), pp. E2110-6.

Fitzgerald, S. D., Schooley, A. M., Berry, D. E. and Kaneene, J. B. (2010) 'Antimicrobial susceptibility testing of *Mycobacterium bovis* isolates from Michigan white-tailed deer during the 2009 hunting season', *Vet Med Int,* 2011, pp. 903683.

Flannagan, R. S., Cosio, G. and Grinstein, S. (2009) 'Antimicrobial mechanisms of phagocytes and bacterial evasion strategies', *Nature Reviews. Microbiology,* 7(5), pp. 355-66.

Forrest, A. R., Kanamori-Katayama, M., Tomaru, Y., Lassmann, T., Ninomiya, N., Takahashi, Y., de Hoon, M. J., Kubosaki, A., Kaiho, A., Suzuki, M., Yasuda, J., Kawai, J., Hayashizaki, Y., Hume, D. A. and Suzuki, H. (2010) 'Induction of microRNAs, mir-155, mir-222, mir-424 and mir-503, promotes monocytic differentiation through combinatorial regulation', *Leukemia,* 24(2), pp. 460-6.

Frankel, L. B. and Lund, A. H. (2012) 'MicroRNA regulation of autophagy', *Carcinogenesis,* 33(11), pp. 2018-25.

Fremond, C. M., Togbe, D., Doz, E., Rose, S., Vasseur, V., Maillet, I., Jacobs, M., Ryffel, B. and Quesniaux, V. F. (2007) 'IL-1 receptor-mediated signal is an essential component of MyD88-dependent innate response to *Mycobacterium tuberculosis* infection', *Journal of Immunology,* 179(2), pp. 1178-89.

Friedlander, M. R., Chen, W., Adamidi, C., Maaskola, J., Einspanier, R., Knespel, S. and Rajewsky, N. (2008) 'Discovering microRNAs from deep sequencing data using miRDeep', *Nature Biotechnology,* 26(4), pp. 407-15.

Friedman, R. C., Farh, K. K., Burge, C. B. and Bartel, D. P. (2009) 'Most mammalian mRNAs are conserved targets of microRNAs', *Genome Research,* 19(1), pp. 92-105.

Fu, Y., Yi, Z., Wu, X., Li, J. and Xu, F. (2011) 'Circulating microRNAs in patients with active pulmonary tuberculosis', *Journal of Clinical Microbiology,* 49(12), pp. 4246-51.

Gantier, M. P. (2010) 'New perspectives in MicroRNA regulation of innate immunity', *J Interferon Cytokine Res,* 30(5), pp. 283-9.

Garmire, L. X., Shen, Z., Briggs, S., Yeo, G., Subramaniam, S. and Glass, C. (2010) 'Regulatory network of microRNAs in RAW 264.7 macrophage cells', *Conf Proc IEEE Eng Med Biol Soc,* 2010, pp. 6198-201.

Garmire, L. X. and Subramaniam, S. (2012) 'Evaluation of normalization methods in mammalian microRNA-Seq data', *RNA,* 18(6), pp. 1279-88.

Garnier, T., Eiglmeier, K., Camus, J. C., Medina, N., Mansoor, H., Pryor, M., Duthoy, S., Grondin, S., Lacroix, C., Monsempe, C., Simon, S., Harris, B., Atkin, R., Doggett, J., Mayes, R., Keating, L., Wheeler, P. R., Parkhill, J., Barrell, B. G., Cole, S. T., Gordon, S. V. and Hewinson, R. G. (2003) 'The complete genome sequence of *Mycobacterium bovis*', *Proceedings of the National Academy of Sciences of the United States of America,* 100(13), pp. 7877-82.

Ghorpade, D. S., Holla, S., Kaveri, S. V., Bayry, J., Patil, S. A. and Balaji, K. N. (2013) 'Sonic hedgehog-dependent induction of microRNA 31 and microRNA 150 regulates *Mycobacterium bovis* BCG-driven toll-like receptor 2 signaling', *Molecular and Cellular Biology,* 33(3), pp. 543-56.

Ghorpade, D. S., Leyland, R., Kurowska-Stolarska, M., Patil, S. A. and Balaji, K. N. (2012) 'MicroRNA-155 is required for *Mycobacterium bovis* BCG-mediated apoptosis of macrophages', *Molecular and cellular biology,* 32(12), pp. 2239-53.

Git, A., Dvinge, H., Salmon-Divon, M., Osborne, M., Kutter, C., Hadfield, J., Bertone, P. and Caldas, C. (2010) 'Systematic comparison of microarray profiling, real-time PCR, and next-generation sequencing technologies for measuring differential microRNA expression', *RNA,* 16(5), pp. 991-1006.

Glazov, E. A., Kongsuwan, K., Assavalapsakul, W., Horwood, P. F., Mitter, N. and Mahony, T. J. (2009) 'Repertoire of bovine miRNA and miRNA-like small regulatory RNAs expressed upon viral infection', *PLoS One,* 4(7), pp. e6349.

Golby, P., Villarreal-Ramos, B., Dean, G., Jones, G. J. and Vordermeier, M. (2014) 'MicroRNA expression profiling of PPD-B stimulated PBMC from *M. bovis*-challenged unvaccinated and BCG vaccinated cattle', *Vaccine,* 32(44), pp. 5839-44.

Gong, D., Shi, W., Yi, S. J., Chen, H., Groffen, J. and Heisterkamp, N. (2012) 'TGF-beta signaling plays a critical role in promoting alternative macrophage activation', *BMC Immunology,* 13, pp. 31.

Goodchild, A. V. and Clifton-Hadley, R. S. (2001) 'Cattle-to-cattle transmission of *Mycobacterium bovis*', *Tuberculosis,* 81(1-2), pp. 23-41.

Graff, J. W., Dickson, A. M., Clay, G., McCaffrey, A. P. and Wilson, M. E. (2012) 'Identifying functional microRNAs in macrophages with polarized phenotypes', *The Journal of Biological Chemistry,* 287(26), pp. 21816-25.

Grimson, A., Farh, K. K., Johnston, W. K., Garrett-Engele, P., Lim, L. P. and Bartel, D. P. (2007) 'MicroRNA targeting specificity in mammals: determinants beyond seed pairing', *Molecular Cell,* 27(1), pp. 91-105.

Groves, E., Dart, A. E., Covarelli, V. and Caron, E. (2008) 'Molecular mechanisms of phagocytic uptake in mammalian cells', *Cellular and Molecular Life Sciences,* 65(13), pp. 1957-76.

Grueter, C. E., van Rooij, E., Johnson, B. A., DeLeon, S. M., Sutherland, L. B., Qi, X., Gautron, L., Elmquist, J. K., Bassel-Duby, R. and Olson, E. N. (2012) 'A cardiac microRNA governs systemic energy homeostasis by regulation of MED13', *Cell,* 149(3), pp. 671-83.

GTEx Consortium 2013. The Genotype-Tissue Expression (GTEx) project. *Nat Genet.*

Guo, H., Ingolia, N. T., Weissman, J. S. and Bartel, D. P. (2010) 'Mammalian microRNAs predominantly act to decrease target mRNA levels', *Nature,* 466(7308), pp. 835-40.

Ha, M. and Kim, V. N. (2014) 'Regulation of microRNA biogenesis', *Nature Reviews. Molecular Cell Biology,* 15(8), pp. 509-24.

Harapan, H., Fitra, F., Ichsan, I., Mulyadi, M., Miotto, P., Hasan, N. A., Calado, M. and Cirillo, D. M. (2013) 'The roles of microRNAs on tuberculosis infection: meaning or myth?', *Tuberculosis,* 93(6), pp. 596-605.

Harris, H. E., Andersson, U. and Pisetsky, D. S. (2012) 'HMGB1: a multifunctional alarmin driving autoimmune and inflammatory disease', *Nature reviews. Rheumatology,* 8(4), pp. 195-202.

Hartman, M. L. and Kornfeld, H. (2011) 'Interactions between naive and infected macrophages reduce *Mycobacterium tuberculosis* viability', *PLoS One,* 6(11), pp. e27972.

Hata, T., Murakami, K., Nakatani, H., Yamamoto, Y., Matsuda, T. and Aoki, N. (2010) 'Isolation of bovine milk-derived microvesicles carrying mRNAs and microRNAs', *Biochemical and Biophysical Research Communications,* 396(2), pp. 528-33.

He, Y., Jiang, X. and Chen, J. (2014) 'The role of miR-150 in normal and malignant hematopoiesis', *Oncogene,* 33(30), pp. 3887-93.

Holley, C. L. and Topkara, V. K. (2011) 'An introduction to small non-coding RNAs: miRNA and snoRNA', *Cardiovascular Drugs and Therapy,* 25(2), pp. 151-9.

Hou, J., Wang, P., Lin, L., Liu, X., Ma, F., An, H., Wang, Z. and Cao, X. (2009) 'MicroRNA-146a feedback inhibits RIG-I-dependent Type I IFN production in macrophages by targeting TRAF6, IRAK1, and IRAK2', *Journal of Immunology,* 183(3), pp. 2150-8.

Houben, E. N., Nguyen, L. and Pieters, J. (2006) 'Interaction of pathogenic mycobacteria with the host immune system', *Current Opinion in Microbiology,* 9(1), pp. 76-85.

Hsu, S. D., Tseng, Y. T., Shrestha, S., Lin, Y. L., Khaleel, A., Chou, C. H., Chu, C. F., Huang, H. Y., Lin, C. M., Ho, S. Y., Jian, T. Y., Lin, F. M., Chang, T. H., Weng, S. L., Liao, K. W., Liao, I. E., Liu, C. C. and Huang, H. D. (2014) 'miRTarBase update 2014: an information resource for experimentally validated miRNA-target interactions', *Nucleic Acids Research,* 42(Database issue), pp. D78-85.

Huether, S. E. and McCance, K. L. (2004) *Understanding pathophysiology.* 3rd edn.: Mosby.

Huntzinger, E. and Izaurralde, E. (2011) 'Gene silencing by microRNAs: contributions of translational repression and mRNA decay', *Nature Reviews. Genetics,* 12(2), pp. 99-110.

Huynh, K. K., Joshi, S. A. and Brown, E. J. (2011) 'A delicate dance: host response to mycobacteria', *Current Opinion in Immunology,* 23(4), pp. 464-72.

Iliopoulos, D., Hirsch, H. A. and Struhl, K. (2009) 'An epigenetic switch involving NF-kappaB, Lin28, Let-7 MicroRNA, and IL6 links inflammation to cell transformation', *Cell,* 139(4), pp. 693-706.

Illumina (2010) *Illumina Technology Spotlight: Illumina Sequencing* Pub. No. 770-2007-002.

Illumina (2011) *Illumina White Paper: Sequencing* Pub. No. 470-2011-004.

Ivey, K. N. and Srivastava, D. (2010) 'MicroRNAs as regulators of differentiation and cell fate decisions', *Cell Stem Cell,* 7(1), pp. 36-41.

Jayaraman, P., Sada-Ovalle, I., Nishimura, T., Anderson, A. C., Kuchroo, V. K., Remold, H. G. and Behar, S. M. (2013) 'IL-1beta promotes antimicrobial immunity in macrophages by regulating TNFR signaling and caspase-3 activation', *Journal of Immunology,* 190(8), pp. 4196-204.

Jin, H., Tuo, W., Lian, H., Liu, Q., Zhu, X. Q. and Gao, H. (2010) 'Strategies to identify microRNA targets: new advances', *N Biotechnol,* 27(6), pp. 734-8.

Jin, W., Ibeagha-Awemu, E. M., Liang, G., Beaudoin, F., Zhao, X. and Guan le, L. (2014) 'Transcriptome microRNA profiling of bovine mammary epithelial cells challenged with *Escherichia coli* or *Staphylococcus aureus* bacteria reveals pathogen directed microRNA expression profiles', *BMC Genomics,* 15, pp. 181.

Kamato, D., Burch, M. L., Piva, T. J., Rezaei, H. B., Rostam, M. A., Xu, S., Zheng, W., Little, P. J. and Osman, N. (2013) 'Transforming growth factor-beta signalling: role and consequences of Smad linker region phosphorylation', *Cell Signal,* 25(10), pp. 2017-24.

Kanehisa, M., Goto, S., Sato, Y., Furumichi, M. and Tanabe, M. (2012) 'KEGG for integration and interpretation of large-scale molecular data sets', *Nucleic Acids Research,* 40(Database issue), pp. D109-14.

Kang, J. S., Liu, C. and Derynck, R. (2009) 'New regulatory mechanisms of TGF-beta receptor function', *Trends in Cell Biology,* 19(8), pp. 385-94.

Kaufmann, S. H. and Dorhoi, A. (2013) 'Inflammation in tuberculosis: interactions, imbalances and interventions', *Curr Opin Immunol,* 25(4), pp. 441-9.

Kaufmann, S. H. E. and Rubin, E. (2008) *Handbook of Tuberculosis.* Wiley.

Kawaji, H., Lizio, M., Itoh, M., Kanamori-Katayama, M., Kaiho, A., Nishiyori-Sueki, H., Shin, J. W., Kojima-Ishiyama, M., Kawano, M., Murata, M., Ninomiya-Fukuda, N., Ishikawa-Kato, S., Nagao-Sato, S., Noma, S., Hayashizaki, Y., Forrest, A. R. R. and Carninci, P. (2014) 'Comparison of CAGE and RNA-seq transcriptome profiling using clonally amplified and single-molecule next-generation sequencing', *Genome Res,* 24(4), pp. 708-17.

Khan, A. A., Betel, D., Miller, M. L., Sander, C., Leslie, C. S. and Marks, D. S. (2009) 'Transfection of small RNAs globally perturbs gene regulation by endogenous microRNAs', *Nat Biotechnol,* 27(6), pp. 549-55.

Kim, D., Pertea, G., Trapnell, C., Pimentel, H., Kelley, R. and Salzberg, S. L. (2013) 'TopHat2: accurate alignment of transcriptomes in the presence of insertions, deletions and gene fusions', *Genome Biology,* 14(4), pp. R36.

Kim, Y. K., Yu, J., Han, T. S., Park, S. Y., Namkoong, B., Kim, D. H., Hur, K., Yoo, M. W., Lee, H. J., Yang, H. K. and Kim, V. N. (2009) 'Functional links between clustered microRNAs: suppression of cell-cycle inhibitors by microRNA clusters in gastric cancer', *Nucleic Acids Research,* 37(5), pp. 1672-81.

Kleinnijenhuis, J., Quintin, J., Preijers, F., Joosten, L. A., Ifrim, D. C., Saeed, S., Jacobs, C., van Loenhout, J., de Jong, D., Stunnenberg, H. G., Xavier, R. J., van der Meer, J. W., van Crevel, R. and Netea, M. G. (2012) 'Bacille Calmette-Guerin induces NOD2-dependent nonspecific protection from reinfection via epigenetic reprogramming of monocytes', *Proceedings of the National Academy of Sciences of the United States of America,* 109(43), pp. 17537-42.

Kosaka, N., Izumi, H., Sekine, K. and Ochiya, T. (2010) 'microRNA as a new immune-regulatory agent in breast milk', *Silence,* 1(1), pp. 7.

Kozomara, A. and Griffiths-Jones, S. (2011) 'miRBase: integrating microRNA annotation and deep-sequencing data', *Nucleic acids research,* 39(Database issue), pp. D152-7.

Kramer, A., Green, J., Pollard, J., Jr. and Tugendreich, S. (2014) 'Causal analysis approaches in Ingenuity Pathway Analysis', *Bioinformatics,* 30(4), pp. 523-30.

Krol, J., Loedige, I. and Filipowicz, W. (2010) 'The widespread regulation of microRNA biogenesis, function and decay', *Nature Reviews. Genetics,* 11(9), pp. 597-610.

Kuhn, D. E., Martin, M. M., Feldman, D. S., Terry, A. V., Jr., Nuovo, G. J. and Elton, T. S. (2008) 'Experimental validation of miRNA targets', *Methods,* 44(1), pp. 47-54.

Kumar, M., Sahu, S. K., Kumar, R., Subuddhi, A., Maji, R. K., Jana, K., Gupta, P., Raffetseder, J., Lerm, M., Ghosh, Z., van Loo, G., Beyaert, R., Gupta, U. D., Kundu, M. and Basu, J. (2015) 'MicroRNA let-7 modulates the immune response to *Mycobacterium tuberculosis* infection via control of A20, an inhibitor of the NF-kappaB pathway', *Cell Host Microbe,* 17(3), pp. 345-56.

Kumar, R., Halder, P., Sahu, S. K., Kumar, M., Kumari, M., Jana, K., Ghosh, Z., Sharma, P., Kundu, M. and Basu, J. (2012) 'Identification of a novel role of ESAT-6-dependent miR-155 induction during infection of macrophages with *Mycobacterium tuberculosis*', *Cellular Microbiology,* 14(10), pp. 1620-31.

Kusuda, R., Cadetti, F., Ravanelli, M. I., Sousa, T. A., Zanon, S., De Lucca, F. L. and Lucas, G. (2011) 'Differential expression of microRNAs in mouse pain models', *Molecular Pain,* 7, pp. 17.

Lagos-Quintana, M., Rauhut, R., Yalcin, A., Meyer, J., Lendeckel, W. and Tuschl, T. (2002) 'Identification of tissue-specific microRNAs from mouse', *Curr Biol,* 12(9), pp. 735-9.

Lambrecht, B. N. (2006) 'Alveolar macrophage in the driver's seat', *Immunity,* 24(4), pp. 366-8.

Lawless, N., Foroushani, A. B., McCabe, M. S., O'Farrelly, C. and Lynn, D. J. (2013) 'Next generation sequencing reveals the expression of a unique miRNA profile in response to a Gram-positive bacterial infection', *PLoS One,* 8(3), pp. e57543.

Lawless, N., Reinhardt, T. A., Bryan, K., Baker, M., Pesch, B., Zimmerman, D., Zuelke, K., Sonstegard, T., O'Farrelly, C., Lippolis, J. D. and Lynn, D. J. (2014) 'MicroRNA regulation of bovine monocyte inflammatory and metabolic networks in an in vivo infection model', *G3 (Bethesda),* 4(6), pp. 957-71.

le Sage, C., Nagel, R., Egan, D. A., Schrier, M., Mesman, E., Mangiola, A., Anile, C., Maira, G., Mercatelli, N., Ciafre, S. A., Farace, M. G. and Agami, R. (2007) 'Regulation of the p27(Kip1) tumor suppressor by miR-221 and miR-222 promotes cancer cell proliferation', *EMBO Journal,* 26(15), pp. 3699-708.

Lee, L. W., Zhang, S., Etheridge, A., Ma, L., Martin, D., Galas, D. and Wang, K. (2010) 'Complexity of the microRNA repertoire revealed by next-generation sequencing', *RNA,* 16(11), pp. 2170-80.

Levine, B., Mizushima, N. and Virgin, H. W. (2011) 'Autophagy in immunity and inflammation', *Nature,* 469(7330), pp. 323-35.

Lewis, B. P., Burge, C. B. and Bartel, D. P. (2005) 'Conserved seed pairing, often flanked by adenosines, indicates that thousands of human genes are microRNA targets', *Cell,* 120(1), pp. 15-20.

Li, G., Luna, C., Qiu, J., Epstein, D. L. and Gonzalez, P. (2011a) 'Role of miR-204 in the regulation of apoptosis, endoplasmic reticulum stress response, and

inflammation in human trabecular meshwork cells', *Investigative Ophthalmology and Visual Science,* 52(6), pp. 2999-3007.

Li, L., Huang, J., Zhang, X., Ju, Z., Qi, C., Zhang, Y., Li, Q., Wang, C., Miao, W., Zhong, J., Hou, M. and Hang, S. (2012) 'One SNP in the 3'-UTR of HMGB1 gene affects the binding of target bta-miR-223 and is involved in mastitis in dairy cattle', *Immunogenetics,* 64(11), pp. 817-24.

Li, Y. P., Gottwein, J. M., Scheel, T. K., Jensen, T. B. and Bukh, J. (2011b) 'MicroRNA-122 antagonism against hepatitis C virus genotypes 1-6 and reduced efficacy by host RNA insertion or mutations in the HCV 5' UTR', *Proceedings of the National Academy of Sciences of the United States of America,* 108(12), pp. 4991-6.

Liao, Y., Smyth, G. K. and Shi, W. (2014) 'featureCounts: an efficient general purpose program for assigning sequence reads to genomic features', *Bioinformatics,* 30(7), pp. 923-30.

Lillebaek, T., Dirksen, A., Baess, I., Strunge, B., Thomsen, V. O. and Andersen, A. B. (2002) 'Molecular evidence of endogenous reactivation of *Mycobacterium tuberculosis* after 33 years of latent infection', *Journal of Infectious Diseases,* 185(3), pp. 401-4.

Lim, L. P., Lau, N. C., Garrett-Engele, P., Grimson, A., Schelter, J. M., Castle, J., Bartel, D. P., Linsley, P. S. and Johnson, J. M. (2005) 'Microarray analysis shows that some microRNAs downregulate large numbers of target mRNAs', *Nature,* 433(7027), pp. 769-73.

Lin, J., Huang, S., Wu, S., Ding, J., Zhao, Y., Liang, L., Tian, Q., Zha, R., Zhan, R. and He, X. (2011) 'MicroRNA-423 promotes cell growth and regulates G(1)/S transition by targeting p21Cip1/Waf1 in hepatocellular carcinoma', *Carcinogenesis,* 32(11), pp. 1641-7.

Liston, A., Linterman, M. and Lu, L. F. (2010) 'MicroRNA in the adaptive immune system, in sickness and in health', *Journal of Clinical Immunology,* 30(3), pp. 339-46.

Liu, G., Friggeri, A., Yang, Y., Park, Y. J., Tsuruta, Y. and Abraham, E. (2009) 'miR-147, a microRNA that is induced upon Toll-like receptor stimulation, regulates murine macrophage inflammatory responses', *Proceedings of the National Academy of Sciences of the United States of America,* 106(37), pp. 15819-24.

Liu, G., Park, Y. J. and Abraham, E. (2008) 'Interleukin-1 receptor-associated kinase (IRAK) -1-mediated NF-kappaB activation requires cytosolic and nuclear activity', *The FASEB Journal,* 22(7), pp. 2285-96.

Liu, P. T., Wheelwright, M., Teles, R., Komisopoulou, E., Edfeldt, K., Ferguson, B., Mehta, M. D., Vazirnia, A., Rea, T. H., Sarno, E. N., Graeber, T. G. and Modlin, R. L. (2012) 'MicroRNA-21 targets the vitamin D-dependent antimicrobial pathway in leprosy', *Nature Medicine,* 18(2), pp. 267-73.

Luan, Y., Lengyel, P. and Liu, C. J. (2008) 'p204, a p200 family protein, as a multifunctional regulator of cell proliferation and differentiation', *Cytokine Growth Factor Rev,* 19(5-6), pp. 357-69.

Lynn, D. J., Winsor, G. L., Chan, C., Richard, N., Laird, M. R., Barsky, A., Gardy, J. L., Roche, F. M., Chan, T. H., Shah, N., Lo, R., Naseer, M., Que, J., Yau, M., Acab, M., Tulpan, D., Whiteside, M. D., Chikatamarla, A., Mah, B., Munzner, T., Hokamp, K., Hancock, R. E. and Brinkman, F. S. (2008) 'InnateDB: facilitating systems-level analyses of the mammalian innate immune response', *Molecular Systems Biology,* 4, pp. 218.

Ma, C., Li, Y., Li, M., Deng, G., Wu, X., Zeng, J., Hao, X., Wang, X., Liu, J., Cho, W. C., Liu, X. and Wang, Y. (2014) 'microRNA-124 negatively regulates TLR signaling in alveolar macrophages in response to mycobacterial infection', *Molecular Immunology,* 62(1), pp. 150-8.

Ma, F., Xu, S., Liu, X., Zhang, Q., Xu, X., Liu, M., Hua, M., Li, N., Yao, H. and Cao, X. (2011) 'The microRNA miR-29 controls innate and adaptive immune responses to intracellular bacterial infection by targeting interferon-gamma', *Nature Immunology,* 12(9), pp. 861-9.

MacHugh, D. E., Gormley, E., Park, S. D., Browne, J. A., Taraktsoglou, M., O'Farrelly, C. and Meade, K. G. (2009) 'Gene expression profiling of the host response to *Mycobacterium bovis* infection in cattle', *Transboundary and Emerging Diseases,* 56(6-7), pp. 204-14.

Magee, D. A., Conlon, K. M., Nalpas, N. C., Browne, J. A., Pirson, C., Healy, C., McLoughlin, K. E., Chen, J., Vordermeier, H. M., Gormley, E., MacHugh, D. E. and Gordon, S. V. (2014) 'Innate cytokine profiling of bovine alveolar macrophages reveals commonalities and divergence in the response to *Mycobacterium bovis* and *Mycobacterium tuberculosis* infection', *Tuberculosis.*

Magee, D. A., Taraktsoglou, M., Killick, K. E., Nalpas, N. C., Browne, J. A., Park, S. D., Conlon, K. M., Lynn, D. J., Hokamp, K., Gordon, S. V., Gormley, E. and MacHugh, D. E. (2012) 'Global gene expression and systems biology analysis of bovine monocyte-derived macrophages in response to in vitro challenge with *Mycobacterium bovis*', *PloS One,* 7(2), pp. e32034.

Marioni, J. C., Mason, C. E., Mane, S. M., Stephens, M. and Gilad, Y. (2008) 'RNA-seq: an assessment of technical reproducibility and comparison with gene expression arrays', *Genome Research,* 18(9), pp. 1509-17.

Marriott, H. M. and Dockrell, D. H. (2007) 'The role of the macrophage in lung disease mediated by bacteria', *Experimental Lung Research,* 33(10), pp. 493-505.

Martin, M. (2011) 'Cutadapt removes adapter sequences from high-throughput sequencing reads', *EMBnet.journal,* 17(1), pp. 10-12.

Martinez-Sanchez, A. and Murphy, C. L. (2013) 'MicroRNA target identification-experimental approaches', *Biology,* 2(1), pp. 189-205.

Maudet, C., Mano, M. and Eulalio, A. (2014) 'MicroRNAs in the interaction between host and bacterial pathogens', *FEBS Lett,* 588(22), pp. 4140-7.

McDonald, R. A. (2014) 'Animal health: How to control bovine tuberculosis', *Nature,* 511(7508), pp. 158-9.

Meade, K. G., Gormley, E., Doyle, M. B., Fitzsimons, T., O'Farrelly, C., Costello, E., Keane, J., Zhao, Y. and MacHugh, D. E. (2007) 'Innate gene repression associated with *Mycobacterium bovis* infection in cattle: toward a gene signature of disease', *BMC Genomics,* 8, pp. 400.

Meade, K. G., Gormley, E., O'Farrelly, C., Park, S. D., Costello, E., Keane, J., Zhao, Y. and MacHugh, D. E. (2008) 'Antigen stimulation of peripheral blood mononuclear cells from Mycobacterium bovis infected cattle yields evidence for a novel gene expression program', *BMC Genomics,* 9, pp. 447.

Medina, R., Zaidi, S. K., Liu, C. G., Stein, J. L., van Wijnen, A. J., Croce, C. M. and Stein, G. S. (2008) 'MicroRNAs 221 and 222 bypass quiescence and compromise cell survival', *Cancer Research,* 68(8), pp. 2773-80.

Mehta, M. D. and Liu, P. T. (2014) 'microRNAs in mycobacterial disease: friend or foe?', *Frontiers in Genetics,* 5, pp. 231.

Menzies, F. D. and Neill, S. D. (2000) 'Cattle-to-cattle transmission of bovine tuberculosis', *Vet J,* 160(2), pp. 92-106.

Meredith, B. K., Berry, D. P., Kearney, F., Finlay, E. K., Fahey, A. G., Bradley, D. G. and Lynn, D. J. (2013) 'A genome-wide association study for somatic cell score using the Illumina high-density bovine beadchip identifies several novel QTL potentially related to mastitis susceptibility', *Frontiers in Genetics,* 4, pp. 229.

Mogensen, T. H. (2009) 'Pathogen recognition and inflammatory signaling in innate immune defenses', *Clin Microbiol Rev,* 22(2), pp. 240-73.

Montagner, S., Orlandi, E. M., Merante, S. and Monticelli, S. (2013) 'The role of miRNAs in mast cells and other innate immune cells', *Immunol Rev,* 253(1), pp. 12-24.

Mosser, D. M. and Edwards, J. P. (2008) 'Exploring the full spectrum of macrophage activation', *Nature Reviews. Immunology,* 8(12), pp. 958-69.

Mullokandov, G., Baccarini, A., Ruzo, A., Jayaprakash, A. D., Tung, N., Israelow, B., Evans, M. J., Sachidanandam, R. and Brown, B. D. (2012) 'High-throughput assessment of microRNA activity and function using microRNA sensor and decoy libraries', *Nature Methods,* 9(8), pp. 840-6.

Murphy, K. P., Travers, P., Walport, M. and Janeway, C. (2008) *Janeway's Immunobiology.* Garland Science.

Naeem, A., Zhong, K., Moisa, S. J., Drackley, J. K., Moyes, K. M. and Loor, J. J. (2012) 'Bioinformatics analysis of microRNA and putative target genes in bovine mammary tissue infected with Streptococcus uberis', *Journal of Dairy Science,* 95(11), pp. 6397-408.

Nalpas, N. C., Park, S. D., Magee, D. A., Taraktsoglou, M., Browne, J. A., Conlon, K. M., Rue-Albrecht, K., Killick, K. E., Hokamp, K., Lohan, A. J., Loftus, B. J., Gormley, E., Gordon, S. V. and Machugh, D. E. (2013) 'Whole-transcriptome, high-throughput RNA sequence analysis of the bovine macrophage response to *Mycobacterium bovis* infection in vitro', *BMC Genomics,* 14(1), pp. 230.

Nam, J. W., Rissland, O. S., Koppstein, D., Abreu-Goodger, C., Jan, C. H., Agarwal, V., Yildirim, M. A., Rodriguez, A. and Bartel, D. P. (2014) 'Global analyses of the effect of different cellular contexts on microRNA targeting', *Mol Cell,* 53(6), pp. 1031-43.

Natarajan, K., Kundu, M., Sharma, P. and Basu, J. (2011) 'Innate immune responses to *M. tuberculosis* infection', *Tuberculosis,* 91(5), pp. 427-31.

Neilsen, C. T., Goodall, G. J. and Bracken, C. P. (2012) 'IsomiRs--the overlooked repertoire in the dynamic microRNAome', *Trends in Genetics,* 28(11), pp. 544-9.

Newman, M. A., Mani, V. and Hammond, S. M. (2011) 'Deep sequencing of microRNA precursors reveals extensive 3' end modification', *RNA,* 17(10), pp. 1795-803.

Ni Cheallaigh, C., Keane, J., Lavelle, E. C., Hope, J. C. and Harris, J. (2011) 'Autophagy in the immune response to tuberculosis: clinical perspectives', *Clinical and Experimental Immunology,* 164(3), pp. 291-300.

O'Connell, R. M., Rao, D. S., Chaudhuri, A. A. and Baltimore, D. (2010) 'Physiological and pathological roles for microRNAs in the immune system', *Nature Reviews. Immunology,* 10(2), pp. 111-22.

O'Connell, R. M., Taganov, K. D., Boldin, M. P., Cheng, G. and Baltimore, D. (2007) 'MicroRNA-155 is induced during the macrophage inflammatory response', *Proceedings of the National Academy of Sciences of the United States of America,* 104(5), pp. 1604-9.

O'Leary, S., O'Sullivan, M. P. and Keane, J. (2011) 'IL-10 blocks phagosome maturation in *Mycobacterium tuberculosis*-infected human macrophages', *American Journal of Respiratory Cell and Molecular Biology,* 45(1), pp. 172-80.

O'Neill, L. A. (2008) 'The interleukin-1 receptor/Toll-like receptor superfamily: 10 years of progress', *Immunological Reviews,* 226, pp. 10-8.

O'Neill, L. A., Sheedy, F. J. and McCoy, C. E. (2011) 'MicroRNAs: the fine-tuners of Toll-like receptor signalling', *Nature Reviews. Immunology,* 11(3), pp. 163-75.

Ottenhoff, T. H. (2012) 'New pathways of protective and pathological host defense to mycobacteria', *Trends in Microbiology,* 20(9), pp. 419-28.

Ouyang, Y. B., Stary, C. M., White, R. E. and Giffard, R. G. (2015) 'The use of microRNAs to modulate redox and immune response to stroke', *Antioxid Redox Signal,* 22(2), pp. 187-202.

Pasquinelli, A. E. (2012) 'MicroRNAs and their targets: recognition, regulation and an emerging reciprocal relationship', *Nature Reviews. Genetics,* 13(4), pp. 271-82.

Pauls, E., Nanda, S. K., Smith, H., Toth, R., Arthur, J. S. and Cohen, P. (2013) 'Two phases of inflammatory mediator production defined by the study of IRAK2 and IRAK1 knock-in mice', *Journal of Immunology,* 191(5), pp. 2717-30.

Perkins, J. R., Dawes, J. M., McMahon, S. B., Bennett, D. L., Orengo, C. and Kohl, M. (2012) 'ReadqPCR and NormqPCR: R packages for the reading, quality checking and normalisation of RT-qPCR quantification cycle (Cq) data', *BMC Genomics,* 13, pp. 296.

Peters-Golden, M. (2004) 'The alveolar macrophage: the forgotten cell in asthma', *American Journal of Respiratory Cell and Molecular Biology,* 31(1), pp. 3-7.

Pfaffl, M. W. (2001) 'A new mathematical model for relative quantification in real-time RT-PCR', *Nucleic Acids Research,* 29(9), pp. e45.

Pilli, M., Arko-Mensah, J., Ponpuak, M., Roberts, E., Master, S., Mandell, M. A., Dupont, N., Ornatowski, W., Jiang, S., Bradfute, S. B., Bruun, J. A., Hansen, T. E., Johansen, T. and Deretic, V. (2012) 'TBK-1 promotes autophagy-mediated antimicrobial defense by controlling autophagosome maturation', *Immunity,* 37(2), pp. 223-34.

Pollock, J. M., Rodgers, J. D., Welsh, M. D. and McNair, J. (2006) 'Pathogenesis of bovine tuberculosis: the role of experimental models of infection', *Veterinary Microbiology,* 112(2-4), pp. 141-50.

Pradervand, S., Weber, J., Lemoine, F., Consales, F., Paillusson, A., Dupasquier, M., Thomas, J., Richter, H., Kaessmann, H., Beaudoing, E., Hagenbuchle, O. and Harshman, K. (2010) 'Concordance among digital gene expression, microarrays, and qPCR when measuring differential expression of microRNAs', *Biotechniques,* 48(3), pp. 219-22.

Qi, Y., Cui, L., Ge, Y., Shi, Z., Zhao, K., Guo, X., Yang, D., Yu, H., Shan, Y., Zhou, M., Wang, H. and Lu, Z. (2012) 'Altered serum microRNAs as biomarkers for the early diagnosis of pulmonary tuberculosis infection', *BMC Infectious Diseases,* 12, pp. 384.

Quinn, S. R. and O'Neill, L. A. (2011) 'A trio of microRNAs that control Toll-like receptor signalling', *International Immunology,* 23(7), pp. 421-5.

Raabe, C. A., Tang, T. H., Brosius, J. and Rozhdestvensky, T. S. (2014) 'Biases in small RNA deep sequencing data', *Nucleic Acids Research,* 42(3), pp. 1414-26.

Rajaram, M. V., Ni, B., Dodd, C. E. and Schlesinger, L. S. (2014) 'Macrophage immunoregulatory pathways in tuberculosis', *Semin Immunol,* 26(6), pp. 471-85.

Rajaram, M. V., Ni, B., Morris, J. D., Brooks, M. N., Carlson, T. K., Bakthavachalu, B., Schoenberg, D. R., Torrelles, J. B. and Schlesinger, L. S. (2011) '*Mycobacterium tuberculosis* lipomannan blocks TNF biosynthesis by regulating

macrophage MAPK-activated protein kinase 2 (MK2) and microRNA miR-125b', *Proceedings of the National Academy of Sciences of the United States of America,* 108(42), pp. 17408-13.

Ramakrishnan, L. (2012) 'Revisiting the role of the granuloma in tuberculosis', *Nature Reviews. Immunology,* 12(5), pp. 352-66.

Redford, P. S., Murray, P. J. and O'Garra, A. (2011) 'The role of IL-10 in immune regulation during *M. tuberculosis* infection', *Mucosal Immunology,* 4(3), pp. 261-70.

Roberts, E. A., Chua, J., Kyei, G. B. and Deretic, V. (2006) 'Higher order Rab programming in phagolysosome biogenesis', *The Journal of Cell Biology,* 174(7), pp. 923-9.

Robinson, M. D., McCarthy, D. J. and Smyth, G. K. (2010) 'edgeR: a Bioconductor package for differential expression analysis of digital gene expression data', *Bioinformatics,* 26(1), pp. 139-40.

Robinson, M. D. and Oshlack, A. (2010) 'A scaling normalization method for differential expression analysis of RNA-seq data', *Genome Biology,* 11(3), pp. R25.

Rodrigues, M. F., Alves, C. C., Figueiredo, B. B., Rezende, A. B., Wohlres-Viana, S., Silva, V. L., Machado, M. A. and Teixeira, H. C. (2013) 'Tumour necrosis factor receptors and apoptosis of alveolar macrophages during early infection with attenuated and virulent *Mycobacterium bovis*', *Immunology,* 139(4), pp. 503-12.

Rossi, R. L., Rossetti, G., Wenandy, L., Curti, S., Ripamonti, A., Bonnal, R. J., Birolo, R. S., Moro, M., Crosti, M. C., Gruarin, P., Maglie, S., Marabita, F., Mascheroni, D., Parente, V., Comelli, M., Trabucchi, E., De Francesco, R., Geginat, J., Abrignani, S. and Pagani, M. (2011) 'Distinct microRNA signatures in human lymphocyte subsets and enforcement of the naive state in CD4+ T cells by the microRNA miR-125b', *Nature Immunology,* 12(8), pp. 796-803.

Rottiers, V. and Naar, A. M. (2012) 'MicroRNAs in metabolism and metabolic disorders', *Nature Reviews. Molecular Cell Biology,* 13(4), pp. 239-50.

Rusca, N. and Monticelli, S. (2011) 'MiR-146a in Immunity and Disease', *Mol Biol Int,* 2011, pp. 437301.

Sager, H., Davis, W. C. and Jungi, T. W. (1999) 'Bovine monocytoid cells transformed to proliferate cease to exhibit lineage-specific functions', *Veterinary Immunology and Immunopathology,* 68(2-4), pp. 113-30.

Sasindran, S. J. and Torrelles, J. B. (2011) '*Mycobacterium tuberculosis* infection and inflammation: what is beneficial for the host and for the bacterium?', *Frontiers in Microbiology,* 2, pp. 2.

Satoh, M., Tabuchi, T., Minami, Y., Takahashi, Y., Itoh, T. and Nakamura, M. (2012) 'Expression of let-7i is associated with Toll-like receptor 4 signal in coronary artery disease: effect of statins on let-7i and Toll-like receptor 4 signal', *Immunobiology,* 217(5), pp. 533-9.

Schnitger, A. K. D., Machova, A., Mueller, R. U., Androulidaki, A., Schermer, B., Pasparakis, M., Krönke, M. and Papadopoulou, N. (2011) '*Listeria monocytogenes* infection in macrophages induces vacuolar-dependent host miRNA response', *PLoS One,* 6(11), pp. e27435.

Schulte, L. N., Eulalio, A., Mollenkopf, H. J., Reinhardt, R. and Vogel, J. (2011) 'Analysis of the host microRNA response to *Salmonella* uncovers the control of major cytokines by the let-7 family', *The EMBO Journal,* 30(10), pp. 1977-89.

Shaler, C. R., Horvath, C., Lai, R. and Xing, Z. (2012) 'Understanding delayed T-cell priming, lung recruitment, and airway luminal T-cell responses in host defense against pulmonary tuberculosis', *Clin Dev Immunol,* 2012, pp. 628293.

Shapiro, E., Biezuner, T. and Linnarsson, S. (2013) 'Single-cell sequencing-based technologies will revolutionize whole-organism science', *Nature Reviews. Genetics,* 14(9), pp. 618-30.

Sharbati, J., Lewin, A., Kutz-Lohroff, B., Kamal, E., Einspanier, R. and Sharbati, S. (2011) 'Integrated microRNA-mRNA-analysis of human monocyte derived macrophages upon *Mycobacterium avium* subsp. *hominissuis* infection', *PLoS One,* 6(5), pp. e20258.

Sharbati, S., Sharbati, J., Hoeke, L., Bohmer, M. and Einspanier, R. (2012) 'Quantification and accurate normalisation of small RNAs through new custom RT-qPCR arrays demonstrates *Salmonella*-induced microRNAs in human monocytes', *BMC Genomics,* 13, pp. 23.

Singh, P. K., Singh, A. V. and Chauhan, D. S. (2013a) 'Current understanding on micro RNAs and its regulation in response to Mycobacterial infections', *Journal of Biomedical Science,* 20, pp. 14.

Singh, Y., Kaul, V., Mehra, A., Chatterjee, S., Tousif, S., Dwivedi, V. P., Suar, M., Van Kaer, L., Bishai, W. R. and Das, G. (2013b) 'Mycobacterium tuberculosis controls microRNA-99b (miR-99b) expression in infected murine dendritic cells

to modulate host immunity', *The Journal of Biological Chemistry,* 288(7), pp. 5056-61.

So, A. Y., Zhao, J. L. and Baltimore, D. (2013) 'The Yin and Yang of microRNAs: leukemia and immunity', *Immunol Rev,* 253(1), pp. 129-45.

Sopp, P., Coad, M., Hewinson, G., Howard, C. J., Cheallaigh, C. N., Keane, J., Harris, J. and Hope, J. C. (2008) 'Development of a simple, sensitive, rapid test which discriminates BCG-vaccinated from *Mycobacterium bovis*-infected cattle', *Vaccine,* 26(43), pp. 5470-6.

Stanley, S. A., Grant, S. S., Kawate, T., Iwase, N., Shimizu, M., Wivagg, C., Silvis, M., Kazyanskaya, E., Aquadro, J., Golas, A., Fitzgerald, M., Dai, H., Zhang, L. and Hung, D. T. (2012) 'Identification of novel inhibitors of *M. tuberculosis* growth using whole cell based high-throughput screening', *ACS Chem Biol,* 7(8), pp. 1377-84.

Subbian, S., Bandyopadhyay, N., Tsenova, L., P, O. B., Khetani, V., Kushner, N. L., Peixoto, B., Soteropoulos, P., Bader, J. S., Karakousis, P. C., Fallows, D. and Kaplan, G. (2013) 'Early innate immunity determines outcome of *Mycobacterium tuberculosis* pulmonary infection in rabbits', *Cell Commun Signal,* 11(1), pp. 60.

Sung, T. L. and Rice, A. P. (2009) 'miR-198 inhibits HIV-1 gene expression and replication in monocytes and its mechanism of action appears to involve repression of cyclin T1', *PLoS Pathogens,* 5(1), pp. e1000263.

Taganov, K. D., Boldin, M. P., Chang, K. J. and Baltimore, D. (2006) 'NF-kappaB-dependent induction of microRNA miR-146, an inhibitor targeted to signaling proteins of innate immune responses', *Proceedings of the National Academy of Sciences of the United States of America,* 103(33), pp. 12481-6.

Tam, S., de Borja, R., Tsao, M. S. and McPherson, J. D. (2014) 'Robust global microRNA expression profiling using next-generation sequencing technologies', *Lab Invest,* 94(3), pp. 350-8.

Tanaka, T. and Kishimoto, T. (2014) 'The biology and medical implications of interleukin-6', *Cancer Immunol Res,* 2(4), pp. 288-94.

Tang, F., Barbacioru, C., Wang, Y., Nordman, E., Lee, C., Xu, N., Wang, X., Bodeau, J., Tuch, B. B., Siddiqui, A., Lao, K. and Surani, M. A. (2009) 'mRNA-Seq whole-transcriptome analysis of a single cell', *Nature Methods,* 6(5), pp. 377-82.

Tanzer, A. and Stadler, P. F. (2004) 'Molecular evolution of a microRNA cluster', *Journal of Molecular Biology,* 339(2), pp. 327-35.

Taraktsoglou, M., Szalabska, U., Magee, D. A., Browne, J. A., Sweeney, T., Gormley, E. and MacHugh, D. E. (2011) 'Transcriptional profiling of immune genes in bovine monocyte-derived macrophages exposed to bacterial antigens', *Veterinary Immunology and Immunopathology,* 140(1-2), pp. 130-9.

Tarang, S. and Weston, M. D. (2014) 'Macros in microRNA target identification: a comparative analysis of in *silico, in vitro,* and *in vivo* approaches to microRNA target identification', *RNA Biology,* 11(4), pp. 324-33.

Thomson, D. W., Bracken, C. P. and Goodall, G. J. (2011) 'Experimental strategies for microRNA target identification', *Nucleic Acids Research,* 39(16), pp. 6845-53.

Tili, E., Michaille, J. J., Cimino, A., Costinean, S., Dumitru, C. D., Adair, B., Fabbri, M., Alder, H., Liu, C. G., Calin, G. A. and Croce, C. M. (2007) 'Modulation of miR-155 and miR-125b levels following lipopolysaccharide/TNF-alpha stimulation and their possible roles in regulating the response to endotoxin shock', *Journal of Immunology,* 179(8), pp. 5082-9.

Toossi, Z. and Ellner, J. J. (1998) 'The role of TGF beta in the pathogenesis of human tuberculosis', *Clinical Immunology and Immunopathology,* 87(2), pp. 107-14.

Trapnell, C., Pachter, L. and Salzberg, S. L. (2009) 'TopHat: discovering splice junctions with RNA-Seq', *Bioinformatics,* 25(9), pp. 1105-11.

Undi, R. B., Kandi, R. and Gutti, R. K. (2013) 'MicroRNAs as haematopoiesis regulators', *Advances in Hematology,* 2013, pp. 695754.

Unterholzner, L., Keating, S. E., Baran, M., Horan, K. A., Jensen, S. B., Sharma, S., Sirois, C. M., Jin, T., Latz, E., Xiao, T. S., Fitzgerald, K. A., Paludan, S. R. and Bowie, A. G. (2010) 'IFI16 is an innate immune sensor for intracellular DNA', *Nat Immunol,* 11(11), pp. 997-1004.

Upadhyay, V. and Fu, Y. X. (2013) 'Lymphotoxin signalling in immune homeostasis and the control of microorganisms', *Nature Reviews. Immunology,* 13(4), pp. 270-9.

van Rooij, E. and Kauppinen, S. (2014) 'Development of microRNA therapeutics is coming of age', *EMBO Molecular Medicine,* 6(7), pp. 851-864.

van Rooij, E., Sutherland, L. B., Qi, X., Richardson, J. A., Hill, J. and Olson, E. N. (2007) 'Control of stress-dependent cardiac growth and gene expression by a microRNA', *Science,* 316(5824), pp. 575-9.

Vandesompele, J., De Preter, K., Pattyn, F., Poppe, B., Van Roy, N., De Paepe, A. and Speleman, F. (2002) 'Accurate normalization of real-time quantitative RT-PCR data by geometric averaging of multiple internal control genes', *Genome Biology,* 3(7), pp. 34.

Vasudevan, S. (2012) 'Posttranscriptional upregulation by microRNAs', *Wiley Interdiscip Rev RNA,* 3(3), pp. 311-30.

Vegh, P., Foroushani, A. B., Magee, D. A., McCabe, M. S., Browne, J. A., Nalpas, N. C., Conlon, K. M., Gordon, S. V., Bradley, D. G., MacHugh, D. E. and Lynn, D. J. (2013) 'Profiling microRNA expression in bovine alveolar macrophages using RNA-seq', *Veterinary Immunology and Immunopathology,* 155(4), pp. 238-44.

Vergne, I., Fratti, R. A., Hill, P. J., Chua, J., Belisle, J. and Deretic, V. (2004) '*Mycobacterium tuberculosis* phagosome maturation arrest: mycobacterial phosphatidylinositol analog phosphatidylinositol mannoside stimulates early endosomal fusion', *Molecular Biology of the Cell,* 15(2), pp. 751-60.

Wang, C., Yang, S., Sun, G., Tang, X., Lu, S., Neyrolles, O. and Gao, Q. (2011) 'Comparative miRNA expression profiles in individuals with latent and active tuberculosis', *PLoS One,* 6(10), pp. e25832.

Wang, D., Zhang, H., Li, M., Frid, M. G., Flockton, A. R., McKeon, B. A., Yeager, M. E., Fini, M. A., Morrell, N. W., Pullamsetti, S. S., Velegala, S., Seeger, W., McKinsey, T. A., Sucharov, C. C. and Stenmark, K. R. (2014) 'MicroRNA-124 controls the proliferative, migratory, and inflammatory phenotype of pulmonary vascular fibroblasts', *Circulation Research,* 114(1), pp. 67-78.

Wang, F. E., Zhang, C., Maminishkis, A., Dong, L., Zhi, C., Li, R., Zhao, J., Majerciak, V., Gaur, A. B., Chen, S. and Miller, S. S. (2010) 'MicroRNA-204/211 alters epithelial physiology', *The FASEB Journal,* 24(5), pp. 1552-71.

Wang, Z., Gerstein, M. and Snyder, M. (2009) 'RNA-Seq: a revolutionary tool for transcriptomics', *Nature Reviews. Genetics,* 10(1), pp. 57-63.

Welin, A. and Lerm, M. (2012) 'Inside or outside the phagosome? The controversy of the intracellular localization of *Mycobacterium tuberculosis*', *Tuberculosis,* 92(2), pp. 113-20.

Wen, J., Parker, B. J., Jacobsen, A. and Krogh, A. (2011) 'MicroRNA transfection and AGO-bound CLIP-seq data sets reveal distinct determinants of miRNA action', *RNA,* 17(5), pp. 820-34.

WHO (2013) 'Global Tuberculosis Report'.

Widdison, S., Watson, M. and Coffey, T. J. (2011) 'Early response of bovine alveolar macrophages to infection with live and heat-killed *Mycobacterium bovis*', *Developmental and Comparative Immunology,* 35(5), pp. 580-91.

Winter, J., Jung, S., Keller, S., Gregory, R. I. and Diederichs, S. (2009) 'Many roads to maturity: microRNA biogenesis pathways and their regulation', *Nature Cell Biology,* 11(3), pp. 228-34.

Wood, P. R. and Jones, S. L. (2001) 'BOVIGAM: an in vitro cellular diagnostic test for bovine tuberculosis', *Tuberculosis,* 81(1-2), pp. 147-55.

Wright, J. R. (2005) 'Immunoregulatory functions of surfactant proteins', *Nature Reviews. Immunology,* 5(1), pp. 58-68.

Wu, J., Lu, C., Diao, N., Zhang, S., Wang, S., Wang, F., Gao, Y., Chen, J., Shao, L., Lu, J., Zhang, X., Weng, X., Wang, H., Zhang, W. and Huang, Y. (2012a) 'Analysis of microRNA expression profiling identifies miR-155 and miR-155* as potential diagnostic markers for active tuberculosis: a preliminary study', *Human Immunology,* 73(1), pp. 31-7.

Wu, M., Aung, H., Hirsch, C. S. and Toossi, Z. (2012b) 'Inhibition of *Mycobacterium tuberculosis*-induced signalling by transforming growth factor-beta in human mononuclear phagocytes', *Scandinavian Journal of Immunology,* 75(3), pp. 301-4.

Xiao, C. and Rajewsky, K. (2009) 'MicroRNA control in the immune system: basic principles', *Cell,* 136(1), pp. 26-36.

Xu, G., Fewell, C., Taylor, C., Deng, N., Hedges, D., Wang, X., Zhang, K., Lacey, M., Zhang, H., Yin, Q., Cameron, J., Lin, Z., Zhu, D. and Flemington, E. K. (2010) 'Transcriptome and targetome analysis in MIR155 expressing cells using RNA-seq', *RNA,* 16(8), pp. 1610-22.

Xu, G., Zhang, Y., Jia, H., Li, J., Liu, X., Engelhardt, J. F. and Wang, Y. (2009) 'Cloning and identification of microRNAs in bovine alveolar macrophages', *Molecular and Cellular Biochemistry,* 332(1-2), pp. 9-16.

Xu, G., Zhang, Z., Wei, J., Zhang, Y., Guo, L. and Liu, X. (2013) 'microR-142-3p down-regulates IRAK-1 in response to *Mycobacterium bovis* BCG infection in macrophages', *Tuberculosis,* 93(6), pp. 606-11.

Yi, Z., Fu, Y., Ji, R., Li, R. and Guan, Z. (2012) 'Altered microRNA signatures in sputum of patients with active pulmonary tuberculosis', *PLoS One,* 7(8), pp. e43184.

Yin, Q., Wang, X., Fewell, C., Cameron, J., Zhu, H., Baddoo, M., Lin, Z. and Flemington, E. K. (2010) 'MicroRNA miR-155 inhibits bone morphogenetic protein (BMP) signaling and BMP-mediated Epstein-Barr virus reactivation', *J Virol,* 84(13), pp. 6318-27.

Yoshida, Y. and Tanaka, T. (2014) 'Interleukin 6 and rheumatoid arthritis', *Biomed Res Int,* 2014, pp. 698313.

Young, M. D., Wakefield, M. J., Smyth, G. K. and Oshlack, A. (2010) 'Gene ontology analysis for RNA-seq: accounting for selection bias', *Genome biology,* 11(2), pp. R14.

Zarogoulidis, P., Katsikogianni, F., Tsiouda, T., Sakkas, A., Katsikogiannis, N. and Zarogoulidis, K. (2014) 'Interleukin-8 and interleukin-17 for cancer', *Cancer Invest,* 32(5), pp. 197-205.

Zhang, H., Sun, Z., Wei, W., Liu, Z., Fleming, J., Zhang, S., Lin, N., Wang, M., Chen, M., Xu, Y., Zhou, J., Li, C., Bi, L. and Zhou, G. (2014) 'Identification of serum microRNA biomarkers for tuberculosis using RNA-seq', *PLoS One,* 9(2), pp. e88909.

Zhao, J. L. and Starczynowski, D. T. (2014) 'Role of microRNA-146a in normal and malignant hematopoietic stem cell function', *Frontiers in Genetics,* 5, pp. 219.

Zimin, A. V., Delcher, A. L., Florea, L., Kelley, D. R., Schatz, M. C., Puiu, D., Hanrahan, F., Pertea, G., Van Tassell, C. P., Sonstegard, T. S., Marcais, G., Roberts, M., Subramanian, P., Yorke, J. A. and Salzberg, S. L. (2009) 'A whole-genome assembly of the domestic cow, *Bos taurus*', *Genome Biology,* 10(4), pp. R42.

Appendix

Appendix 1 | Total and small RNA concentrations, as measured by Bioanalyzer (Chapter 2).

Sample	Small RNA [pg/µl]	miRNA [pg/µl]	RNA [ng/ul]	rRNA Ratio [28s / 18s]	RNA Integrity Number (RIN)
1	15674	746	383	1.60	9.4
2	19602	1144	530	1.59	9.4
3	18441	1404	483	1.66	9.4
4	13306	1005	446	1.62	9.6
5	17380	1875	372	1.72	9.7
6	11565	1830	470	1.69	9.6
7	9854	1820	656	1.55	9.4
8	9869	660	72	1.82	9.2

Appendix 2 | Small RNA concentrations, as measured by Bioanalyzer (Chapter 3).

Sample Code	Animal ID	Timepoint (hpi)	Treatment	Small RNA [pg/µl]	miRNA [pg/µl]
1	N1178	48	control	17158	513
2	N1178	24	infected	8808	233
3	N121	6	infected	16608	597
4	N121	6	control	12236	455
5	N121	24	infected	9371	347
6	N121	24	control	9634	276
7	N138	2	control	8823	186
8	N158	48	infected	10569	353
9	N158	48	control	7429	264
10	N1855	6	control	7258	389
11	N1859	24	control	4449	505
12	N1859	6	infected	8643	328
13	N1861	0	control	11693	518
14	N1861	2	infected	10395	539
15	N1864	0	control	12684	360
16	N1864	48	control	4618	255
17	N1870	48	control	6646	320
18	N1870	24	infected	7710	386
19	N1178	6	infected	9873	208
20	N121	0	control	10933	504
21	N121	48	control	6328	328
22	N121	2	control	5205	346
23	N138	24	control	5686	323
24	N138	6	infected	13945	377
25	N138	48	control	7914	424
26	N138	48	infected	12853	613
27	N158	2	control	11506	409
28	N1855	6	infected	13084	407
29	N1855	24	control	7704	344
30	N1859	0	control	8727	385
31	N1859	6	control	6767	247
32	N1861	24	control	6399	237
33	N1864	2	infected	5509	418
34	N1870	0	control	11189	379
35	N1870	48	infected	14366	473
36	N98	6	infected	6687	494
37	N1178	24	control	10030	220
38	N1178	2	control	11947	277
39	N121	2	infected	12904	708
40	N138	2	infected	8299	398
41	N158	6	control	8167	353
42	N158	0	control	7497	394

43	N158	24	infected	7410	431
44	N158	6	infected	8874	475
45	N1855	48	control	9190	448
46	N1855	0	control	10939	377
47	N1859	24	infected	12567	397
48	N1859	48	infected	10067	597
49	N1861	24	infected	7972	325
50	N1864	48	infected	6678	765
51	N1864	24	control	8130	287
52	N1864	6	infected	6683	245
53	N1870	2	infected	9852	555
54	N98	24	infected	4445	418
55	N1178	2	infected	8752	332
56	N1178	48	infected	14717	504
57	N1178	6	control	10940	209
58	N121	48	infected	9976	1425
59	N138	6	control	10331	309
60	N158	2	infected	10265	448
61	N1855	24	infected	16634	481
62	N1855	2	infected	10705	390
63	N1859	2	control	8951	417
64	N1861	6	control	4610	303
65	N1861	6	infected	6588	304
66	N1864	2	control	7209	326
67	N1864	6	control	6830	218
68	N1870	6	infected	9624	321
69	N1870	6	control	10850	292
70	N1870	2	control	13028	400
71	N98	6	control	6374	572
72	N98	2	infected	8232	988
73	N1178	0	control	12315	302
74	N138	0	control	5507	152
75	N138	24	infected	8003	288
76	N158	24	control	4525	222
77	N1855	48	infected	8783	619
78	N1855	2	control	12966	865
79	N1859	2	infected	12668	567
80	N1859	48	control	7130	171
81	N1861	2	control	9911	231
82	N1864	24	infected	11598	218
83	N1870	24	control	6151	322
84	N98	48	infected	3431	381
85	N98	48	control	4129	143
86	N98	2	control	7603	638
87	N98	24	control	4028	209
88	N98	0	control	5466	577

Appendix 3 | Library quantity, Truseq index, and flowcell lane number for each sample.

Sample code	Animal ID	Timepoint (hpi)	Treatment	Quantity (μg)	Truseq index	Lane number
1	N1178	48	control	18.1	21	2
2	N1178	24	infected	18.1	29	6
3	N121	6	infected	16.6	6	4
4	N121	6	control	21.1	11	10
5	N121	24	infected	28.1	41	9
6	N121	24	control	15.5	46	17
7	N138	2	control	19.4	20	16
8	N158	48	infected	19.3	9	1
9	N158	48	control	20.2	38	7
10	N1855	6	control	21.7	28	11
11	N1859	24	control	15.6	33	6
12	N1859	6	infected	14.9	34	14
13	N1861	0	control	16.6	4	7
14	N1861	2	infected	16.2	37	12
15	N1864	0	control	14.2	21	13
16	N1864	48	control	11.8	37	7
17	N1870	48	control	17.8	17	9
18	N1870	24	infected	12.4	30	6
19	N1178	6	infected	12.3	28	3
20	N121	0	control	45.9	5	1
21	N121	48	control	25.5	39	5
22	N121	2	control	14.3	43	12
23	N138	24	control	24.0	5	12
24	N138	6	infected	9.8	31	16
25	N138	48	control	18.6	32	13
26	N138	48	infected	22.5	32	7
27	N158	2	control	20.8	33	15
28	N1855	6	infected	18.1	19	5
29	N1855	24	control	31.9	40	14
30	N1859	0	control	23.1	22	15
31	N1859	6	control	12.1	30	15
32	N1861	24	control	18.5	35	4
33	N1864	2	infected	17.2	18	5
34	N1870	0	control	26.3	7	8
35	N1870	48	infected	19.3	9	9
36	N98	6	infected	24.1	16	9
37	N1178	24	control	27.9	17	2
38	N1178	2	control	20.5	25	10
39	N121	2	infected	49.4	3	6
40	N138	2	infected	17.2	36	17
41	N158	6	control	27.6	6	16
42	N158	0	control	12.7	10	4
43	N158	24	infected	32.9	38	12
44	N158	6	infected	31.9	42	1
45	N1855	48	control	17.3	26	2
46	N1855	0	control	27.5	44	11
47	N1859	24	infected	19.4	15	5

48	N1859	48	infected	14.8	27	5
49	N1861	24	infected	27.5	2	3
50	N1864	48	infected	14.5	24	18
51	N1864	24	control	23.8	40	2
52	N1864	6	infected	15.7	41	4
53	N1870	2	infected	27.0	44	3
54	N98	24	infected	20.6	26	14
55	N1178	2	infected	27.8	27	13
56	N1178	48	infected	24.9	34	1
57	N1178	6	control	24.5	35	10
58	N121	48	infected	21.9	15	18
59	N138	6	control	23.0	43	6
60	N158	2	infected	33.0	4	14
61	N1855	24	infected	35.5	1	13
62	N1855	2	infected	15.4	23	13
63	N1859	2	control	26.9	11	3
64	N1861	6	control	13.2	10	10
65	N1861	6	infected	10.0	23	8
66	N1864	2	control	20.9	13	12
67	N1864	6	control	12.3	45	17
68	N1870	6	infected	28.1	3	11
69	N1870	6	control	10.2	16	8
70	N1870	2	control	25.3	29	16
71	N98	6	control	25.8	20	4
72	N98	2	infected	28.4	22	7
73	N1178	0	control	27.0	2	16
74	N138	0	control	20.3	13	8
75	N138	24	infected	28.9	42	9
76	N158	24	control	8.3	47	17
77	N1855	48	infected	21.5	12	17
78	N1855	2	control	26.9	39	11
79	N1859	2	infected	25.3	18	15
80	N1859	48	control	4.4	25	1
81	N1861	2	control	23.1	31	2
82	N1864	24	infected	10.8	47	15
83	N1870	24	control	17.6	14	3
84	N98	48	infected	35.0	1	8
85	N98	48	control	8.4	7	11
86	N98	2	control	32.4	14	18
87	N98	24	control	27.4	19	14
88	N98	0	control	24.8	45	10

Appendix 4 | The efficiency-corrected C_t values for the six miRNA genes measured with RT-qPCR.

Status	Animal	miR-142-5p	miR-146a	miR-423-3p	miR-22-3p	miR-16b	miR-26b
Control	N1178	24.53417	29.439566	24.396362	23.809377	21.899681	22.365517
Infected	N1178	25.352686	28.385516	25.194137	24.463146	22.208334	22.762029
Control	N138	24.868014	31.158087	25.267732	24.633568	22.951665	23.013894
Infected	N138	24.092343	28.486106	25.08384	23.807755	21.673489	22.033469
Control	N1859	26.820171	30.870788	26.316532	25.680712	24.327334	24.783107
Infected	N1859	24.628555	28.328881	25.889646	24.303286	23.38106	23.079219
Control	N1864	26.491576	31.470069	26.265963	25.674008	24.433305	24.774106
Infected	N1864	24.484526	27.538022	25.99276	24.172018	23.184378	22.723179
Control	N98	26.812393	29.8518	27.255631	25.578893	24.983508	25.088582
Infected	N98	25.580287	27.351854	27.244683	24.370542	24.42623	23.736762
Control	N1870	26.520255	32.214775	25.952544	25.680161	23.692615	23.792721
Infected	N1870	25.498707	30.309308	25.354941	24.663722	22.459404	22.78794
Control	N1855	24.529996	30.101839	24.987502	23.608771	22.379388	22.592828
Infected	N1855	22.812491	27.044538	25.141153	22.008544	21.725855	21.792409
Control	N158	25.139788	28.347613	24.916448	23.659956	22.202008	22.472405
Infected	N158	23.572162	25.882526	25.292828	22.360531	22.214529	21.917481
Control	N121	24.582264	27.26587	25.349734	22.798142	22.003793	22.675857
Infected	N121	23.231772	25.839653	25.357796	22.102495	22.4252	21.437279

Appendix 5 | Total RNA concentrations and quality, as measured by Bioanalyzer (Chapter 4).

Sample	RNA [ng/ul]	rRNA Ratio [28s / 18s]	RNA Integrity Number (RIN)
Untreated 1	67	2.16	10
Untreated 2	69	2.29	10
Untreated 3	75	2.14	10
Negative control mimic 1	62	2.14	9.8
Negative control mimic 2	61	2.28	10
Negative control mimic 3	69	2.32	9.8
miR-146a mimic 1	54	1.92	9.5
miR-146a mimic 2	55	2.09	9.7
miR-146a mimic 3	48	1.99	10

Appendix 6 | Differentially expressed genes in the negative control miRNA mimic-transfected Bomac cells, in comparison with untreated cells.

Upregulated genes:

Ensembl gene ID	Gene name	Fold change	p-value (FDR)
ENSBTAG00000033695	IFNB2	11.7	1.82×10^{-15}
ENSBTAG00000046324		9.6	6.22×10^{-9}
ENSBTAG00000046849	IFNB3	9.4	2.86×10^{-42}
ENSBTAG00000019716	CXCL8	8.8	4.85×10^{-44}
ENSBTAG00000046456	IL6	7.6	2.59×10^{-22}
ENSBTAG00000037558	GRO1	6.7	1.59×10^{-26}
ENSBTAG00000037811	CCL2	6.2	7.59×10^{-22}
ENSBTAG00000015060	GBP5	6.0	1.29×10^{-11}
ENSBTAG00000007191	CCL5	5.4	2.63×10^{-249}
ENSBTAG00000005990	S1PR1	5.2	5.34×10^{-81}
ENSBTAG00000046336	RNPS1	5.1	3.77×10^{-11}
ENSBTAG00000009768	IFIT3	5.1	1.79×10^{-79}
ENSBTAG00000034918	IFIT2	4.8	5.11×10^{-46}
ENSBTAG00000030921	FAM3B	4.6	2.81×10^{-43}
ENSBTAG00000018366	SLC15A3	4.6	6.19×10^{-15}
ENSBTAG00000008471	MX2	4.5	1.02×10^{-46}
ENSBTAG00000015727	IFI47	4.5	1.15×10^{-31}
ENSBTAG00000004381	TACSTD2	4.4	4.07×10^{-19}
ENSBTAG00000022396	SAA3	4.3	2.04×10^{-11}
ENSBTAG00000039035	HSPA6	4.2	4.91×10^{-44}
ENSBTAG00000004221	ESM1	4.1	4.45×10^{-142}
ENSBTAG00000009812	CXCL6	4.0	5.32×10^{-18}
ENSBTAG00000016061	RSAD2	4.0	2.36×10^{-44}
ENSBTAG00000011936	ATP8B4	3.9	5.54×10^{-93}
ENSBTAG00000019017	IFITM2	3.8	1.04×10^{-47}
ENSBTAG00000038625		3.5	7.49×10^{-42}
ENSBTAG00000006864		3.4	1.23×10^{-48}
ENSBTAG00000045907	TNFSF13B	3.4	9.73×10^{-15}
ENSBTAG00000007450	C2	3.3	1.49×10^{-38}
ENSBTAG00000038233		3.3	1.65×10^{-57}
ENSBTAG00000020283	DUSP5	3.2	4.68×10^{-78}
ENSBTAG00000024272		3.2	1.48×10^{-74}
ENSBTAG00000038938		3.1	4.68×10^{-19}
ENSBTAG00000011563	TNFSF13B	3.1	5.38×10^{-38}
ENSBTAG00000037533		3.0	1.59×10^{-162}
ENSBTAG00000014762	ISG20	2.9	1.32×10^{-65}
ENSBTAG00000008021		2.9	9.05×10^{-72}
ENSBTAG00000017824	IRF8	2.9	7.62×10^{-70}
ENSBTAG00000037778	CXCL3	2.8	1.29×10^{-15}

ENSBTAG00000002416		2.8	1.51×10^{-48}
ENSBTAG00000031750	PLAC8	2.8	1.12×10^{-44}
ENSBTAG00000019517	ELN	2.8	5.02×10^{-20}
ENSBTAG00000014127	PGHS-2	2.7	1.84×10^{-28}
ENSBTAG00000031214		2.7	3.32×10^{-57}
ENSBTAG00000009206	FOXS1	2.7	1.59×10^{-45}
ENSBTAG00000019979	CMPK2	2.6	1.09×10^{-37}
ENSBTAG00000037634		2.6	1.12×10^{-33}
ENSBTAG00000015582	HMOX1	2.5	5.13×10^{-88}
ENSBTAG00000003737	SLC51B	2.5	6.66×10^{-17}
ENSBTAG00000043567		2.5	4.30×10^{-27}
ENSBTAG00000014707	ISG15	2.5	2.65×10^{-57}
ENSBTAG00000008062	DMRT2	2.5	1.10×10^{-6}
ENSBTAG00000044118	HMGA2	2.4	1.14×10^{-13}
ENSBTAG00000046512	CMYA1	2.4	1.66×10^{-21}
ENSBTAG00000039524		2.4	3.80×10^{-20}
ENSBTAG00000032265	RTP4	2.4	2.51×10^{-38}
ENSBTAG00000021959	CDC20B	2.4	2.39×10^{-6}
ENSBTAG00000001034	IL18R1	2.4	4.86×10^{-37}
ENSBTAG00000034529	HMGA1	2.4	7.70×10^{-111}
ENSBTAG00000008250	SPRY4	2.4	5.53×10^{-31}
ENSBTAG00000003994	IGFBP3	2.4	3.20×10^{-5}
ENSBTAG00000005382	CCDC85B	2.4	2.58×10^{-31}
ENSBTAG00000020745	HIVEP3	2.4	2.68×10^{-18}
ENSBTAG00000047225	BCL2L14	2.3	7.46×10^{-16}
ENSBTAG00000015493		2.3	6.43×10^{-6}
ENSBTAG00000014705	HES4	2.3	3.54×10^{-8}
ENSBTAG00000006951	LMO2	2.3	7.92×10^{-26}
ENSBTAG00000014628	OAS2	2.3	2.59×10^{-44}
ENSBTAG00000009177	PLEKHA4	2.3	8.01×10^{-80}
ENSBTAG00000006846	LGALS9	2.3	8.60×10^{-79}
ENSBTAG00000000095	PD-L1	2.3	1.27×10^{-27}
ENSBTAG00000019432	ICAM2	2.2	1.05×10^{-9}
ENSBTAG00000014529	GBP4	2.2	3.86×10^{-48}
ENSBTAG00000000507	NR4A1	2.2	1.40×10^{-54}
ENSBTAG00000030932	IFI44L	2.2	4.12×10^{-37}
ENSBTAG00000001221	NKX3-1	2.2	9.68×10^{-05}
ENSBTAG00000006194	FOSL1	2.2	2.89×10^{-59}
ENSBTAG00000037989		2.2	2.56×10^{-31}
ENSBTAG00000007969	CIDEC	2.2	7.45×10^{-08}
ENSBTAG00000009132	TMPRSS2	2.2	7.61×10^{-10}
ENSBTAG00000016505	TMC7	2.2	1.89×10^{-26}
ENSBTAG00000021308	IRS1	2.2	4.16×10^{-44}
ENSBTAG00000011467	BATF2	2.2	9.67×10^{-16}
ENSBTAG00000015919	DKFZP 564O0823	2.2	4.36×10^{-72}

ENSBTAG00000008333	ETV4	2.1	1.84×10^{-35}
ENSBTAG00000000436	TNFAIP3	2.1	8.62×10^{-17}
ENSBTAG00000009051	MMP19	2.1	2.88×10^{-9}
ENSBTAG00000007883		2.1	5.57×10^{-21}
ENSBTAG00000012451	HLA-DMB	2.1	6.27×10^{-51}
ENSBTAG00000005251		2.1	3.85×10^{-20}
ENSBTAG00000017040	LY6E	2.1	1.45×10^{-80}
ENSBTAG00000001864	NR4A3	2.1	3.37×10^{-50}
ENSBTAG00000007773	VCAM1	2.1	3.77×10^{-8}
ENSBTAG00000007881	IFIT1	2.1	6.22×10^{-21}
ENSBTAG00000045588		2.1	9.05×10^{-33}
ENSBTAG00000018474	IL6R	2.1	4.83×10^{-18}
ENSBTAG00000027534		2.1	8.76×10^{-7}
ENSBTAG00000015752	SP110	2.1	7.41×10^{-52}
ENSBTAG00000046580	LGP2	2.1	1.96×10^{-50}
ENSBTAG00000008573	ZFP36	2.1	2.89×10^{-83}
ENSBTAG00000045976	NT5E	2.1	1.98×10^{-34}
ENSBTAG00000037604	EFNB3	2.1	6.88×10^{-8}
ENSBTAG00000006557	RHEBL1	2.1	1.01×10^{-17}
ENSBTAG00000016709	NT5C3	2.0	3.08×10^{-38}
ENSBTAG00000042711	snoU2_19	2.0	8.92×10^{-7}
ENSBTAG00000020172	DENND2D	2.0	1.41×10^{-12}
ENSBTAG00000000892	MB21D1	2.0	3.50×10^{-64}
ENSBTAG00000020884	CASP13	2.0	8.73×10^{-55}

Downregulated genes:

Ensembl gene ID	Gene name	Fold change	p-value (FDR)
ENSBTAG00000043583		-3.6	1.55×10^{-57}
ENSBTAG00000038639	CXCL9	-3.2	1.20×10^{-11}
ENSBTAG00000033160	FAM114A1	-3.2	1.74×10^{-129}
ENSBTAG00000006326	ALDH1L2	-2.9	1.23×10^{-136}
ENSBTAG00000015441	ACTB	-2.8	4.98×10^{-10}
ENSBTAG00000006037	WISP2	-2.8	1.73×10^{-26}
ENSBTAG00000043550	MT-CYB	-2.7	9.39×10^{-126}
ENSBTAG00000003791	LPAR3	-2.7	4.97×10^{-60}
ENSBTAG00000018400	BRMS1L	-2.7	3.05×10^{-94}
ENSBTAG00000007962	ATP9A	-2.7	3.30×10^{-124}
ENSBTAG00000005871	MECOM	-2.7	7.61×10^{-9}
ENSBTAG00000007444	C1H21ORF7	-2.6	3.19×10^{-12}
ENSBTAG00000043559	MT-ND4L	-2.5	4.59×10^{-123}
ENSBTAG00000034075	SLC7A11	-2.5	3.08×10^{-21}
ENSBTAG00000001745	LUM	-2.5	1.35×10^{-42}
ENSBTAG00000015214	CA3	-2.5	4.79×10^{-16}
ENSBTAG00000018829	SPRYD7	-2.5	1.78×10^{-49}
ENSBTAG00000012693		-2.5	1.58×10^{-20}

ENSBTAG00000043577	MT-ND4	-2.4	3.46×10^{-111}
ENSBTAG00000006599	INHBE	-2.4	4.77×10^{-37}
ENSBTAG00000016373	TTC26	-2.4	3.82×10^{-34}
ENSBTAG00000011934	PCK2	-2.4	3.13×10^{-137}
ENSBTAG00000009984	SGPL1	-2.4	1.71×10^{-83}
ENSBTAG00000043568	MT-ND3	-2.4	1.18×10^{-115}
ENSBTAG00000008274		-2.4	1.55×10^{-8}
ENSBTAG00000018460	ADAMTS16	-2.4	2.70×10^{-16}
ENSBTAG00000004231	GPM6A	-2.3	6.37×10^{-74}
ENSBTAG00000026977	PTPRQ	-2.3	1.49×10^{-52}
ENSBTAG00000033679	HLCS	-2.3	1.52×10^{-57}
ENSBTAG00000006234	NPR1	-2.3	1.57×10^{-21}
ENSBTAG00000002978	PRKG2	-2.3	1.58×10^{-56}
ENSBTAG00000007977	LAMP5	-2.3	2.99×10^{-7}
ENSBTAG00000005476	METTL21A	-2.3	1.89×10^{-46}
ENSBTAG00000021217	COL11A1	-2.3	2.16×10^{-182}
ENSBTAG00000001244	PLAT	-2.2	1.72×10^{-121}
ENSBTAG00000012963	VILL	-2.2	3.11×10^{-14}
ENSBTAG00000022114	TMEM65	-2.2	2.09×10^{-67}
ENSBTAG00000005493	TBC1D14	-2.2	4.79×10^{-119}
ENSBTAG00000043582		-2.2	1.68×10^{-90}
ENSBTAG00000013960	PSAT1	-2.2	1.95×10^{-101}
ENSBTAG00000020387	MARF1	-2.2	2.95×10^{-137}
ENSBTAG00000021372	SEPT11	-2.2	3.34×10^{-139}
ENSBTAG00000030599	SMOC1	-2.2	3.39×10^{-118}
ENSBTAG00000014838	VPS26B	-2.2	1.24×10^{-52}
ENSBTAG00000009086	LOXL1	-2.2	7.72×10^{-64}
ENSBTAG00000012994	LOX	-2.2	1.72×10^{-197}
ENSBTAG00000019402	CCDC37	-2.1	1.11×10^{-5}
ENSBTAG00000045628	C15orf61	-2.1	1.17×10^{-8}
ENSBTAG00000007235	NTNG2	-2.1	5.02×10^{-15}
ENSBTAG00000009746	MPHOSPH6	-2.1	1.23×10^{-39}
ENSBTAG00000001702	TMEM107	-2.1	2.52×10^{-7}
ENSBTAG00000014614	ACTA2	-2.1	3.64×10^{-65}
ENSBTAG00000043563	ND5	-2.1	1.22×10^{-89}
ENSBTAG00000000037	CWC27	-2.1	1.70×10^{-36}
ENSBTAG00000011836	OMD	-2.1	5.51×10^{-14}
ENSBTAG00000021570	PLEKHG4	-2.1	5.53×10^{-6}
ENSBTAG00000010704	LRRC4	-2.1	2.49×10^{-9}
ENSBTAG00000014567	MYLK	-2.1	8.79×10^{-23}
ENSBTAG00000013760	COL4A6	-2.1	6.05×10^{-25}
ENSBTAG00000021838	ESRP1	-2.1	7.49×10^{-42}
ENSBTAG00000043556	COII	-2.0	5.68×10^{-98}
ENSBTAG00000008816	TRIM2	-2.0	9.48×10^{-78}
ENSBTAG00000006731	LAT	-2.0	1.03×10^{-41}
ENSBTAG00000002993	SFT2D1	-2.0	6.70×10^{-45}

ENSBTAG00000012545	CASC4	-2.0	8.56×10^{-68}
ENSBTAG00000010620	ATP6V1B1	-2.0	1.50×10^{-15}
ENSBTAG00000014665	ADAMTS2	-2.0	1.94×10^{-32}
ENSBTAG00000006745	FGG	-2.0	9.22×10^{-42}
ENSBTAG00000043560	COX3	-2.0	4.61×10^{-98}
ENSBTAG00000013801	PBX1	-2.0	3.60×10^{-27}

Appendix 7 | Differentially expressed genes in the miR-146a-mimic transfected cells, in comparison with negative control.

Upregulated genes:

Ensembl gene ID	Gene name	Fold change	p-value (FDR)
ENSBTAG00000046324		3.4	5.49×10^{-12}
ENSBTAG00000007423	TNFRSF11B	3.3	6.43×10^{-32}
ENSBTAG00000007191	CCL5	3.1	2.16×10^{-139}
ENSBTAG00000037539	VCAM1	3.1	2.20×10^{-10}
ENSBTAG00000046054	RHOB	2.9	1.12×10^{-174}
ENSBTAG00000008612	C1R	2.8	1.34×10^{-37}
ENSBTAG00000009153	MLXIPL	2.7	7.59×10^{-12}
ENSBTAG00000018400	BRMS1L	2.6	5.57×10^{-87}
ENSBTAG00000009984	SGPL1	2.5	1.52×10^{-96}
ENSBTAG00000007962	ATP9A	2.5	3.31×10^{-108}
ENSBTAG00000001785	TGM3	2.5	1.44×10^{-8}
ENSBTAG00000006048	DCAKD	2.4	1.09×10^{-45}
ENSBTAG00000008105	RBM38	2.4	4.33×10^{-31}
ENSBTAG00000033695	IFNB2	2.3	4.86×10^{-8}
ENSBTAG00000004840	C1S	2.3	8.29×10^{-10}
ENSBTAG00000005871	MECOM	2.3	1.52×10^{-6}
ENSBTAG00000018948	HIF3A	2.3	4.47×10^{-7}
ENSBTAG00000033160	FAM114A1	2.3	4.26×10^{-67}
ENSBTAG00000004438	XPNPEP1	2.3	5.30×10^{-144}
ENSBTAG00000002850	HEATR9	2.3	7.10×10^{-11}
ENSBTAG00000007773	VCAM1	2.3	2.38×10^{-10}
ENSBTAG00000015228	CD74	2.2	1.11×10^{-15}
ENSBTAG00000001021	CYP1A1	2.2	6.05×10^{-40}
ENSBTAG00000020080	MYBPC2	2.2	4.39×10^{-9}
ENSBTAG00000002993	SFT2D1	2.2	3.34×10^{-59}
ENSBTAG00000015060	GBP5	2.2	5.39×10^{-7}
ENSBTAG00000007450	C2	2.2	3.96×10^{-28}
ENSBTAG00000009746	MPHOSPH6	2.2	7.78×10^{-43}
ENSBTAG00000000037	CWC27	2.2	6.31×10^{-41}
ENSBTAG00000044118	HMGA2	2.1	1.61×10^{-17}
ENSBTAG00000016343	KCNIP2	2.1	2.31×10^{-5}
ENSBTAG00000021372	SEPT11	2.1	7.86×10^{-133}
ENSBTAG00000005493	TBC1D14	2.1	1.50×10^{-107}
ENSBTAG00000007235	NTNG2	2.1	6.57×10^{-15}
ENSBTAG00000046456	IL6	2.1	5.13×10^{-9}
ENSBTAG00000008816	TRIM2	2.1	5.55×10^{-86}

ENSBTAG00000009051	MMP19	2.1	4.61×10^{-12}
ENSBTAG00000001244	PLAT	2.1	5.73×10^{-101}
ENSBTAG00000009132	TMPRSS2	2.1	1.60×10^{-13}
ENSBTAG00000022114	TMEM65	2.1	1.11×10^{-56}
ENSBTAG00000017733	CA2	2.1	8.17×10^{-16}
ENSBTAG00000006928	OAT	2.1	4.09×10^{-117}
ENSBTAG00000002329	ASAP2	2.1	1.49×10^{-74}
ENSBTAG00000016373	TTC26	2.1	4.43×10^{-23}
ENSBTAG00000021417	DMWD	2.0	2.57×10^{-34}
ENSBTAG00000012433	DENND1B	2.0	3.00×10^{-15}

Downregulated genes:

Ensembl gene ID	Gene name	Fold change	p-value (FDR)
ENSBTAG00000045661	Metazoa_SRP	-16.5	3.06×10^{-13}
ENSBTAG00000046912	Metazoa_SRP	-15.0	3.63×10^{-12}
ENSBTAG00000042458	RNase_MRP	-13.3	1.35×10^{-10}
ENSBTAG00000047908	Metazoa_SRP	-13.2	1.35×10^{-11}
ENSBTAG00000044427	RNaseP_nuc	-12.6	2.22×10^{-10}
ENSBTAG00000038155	U1	-7.6	4.09×10^{-7}
ENSBTAG00000047122	5S_rRNA	-7.6	2.58×10^{-7}
ENSBTAG00000048148	5_8S_rRNA	-5.5	2.56×10^{-6}
ENSBTAG00000047401	5_8S_rRNA	-5.5	2.71×10^{-6}
ENSBTAG00000045825	5_8S_rRNA	-5.3	4.49×10^{-6}
ENSBTAG00000046797	NRAS	-5.1	0
ENSBTAG00000046304	U1	-4.6	1.12×10^{-4}
ENSBTAG00000043250	7SK	-4.6	4.26×10^{-5}
ENSBTAG00000045741	U1	-4.5	1.18×10^{-4}
ENSBTAG00000003836	ADAM19	-4.3	0
ENSBTAG00000046695		-3.6	1.67×10^{-3}
ENSBTAG00000013168	RPA3	-3.6	6.21×10^{-85}
ENSBTAG00000045952	5_8S_rRNA	-3.5	9.70×10^{-7}
ENSBTAG00000003232	RAB7L1	-3.1	5.39×10^{-137}
ENSBTAG00000010984	CDKN2AIPNL	-3.0	2.23×10^{-121}
ENSBTAG00000048255	5_8S_rRNA	-3.0	4.52×10^{-4}
ENSBTAG00000019930	CLNS1A	-3.0	4.22×10^{-196}
ENSBTAG00000012312	ROR1	-2.9	7.07×10^{-119}
ENSBTAG00000015363	CDC42SE1	-2.7	1.32×10^{-232}
ENSBTAG00000013678	OSGIN2	-2.7	4.91×10^{-118}
ENSBTAG00000038738	PXMP4	-2.7	6.43×10^{-37}
ENSBTAG00000016085	IRAK1	-2.7	3.74×10^{-119}
ENSBTAG00000047381	bta-mir-2904-3	-2.7	8.14×10^{-3}
ENSBTAG00000005351	RFXAP	-2.6	2.37×10^{-40}
ENSBTAG00000047042	bta-mir-2904-3	-2.6	9.06×10^{-3}
ENSBTAG00000048000	bta-mir-2904-3	-2.6	9.00×10^{-3}
ENSBTAG00000047852	bta-mir-2904-1	-2.6	3.30×10^{-3}
ENSBTAG00000025964	MAST4	-2.6	2.36×10^{-63}
ENSBTAG00000019852	PDHA1	-2.6	2.99×10^{-230}

ENSBTAG00000003907	TSPAN14	-2.5	5.46×10^{-68}
ENSBTAG00000045532	bta-mir-2904-3	-2.5	1.24×10^{-2}
ENSBTAG00000045494	bta-mir-2904-3	-2.5	1.28×10^{-2}
ENSBTAG00000001101	IFNLR1	-2.5	8.93×10^{-38}
ENSBTAG00000019761	MANBA	-2.5	1.45×10^{-144}
ENSBTAG00000045632	bta-mir-2904-3	-2.5	1.31×10^{-2}
ENSBTAG00000014333	SLC10A3	-2.5	1.52×10^{-143}
ENSBTAG00000045657	bta-mir-2904-3	-2.5	1.40×10^{-2}
ENSBTAG00000017811	SLC39A9	-2.5	2.48×10^{-181}
ENSBTAG00000046882	5_8S_rRNA	-2.4	6.47×10^{-3}
ENSBTAG00000047046		-2.4	4.94×10^{-3}
ENSBTAG00000046537	bta-mir-2904-3	-2.4	1.82×10^{-2}
ENSBTAG00000047154		-2.4	1.78×10^{-2}
ENSBTAG00000010863	DCP1A	-2.4	4.32×10^{-164}
ENSBTAG00000009423	NIPAL1	-2.4	1.03×10^{-68}
ENSBTAG00000005439	FAM102B	-2.4	1.98×10^{-72}
ENSBTAG00000045710		-2.3	8.40×10^{-3}
ENSBTAG00000046351		-2.3	2.44×10^{-2}
ENSBTAG00000005714	ACTC1	-2.3	6.51×10^{-14}
ENSBTAG00000010360	LRIG1	-2.3	7.51×10^{-40}
ENSBTAG00000007718	TGIF1	-2.2	8.00×10^{-50}
ENSBTAG00000003076	NT5DC1	-2.2	1.59×10^{-58}
ENSBTAG00000008729	FAM45A	-2.2	4.68×10^{-78}
ENSBTAG00000020297	PQLC3	-2.2	2.70×10^{-34}
ENSBTAG00000032914	SLC11A2	-2.2	1.99×10^{-103}
ENSBTAG00000004085	ASF1B	-2.1	1.35×10^{-109}
ENSBTAG00000003386	SUPT4H1	-2.1	1.51×10^{-115}
ENSBTAG00000009112	TRAM2	-2.1	3.04×10^{-107}
ENSBTAG00000030567	ODF2	-2.1	1.26×10^{-132}
ENSBTAG00000018286	RNF181	-2.1	1.47×10^{-97}
ENSBTAG00000043482	7SK	-2.1	2.66×10^{-2}
ENSBTAG00000014151	RCSD1	-2.1	4.25×10^{-104}
ENSBTAG00000037813	IFRG15	-2.1	1.20×10^{-96}
ENSBTAG00000015723	CRIPT	-2.1	9.96×10^{-64}
ENSBTAG00000038949	MRPL30	-2.1	1.49×10^{-61}
ENSBTAG00000016933	IL27RA	-2.1	1.17×10^{-116}
ENSBTAG00000009048	EFHD2	-2.1	2.01×10^{-67}
ENSBTAG00000004549	UPRT	-2.1	1.63×10^{-89}
ENSBTAG00000033748	IL18RAP	-2.1	2.87×10^{-16}
ENSBTAG00000017348	FGF5	-2.0	3.20×10^{-26}
ENSBTAG00000004432	CHRDL1	-2.0	2.19×10^{-35}
ENSBTAG00000019225	SLC39A14	-2.0	1.38×10^{-116}
ENSBTAG00000001754	AHCYL2	-2.0	5.05×10^{-39}
ENSBTAG00000037500	bta-mir-1842	-2.0	1.70×10^{-14}
ENSBTAG00000002746	OSTF1	-2.0	2.49×10^{-106}

Appendix 8 | Normalized count numbers for each differentially expressed miRNA (Chapter 5).

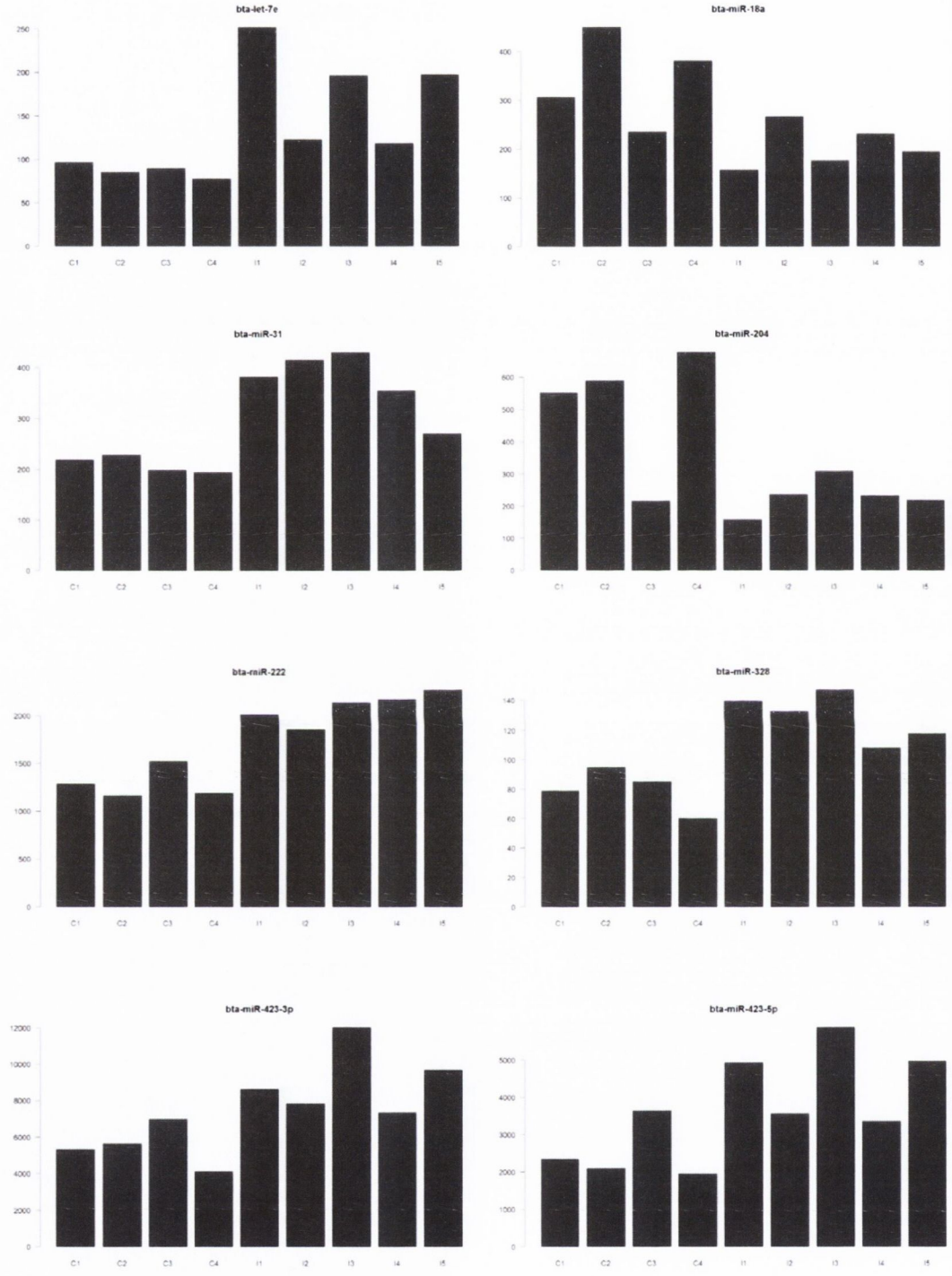

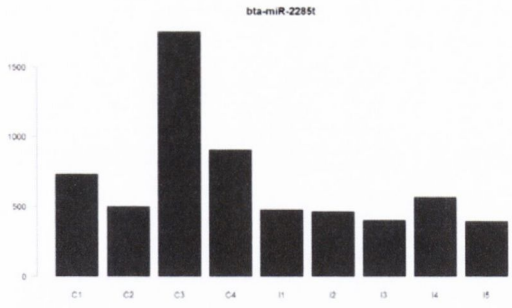

Appendix 9 | Targets of differentially expressed miRNAs.

Targets of upregulated miRNAs:

miRNA	Target	Method
hsa-miR-423-3p	CDKN1A	qRT-PCR//Luciferase reporter assay//Western blot
hsa-miR-222-3p	STAT5A	qRT-PCR//Luciferase reporter assay//Western blot
hsa-miR-222-3p	CDKN1B	Luciferase reporter assay//Western blot//Western blot;Other
hsa-miR-222-3p	CDKN1B	qRT-PCR//Luciferase reporter assay//Western blot
hsa-miR-222-3p	CDKN1B	Western blot//Northern blot
hsa-miR-222-3p	CDKN1B	Luciferase reporter assay//Western blot
hsa-miR-222-3p	CDKN1B	Luciferase reporter assay//qRT-PCR//Western blot
hsa-miR-222-3p	CDKN1B	Luciferase reporter assay
hsa-miR-222-3p	CDKN1B	Luciferase reporter assay
hsa-miR-222-3p	CDKN1B	Luciferase reporter assay
hsa-miR-222-3p	CDKN1B	Northern blot//qRT-PCR//Western blot
hsa-miR-222-3p	CDKN1B	Immunohistochemistry//In situ hybridization//Luciferase reporter assay//Northern blot//Western blot//Reporter assay;Western blot
hsa-miR-222-3p	CDKN1B	Western blot//Reporter assay
hsa-miR-222-3p	CDKN1B	Luciferase reporter assay
hsa-miR-222-3p	CDKN1B	qRT-PCR//Western blot
hsa-miR-222-3p	CDKN1B	Reporter assay
hsa-miR-222-3p	CDKN1B	Reporter assay
hsa-miR-222-3p	SOD2	Flow//Luciferase reporter assay//Microarray//qRT-PCR//Western blot
hsa-miR-222-3p	MMP1	Flow//Luciferase reporter assay//Microarray//qRT-PCR//Western blot
hsa-miR-222-3p	FOXO3	qRT-PCR//ChIP//Luciferase reporter assay//Western blot//Northern blot
hsa-miR-222-3p	DICER1	Luciferase reporter assay
hsa-miR-222-3p	CDKN1C	qRT-PCR//Luciferase reporter assay//Western blot
hsa-miR-222-3p	CDKN1C	Luciferase reporter assay//Western blot
hsa-miR-222-3p	CDKN1C	Luciferase reporter assay//Reporter assay;Other
hsa-miR-222-3p	KIT	qRT-PCR//Western blot
hsa-miR-222-3p	KIT	Luciferase reporter assay
hsa-miR-222-3p	KIT	Luciferase reporter assay
hsa-miR-222-3p	KIT	Northern blot//qRT-PCR//Western blot
hsa-miR-222-3p	KIT	Reporter assay
hsa-miR-222-3p	TMED7	Western blot

hsa-miR-222-3p	TMED7	Western blot;qRT-PCR
hsa-miR-222-3p	ETS1	Luciferase reporter assay//qRT-PCR
hsa-miR-222-3p	PPP2R2A	Luciferase reporter assay//Western blot
hsa-miR-222-3p	PPP2R2A	Reporter assay;Western blot
hsa-miR-222-3p	TIMP3	Flow//Immunohistochemistry//Luciferase reporter assay//qRT-PCR//Western blot
hsa-miR-222-3p	TIMP3	Immunohistochemistry//In situ hybridization//qRT-PCR//Western blot
hsa-miR-222-3p	TIMP3	ELISA//Luciferase reporter assay//qRT-PCR//Western blot
hsa-miR-222-3p	TNFSF10	Western blot
hsa-miR-222-3p	FOS	qRT-PCR//Luciferase reporter assay//Western blot//Northern blot
hsa-miR-222-3p	FOS	Luciferase reporter assay
hsa-miR-222-3p	ICAM1	Luciferase reporter assay
hsa-miR-222-3p	ESR1	Luciferase reporter assay//qRT-PCR//Western blot
hsa-miR-222-3p	BBC3	Immunohistochemistry//In situ hybridization//Luciferase reporter assay//Northern blot//Western blot
hsa-miR-222-3p	PTEN	FACS//Flow//Luciferase reporter assay//Northern blot//Western blot
hsa-miR-222-3p	PTEN	Flow//Immunohistochemistry//Luciferase reporter assay//qRT-PCR//Western blot
hsa-miR-222-3p	PTEN	Western blot
hsa-miR-222-3p	SELE	Luciferase reporter assay
hsa-miR-222-3p	TP53	Western blot
hsa-miR-222-3p	CORO1A	Western blot
hsa-miR-222-3p	TCEAL1	Western blot
hsa-miR-222-3p	RECK	Luciferase reporter assay
hsa-miR-222-3p	CERS2	Luciferase reporter assay//qRT-PCR//Western blot
hsa-miR-31-5p	HIF1AN	Northern blot//qRT-PCR//Western blot
hsa-miR-31-5p	RHOA	Luciferase reporter assay//qRT-PCR//Western blot
hsa-miR-31-5p	RHOA	qRT-PCR//Western blot
hsa-miR-31-5p	PPP2R2A	qRT-PCR//Luciferase reporter assay
hsa-miR-31-5p	LATS2	qRT-PCR//Luciferase reporter assay
hsa-miR-31-5p	SATB2	Luciferase reporter assay
hsa-miR-31-5p	FOXP3	qRT-PCR//Luciferase reporter assay//Western blot
hsa-miR-31-5p	SELE	Immunocytochemistry//Northern blot//qRT-PCR//Western blot
hsa-miR-31-5p	CASR	LacZ assay
hsa-miR-31-5p	YY1	Luciferase reporter assay//qRT-PCR
hsa-miR-31-5p	RET	Luciferase reporter assay//qRT-PCR
hsa-miR-31-5p	NUMB	Luciferase reporter assay//qRT-PCR
hsa-miR-31-5p	NFAT5	Luciferase reporter assay//qRT-PCR
hsa-miR-31-5p	KLF13	Luciferase reporter assay//qRT-PCR
hsa-miR-31-5p	JAZF1	Luciferase reporter assay//qRT-PCR
hsa-miR-31-5p	HOXC13	Luciferase reporter assay//qRT-PCR
hsa-miR-31-5p	ETS1	Luciferase reporter assay//qRT-PCR
hsa-miR-31-5p	ITGA5	Luciferase reporter assay//qRT-PCR//Western blot
hsa-miR-31-5p	MPRIP	Luciferase reporter assay//qRT-PCR
hsa-miR-31-5p	MMP16	Luciferase reporter assay//qRT-PCR//Western blot
hsa-miR-31-5p	RDX	Luciferase reporter assay//qRT-PCR//Western blot
hsa-miR-31-5p	CXCL12	Luciferase reporter assay//qRT-PCR
hsa-miR-31-5p	ARPC5	Luciferase reporter assay//qRT-PCR

hsa-miR-31-5p	FZD3	Luciferase reporter assay//qRT-PCR//Western blot
hsa-miR-31-5p	DMD	Luciferase reporter assay//qRT-PCR//Western blot
hsa-miR-31-5p	TIAM1	Luciferase reporter assay//Microarray//Northern blot//qRT-PCR
hsa-miR-31-5p	ICAM1	Luciferase reporter assay
hsa-miR-31-5p	DKK1	Immunoprecipitaion//Luciferase reporter assay//Microarray//qRT-PCR//Western blot
hsa-miR-31-5p	DACT3	Immunoprecipitaion//Luciferase reporter assay//Microarray//qRT-PCR//Western blot
hsa-miR-31-5p	PRKCE	Luciferase reporter assay
hsa-miR-31-5p	RASA1	Luciferase reporter assay//qRT-PCR//Western blot
hsa-miR-31-5p	STK40	Luciferase reporter assay
hsa-miR-31-5p	MCM2	Luciferase reporter assay
hsa-miR-31-5p	CDK1	Luciferase reporter assay
hsa-miR-31-5p	CREG1	Immunofluorescence//Luciferase reporter assay//qRT-PCR//Western blot
hsa-miR-31-5p	MLH1	Luciferase reporter assay
hsa-miR-31-5p	MET	Luciferase reporter assay
hsa-miR-31-5p	MET	Luciferase reporter assay
hsa-let-7e-5p	MPL	Luciferase reporter assay
hsa-let-7e-5p	HMGA2	Luciferase reporter assay//qRT-PCR
hsa-let-7e-5p	EIF3J	Luciferase reporter assay//Reporter assay
hsa-let-7e-5p	SMC1A	Luciferase reporter assay//Reporter assay;Other
hsa-let-7e-5p	WNT1	Flow//Immunoblot//Luciferase reporter assay//Microarray//qRT-PCR
hsa-let-7e-5p	MYCN	Reporter assay
hsa-miR-328-3p	PTPRJ	qRT-PCR//Western blot
hsa-miR-328-3p	BACE1	Luciferase reporter assay
hsa-miR-328-3p	ABCG2	Luciferase reporter assay//qRT-PCR//Western blot//Reporter assay;Western blot;qRT-PCR;Other
hsa-miR-328-3p	CD44	Luciferase reporter assay//Reporter assay;Other
hsa-miR-328-3p	H2AFX	Reporter assay;Western blot;qRT-PCR

Targets of downregulated miRNAs:

miRNA	Target	Method
hsa-miR-204-5p	CREB5	Immunofluorescence//Microarray//qRT-PCR//Western blot
hsa-miR-204-5p	MEIS1	Luciferase reporter assay//Microarray//Western blot//Reporter assay;Western blot;Other
hsa-miR-204-5p	HOXA10	Microarray//Western blot
hsa-miR-204-5p	BCL2	Luciferase reporter assay
hsa-miR-204-5p	FOXC1	Luciferase reporter assay//Western blot//Reporter assay
hsa-miR-204-5p	TGFBR2	Luciferase reporter assay
hsa-miR-204-5p	SNAI2	Luciferase reporter assay
hsa-miR-204-5p	TGFBR1	Luciferase reporter assay
hsa-miR-204-5p	MAP1LC3B	Immunoblot//Immunofluorescence//qRT-PCR//Western blot
hsa-miR-204-5p	MEIS2	Luciferase reporter assay//Western blot
hsa-miR-204-5p	SNAI1	Luciferase reporter assay
hsa-miR-204-5p	SPDEF	Luciferase reporter assay//Western blot
hsa-miR-204-5p	THRB	Luciferase reporter assay//qRT-PCR//Western blot
hsa-miR-204-5p	CDX2	Luciferase reporter assay

hsa-miR-204-5p	AP1S2	Luciferase reporter assay//Microarray//qRT-PCR
hsa-miR-204-5p	BCL2L2	Immunoblot//Luciferase reporter assay//Microarray//qRT-PCR//Western blot
hsa-miR-204-5p	BIRC2	Immunoblot//Luciferase reporter assay//Microarray//qRT-PCR//Western blot
hsa-miR-204-5p	EDEM1	Luciferase reporter assay//Microarray//qRT-PCR
hsa-miR-204-5p	EZR	Immunoblot//Luciferase reporter assay//Microarray//qRT-PCR//Western blot
hsa-miR-204-5p	EZR	Immunoblot//Luciferase reporter assay
hsa-miR-204-5p	FZD1	Luciferase reporter assay//Microarray//qRT-PCR
hsa-miR-204-5p	IL11	Luciferase reporter assay
hsa-miR-204-5p	M6PR	Immunoblot//Luciferase reporter assay//Microarray//qRT-PCR//Western blot
hsa-miR-204-5p	RAB22A	Luciferase reporter assay//Microarray//qRT-PCR
hsa-miR-204-5p	RAB22A	Immunofluorescence//Microarray//qRT-PCR//Western blot
hsa-miR-204-5p	RAB40B	Luciferase reporter assay//Microarray//qRT-PCR
hsa-miR-204-5p	SERINC3	Luciferase reporter assay//Microarray//qRT-PCR
hsa-miR-204-5p	SERP1	Luciferase reporter assay//Microarray//qRT-PCR//Western blot
hsa-miR-204-5p	TCF12	Luciferase reporter assay//Microarray//qRT-PCR
hsa-miR-204-5p	TCF12	Immunofluorescence//Microarray//qRT-PCR//Western blot
hsa-miR-204-5p	TCF4	Luciferase reporter assay//Microarray//qRT-PCR
hsa-miR-204-5p	ELOVL6	Immunofluorescence//Microarray//qRT-PCR//Western blot
hsa-miR-204-5p	RUNX2	Luciferase reporter assay//qRT-PCR//Western blot
hsa-miR-204-5p	SOX4	Luciferase reporter assay//qRT-PCR//Western blot
hsa-miR-204-5p	EFNB2	Luciferase reporter assay//qRT-PCR//Western blot
hsa-miR-204-5p	ALPL	Luciferase reporter assay
hsa-miR-204-5p	SOST	Luciferase reporter assay
hsa-miR-18a-5p	ESR1	Western blot//Luciferase reporter assay
hsa-miR-18a-5p	ESR1	Luciferase reporter assay//Microarray
hsa-miR-18a-5p	ESR1	Luciferase reporter assay//qRT-PCR//Western blot
hsa-miR-18a-5p	PTEN	Luciferase reporter assay//qRT-PCR//Western blot
hsa-miR-18a-5p	CTGF	Western blot//Microarray//Northern blot//Luciferase reporter assay
hsa-miR-18a-5p	CTGF	Luciferase reporter assay
hsa-miR-18a-5p	NCOA3	Western blot
hsa-miR-18a-5p	TNFSF11	Luciferase reporter assay
hsa-miR-18a-5p	NR3C1	Luciferase reporter assay//Western blot
hsa-miR-18a-5p	TGFBR2	Luciferase reporter assay//Microarray
hsa-miR-18a-5p	Prmt5	immunohistochemistry//Microarray//qRT-PCR//Western blot
hsa-miR-18a-5p	Myc	immunohistochemistry//Microarray//qRT-PCR//Western blot
hsa-miR-18a-5p	SMAD4	Immunoblot//Luciferase reporter assay//Microarray//qRT-PCR//Western blot
hsa-miR-18a-5p	HSF2	Immunofluorescence//In situ hybridization//Luciferase reporter assay//qRT-PCR//Western blot
hsa-miR-18a-5p	ATM	Luciferase reporter assay
hsa-miR-18a-5p	Smad2	Luciferase reporter assay//qRT-PCR//Western blot
hsa-miR-18a-5p	Smad4	Luciferase reporter assay//qRT-PCR//Western blot
hsa-miR-18a-5p	DICER1	Immunohistochemistry//In situ hybridization//Luciferase reporter assay//Microarray//qRT-PCR//Western blot
hsa-miR-18a-5p	SMAD3	Western blot

Electronic Appendix

For the Electronic Appendix files, please see the enclosed CD.

Electronic Appendix 1 | FastQC data (Chapter 2).

Electronic Appendix 2 | Read counts for all known bovine miRNAs expressed in AMs.

Electronic Appendix 3 | List of targets that were predicted by both miRanda and TargetScan.

Electronic Appendix 4 | IsomiR expression analysis results.

Electronic Appendix 5 | FastQC data (Chapter 3).

Electronic Appendix 6 | Summary of the number of reads at each data processing step.

Electronic Appendix 7 | The normalized and efficiency-corrected ΔC_t values. Each sheet contains a data set of reference gene and gene-of-interest ΔC_t values.

Electronic Appendix 8 | List of read counts for all miRNAs at all time-points. CN = control, TB = infected sample.

Electronic Appendix 9 | Normalized count numbers for each differentially expressed miRNA.

Electronic Appendix 10 | Genes with expression values significantly negatively correlated with miRNA expression. These predictions were further refined by removing those miRNA-target predicted relationships that were not supported by a predicted miRNA seed region match in the 3' UTR of the correlated mRNA.

Electronic Appendix 11 | InnateDB pathway overrepresentation analysis of the predicted target genes of upregulated miRNAs.

Electronic Appendix 12 | InnateDB pathway overrepresentation analysis of the predicted target genes of downregulated miRNAs.

Electronic Appendix 13 | FastQC data (Chapter 4). Samples were sequenced on three flowcell lanes, and two files belong to each library (paired-end sequencing).

Electronic Appendix 14 | FastQC data (Chapter 5).

Electronic Appendix 15 | List of read counts for all known miRNAs.

Electronic Appendix 16 | edgeR statistical test results for each tested miRNA.

Electronic Appendix 17 | InnateDB pathway overrepresentation analysis of the predicted target genes of upregulated (A) and downregulated (B) miRNAs.